Supporting Information

Half-sandwich ruthenium(II) complexes with tethered arene-phosphinite ligands: Synthesis, structure and application in catalytic cross dehydrogenative coupling reactions of silanes and alcohols

Rebeca González-Fernández, Pascale Crochet,* and Victorio Cadierno*

Laboratorio de Compuestos Organometálicos y Catálisis (Unidad Asociada al CSIC), Centro de Innovación en Química Avanzada (ORFEO-CINQA), Departamento de Química Orgánica e Inorgánica, Instituto Universitario de Química Organometálica "Enrique Moles", Facultad de Química, Universidad de Oviedo, Julián Clavería 8, E-33006 Oviedo, Spain

E-mail: crochetpascale@uniovi.es (P.C.); vcm@uniovi.es (V.C.).

Contents

NMR spectra of the non-tethered complexes 5-7a-c

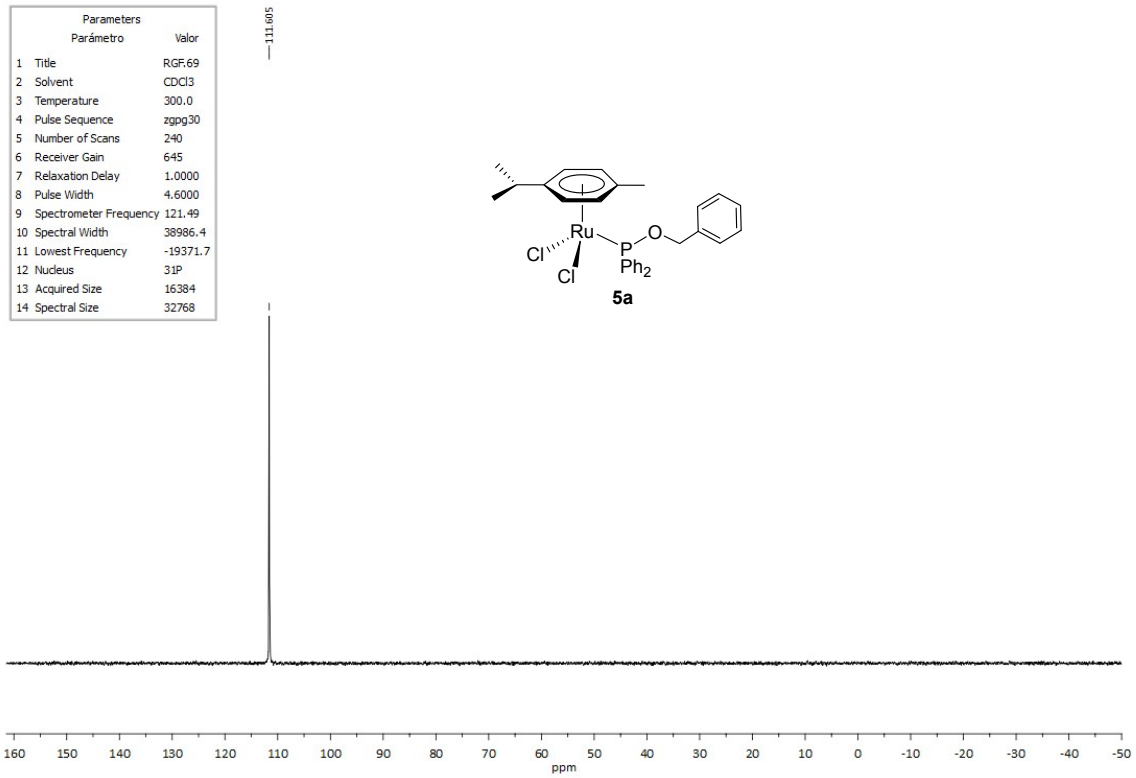

Figure S1: $^{31}P\{^{1}H\}$ NMR spectrum (121 MHz, $CDCl_3$) of complex **5a**.

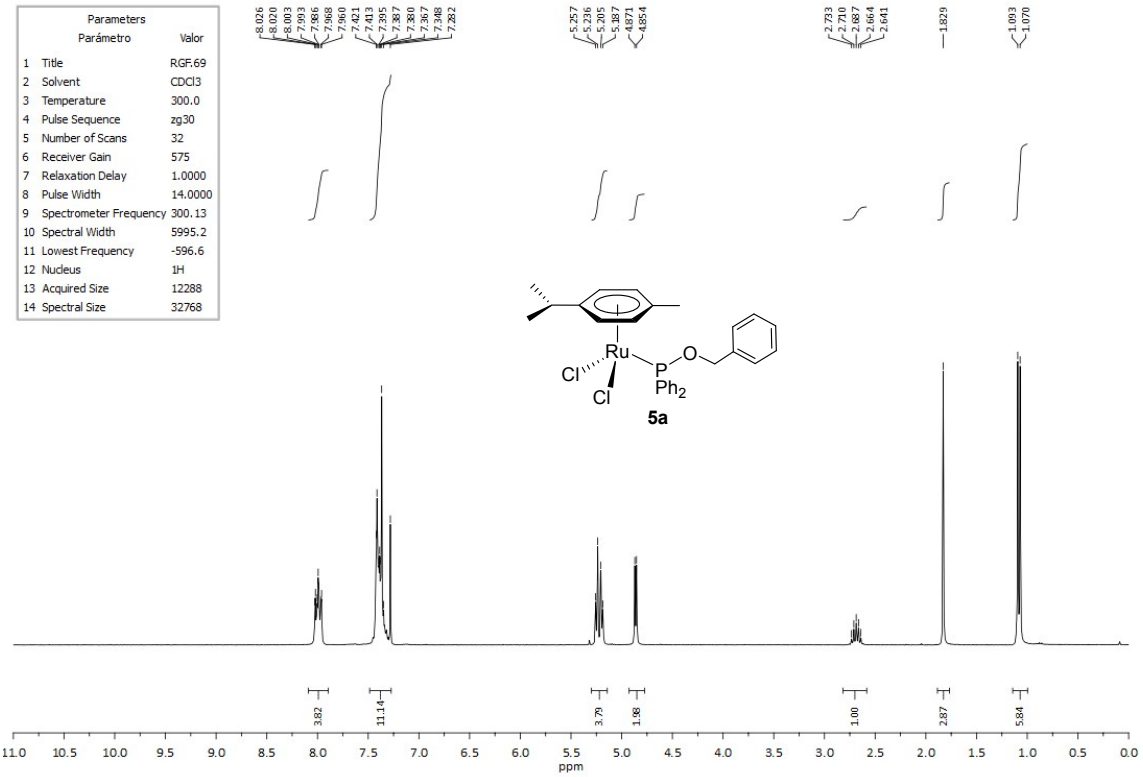

Figure S2: ^{1}H NMR spectrum (300 MHz, $CDCl_3$) of complex **5a**.

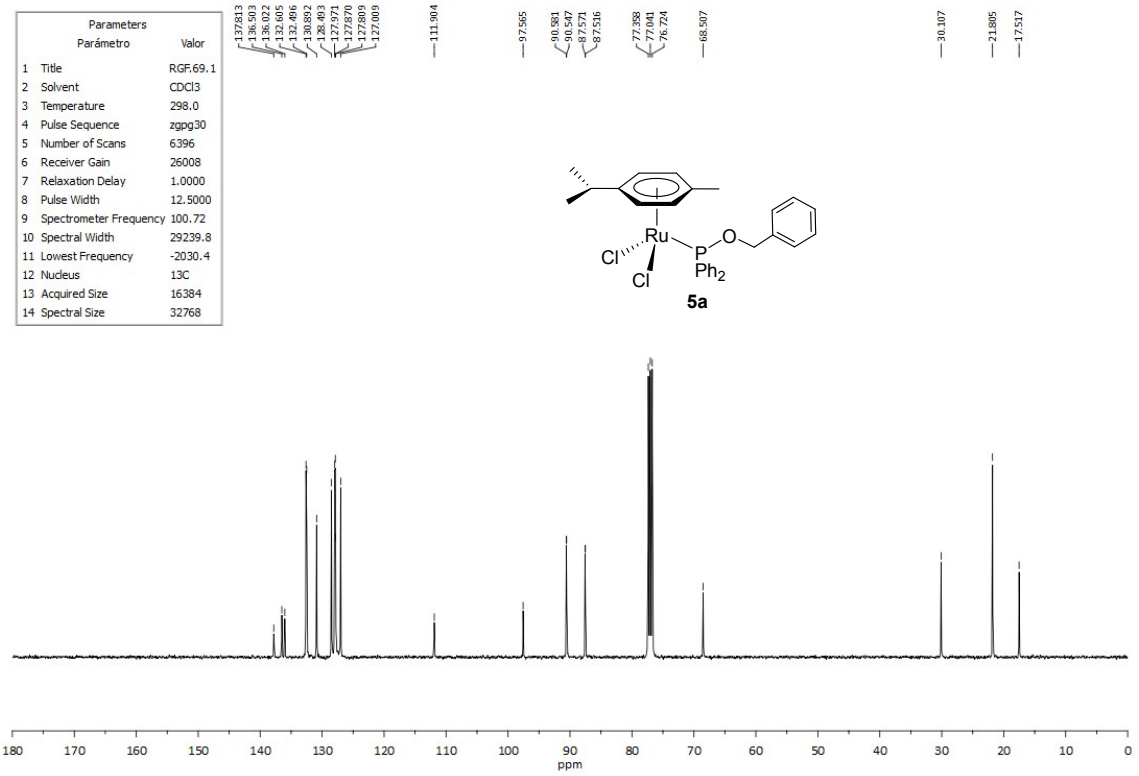

Figure S3: $^{13}C\{^{1}H\}$ NMR spectrum (100 MHz, $CDCl_3$) of complex **5a**.

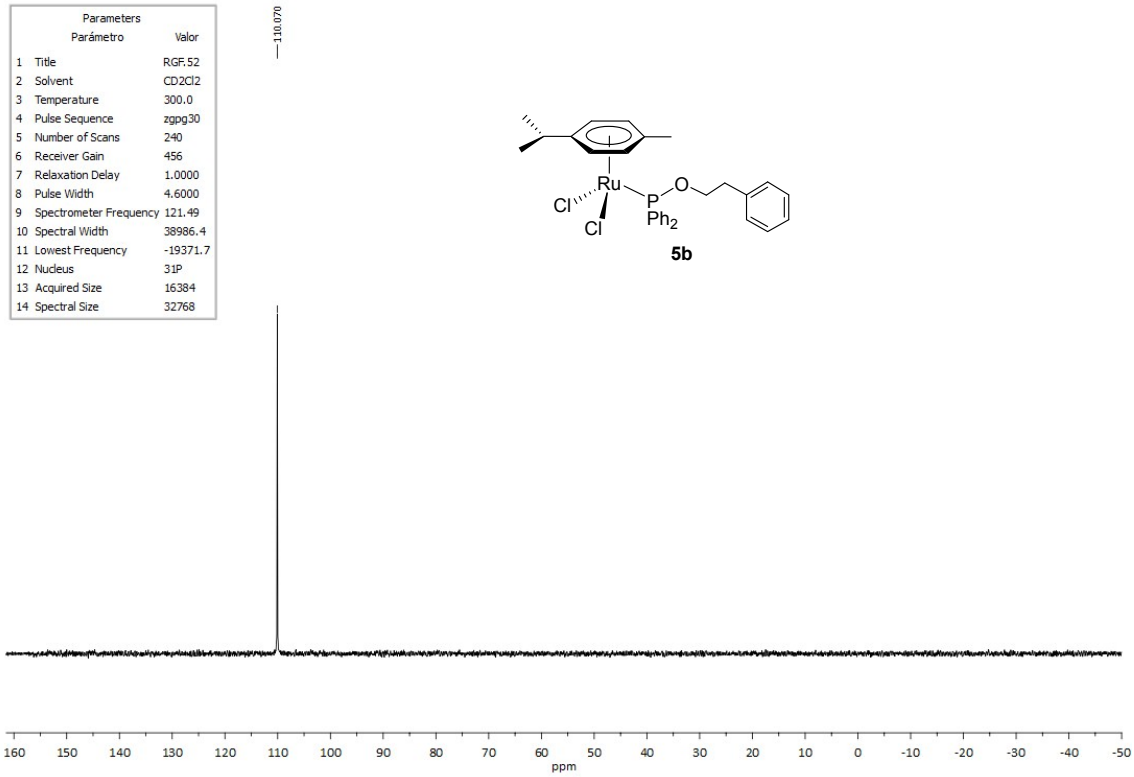

Figure S4: $^{31}P\{^{1}H\}$ NMR spectrum (121 MHz, CD_2Cl_2) of complex **5b**.

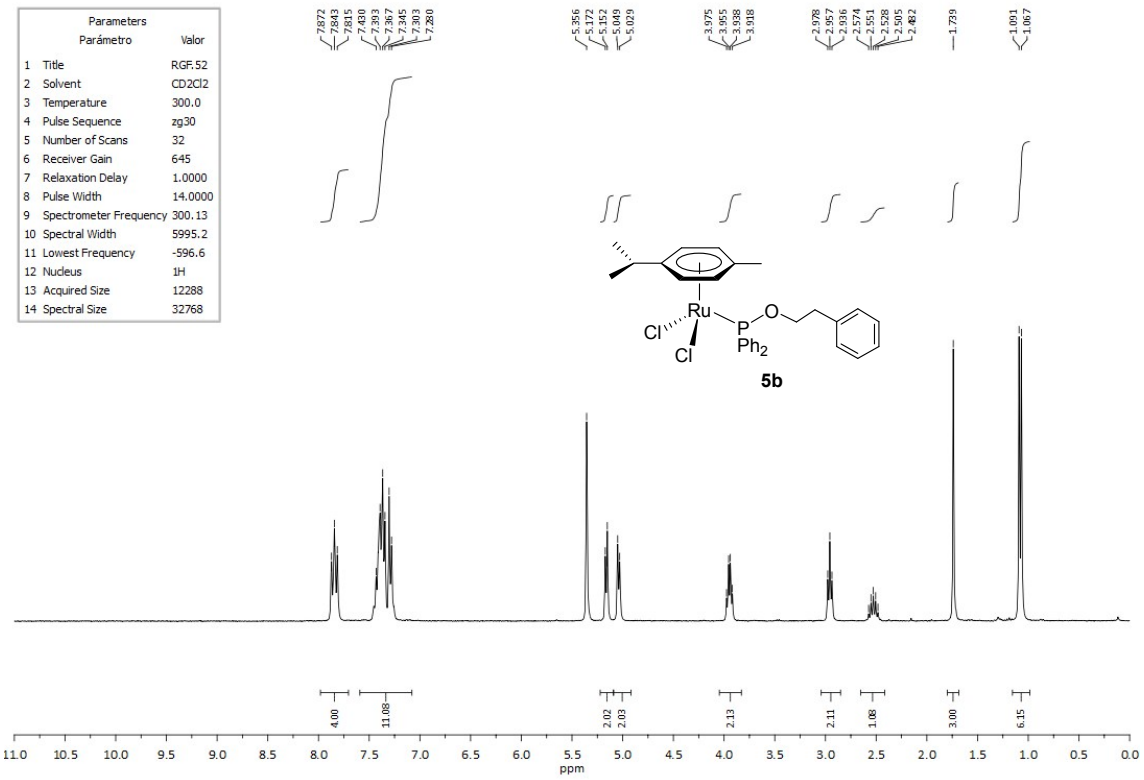

Figure S5: ^{1}H NMR spectrum (300 MHz, CD_2Cl_2) of complex **5b**.

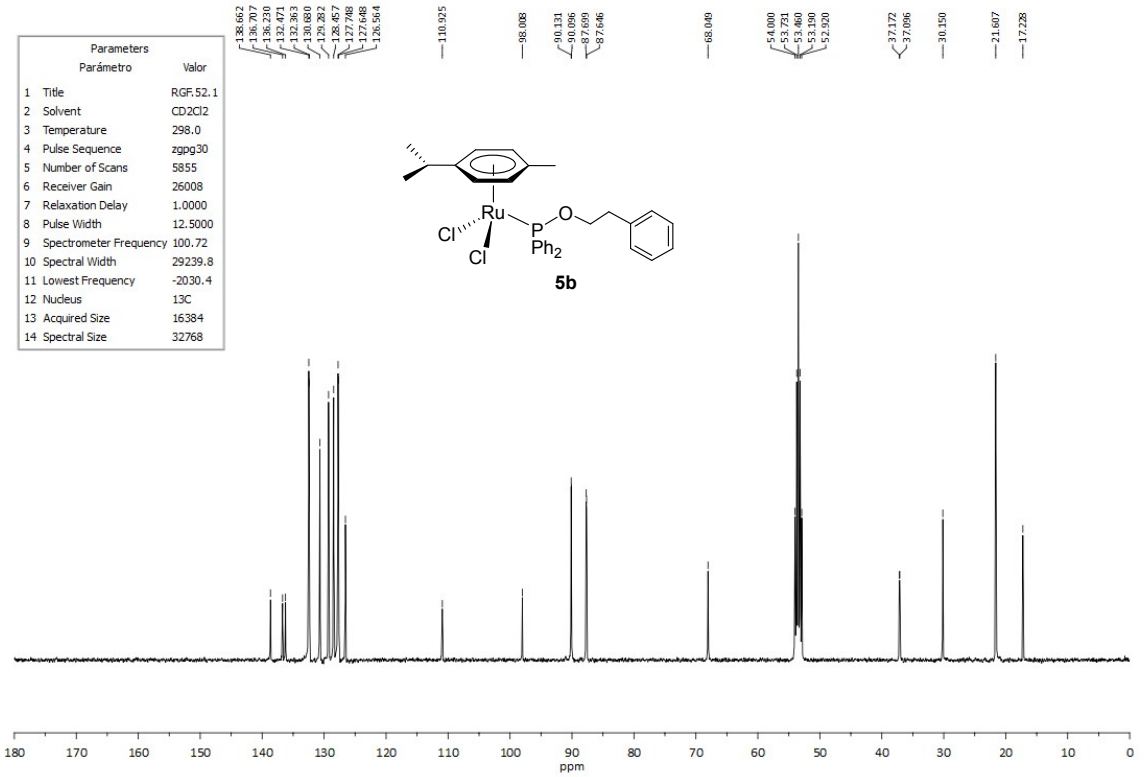

Figure S6: $^{13}C\{^{1}H\}$ NMR spectrum (100 MHz, CD_2Cl_2) of complex **5b**.

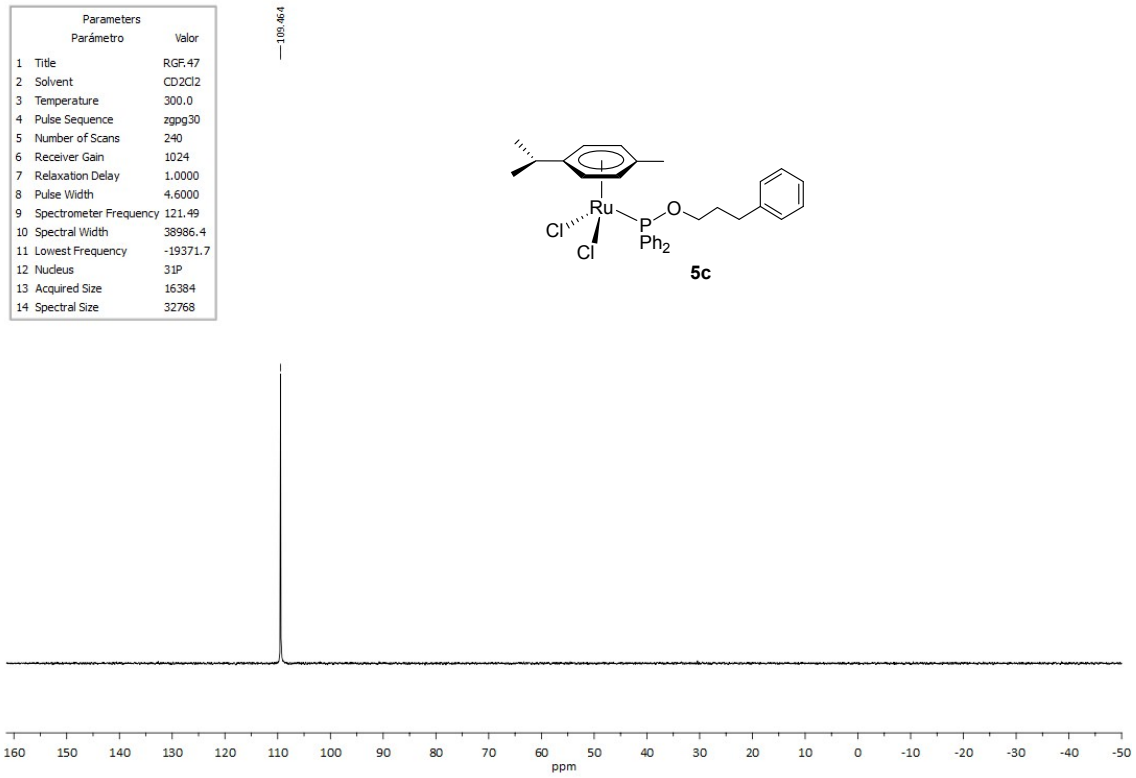

Figure S7: $^{31}P\{^{1}H\}$ NMR spectrum (121 MHz, CD_2Cl_2) of complex **5c**.

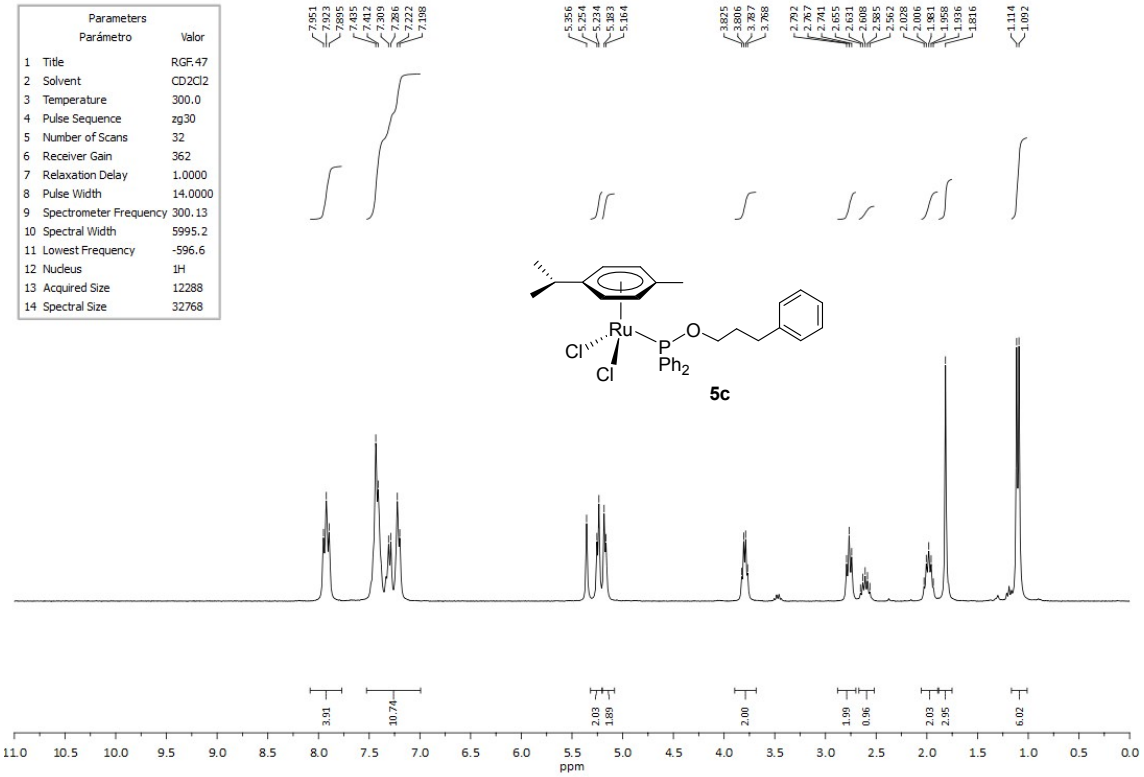

Figure S8: ^{1}H NMR spectrum (300 MHz, CD_2Cl_2) of complex **5c**.

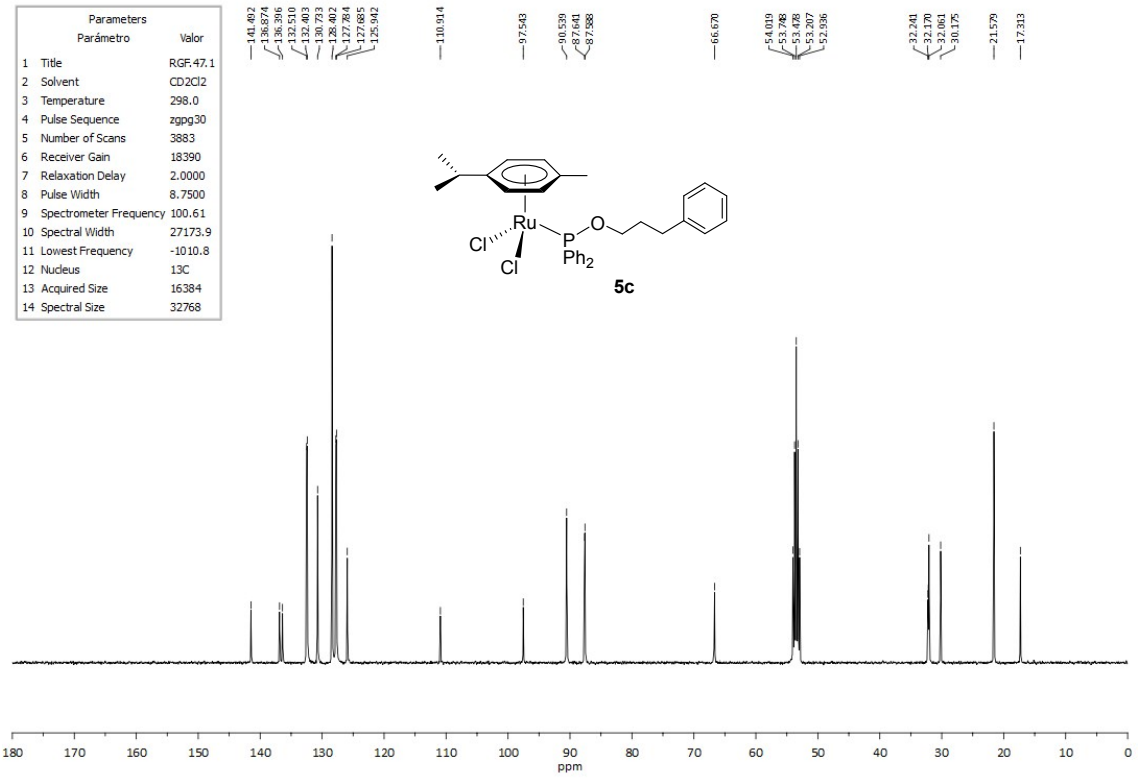

Figure S9: $^{13}C\{^{1}H\}$ NMR spectrum (100 MHz, CD_2Cl_2) of complex **5c**.

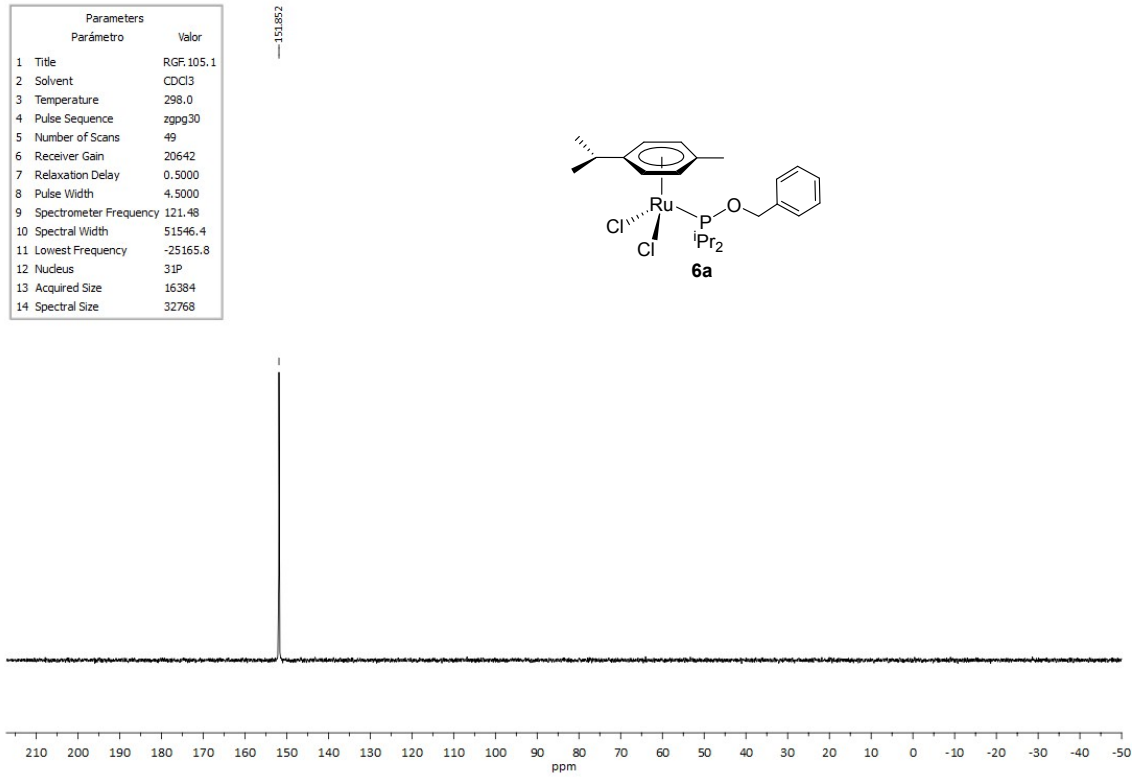

Figure S10: $^{31}P\{^{1}H\}$ NMR spectrum (121 MHz, $CDCl_3$) of complex **6a**.

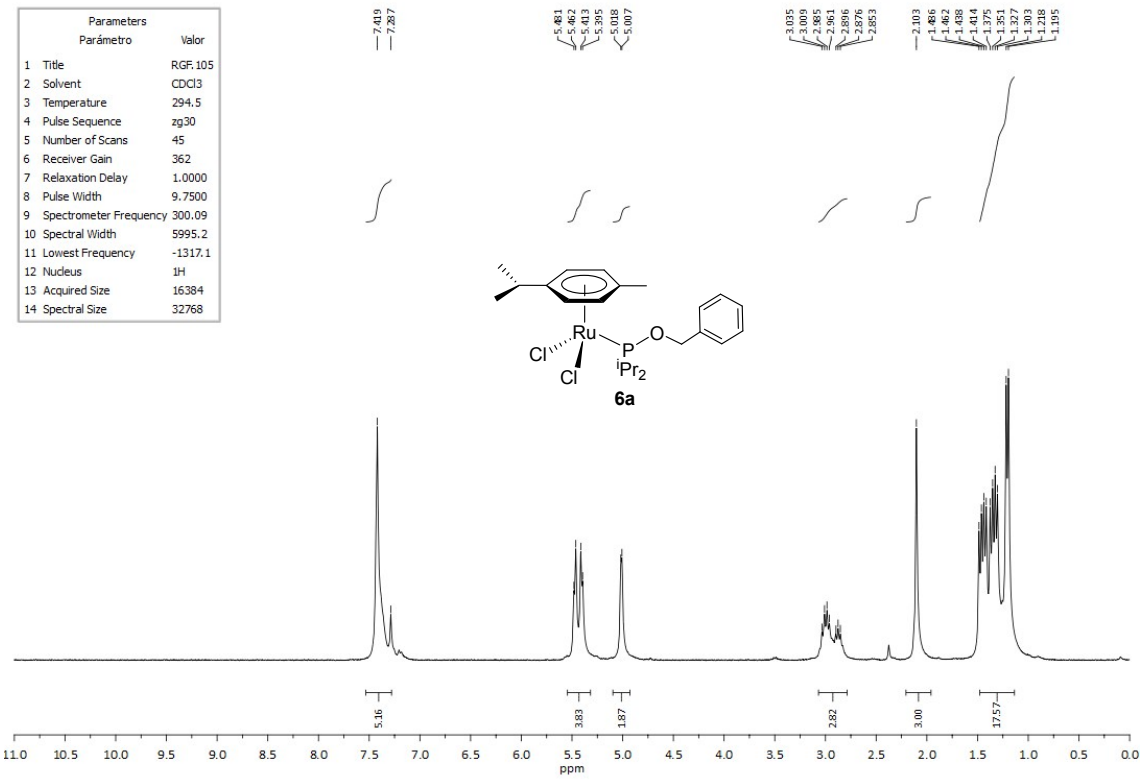

Figure S11: ^{1}H NMR spectrum (300 MHz, $CDCl_3$) of complex **6a**.

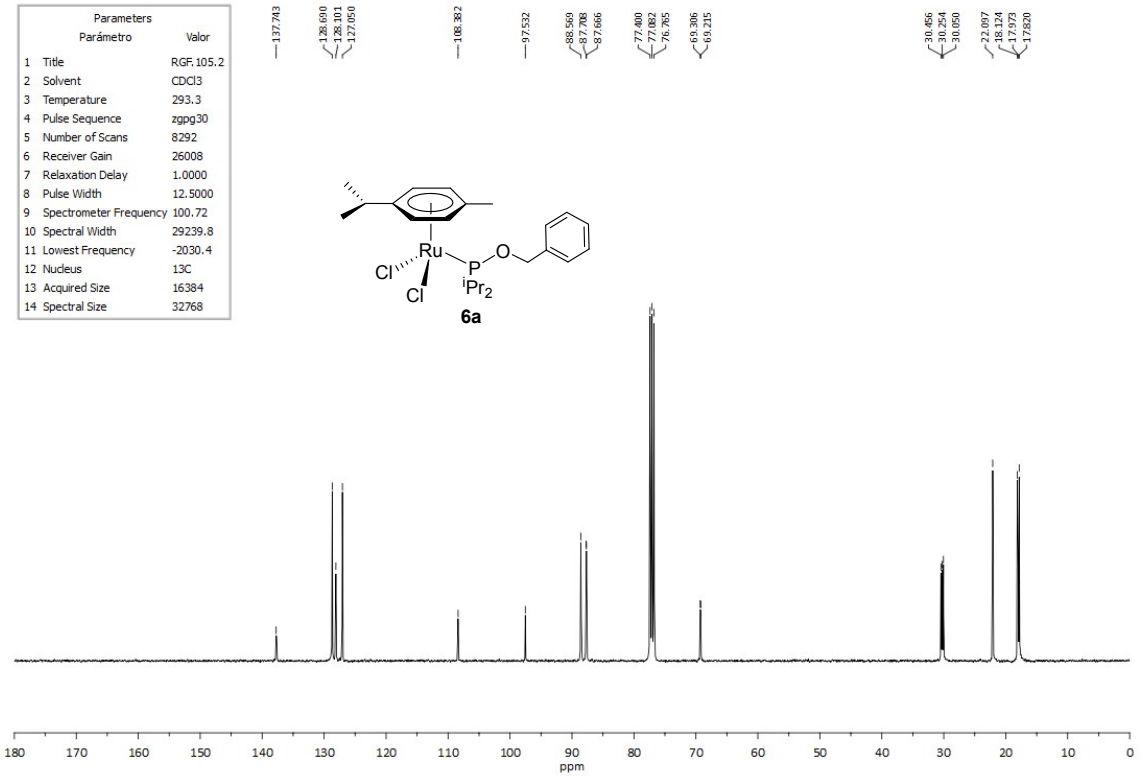

Figure S12: $^{13}C\{^{1}H\}$ NMR spectrum (100 MHz, $CDCl_3$) of complex **6a**.

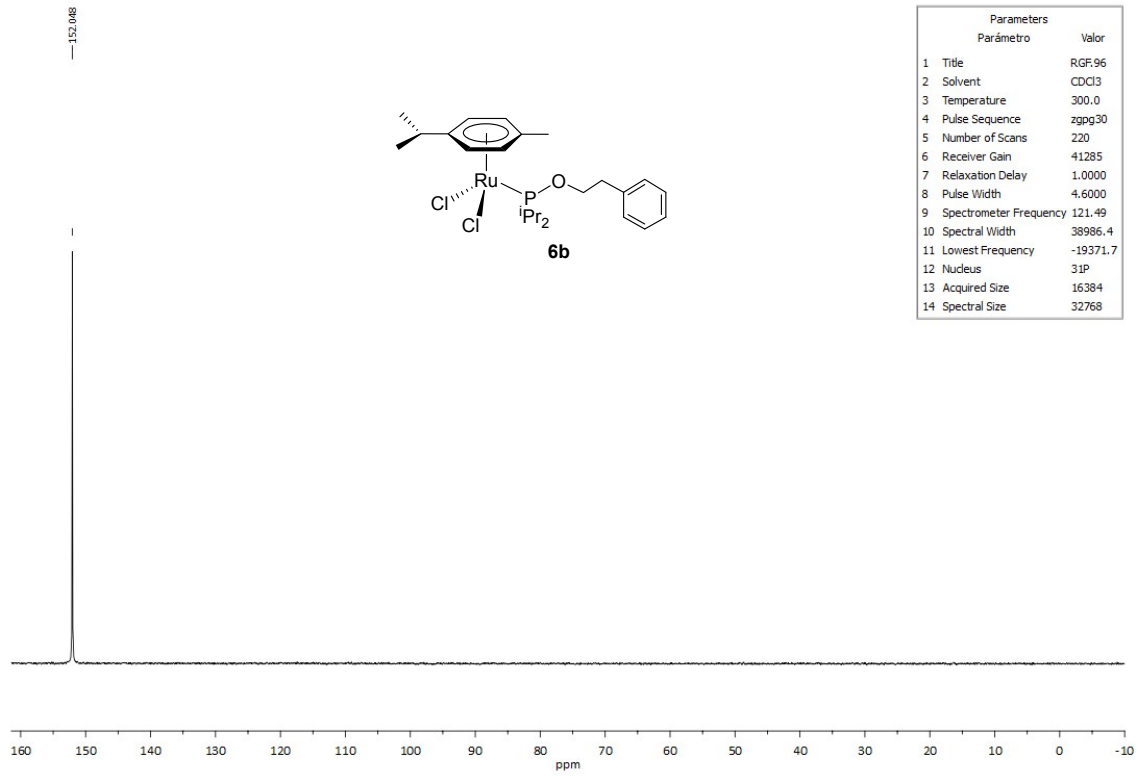

Figure S13: $^{31}P\{^{1}H\}$ NMR spectrum (121 MHz, $CDCl_3$) of complex **6b**.

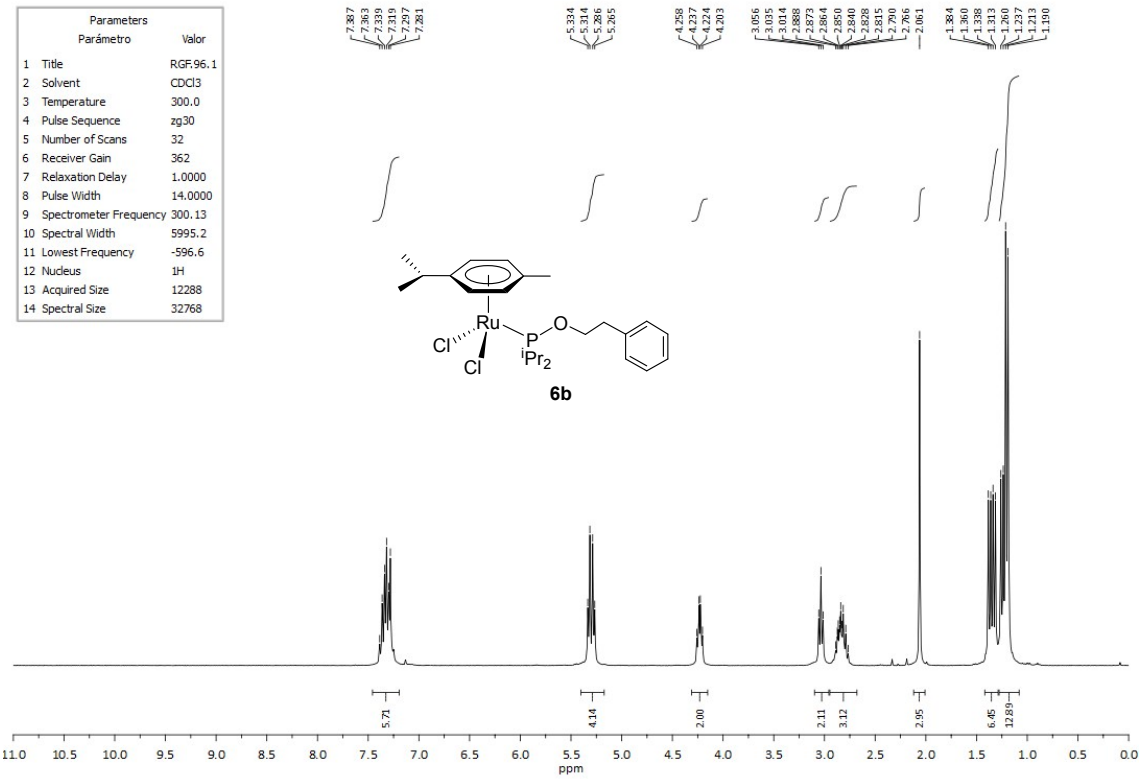

Figure S14: ^{1}H NMR spectrum (300 MHz, $CDCl_3$) of complex **6b**.

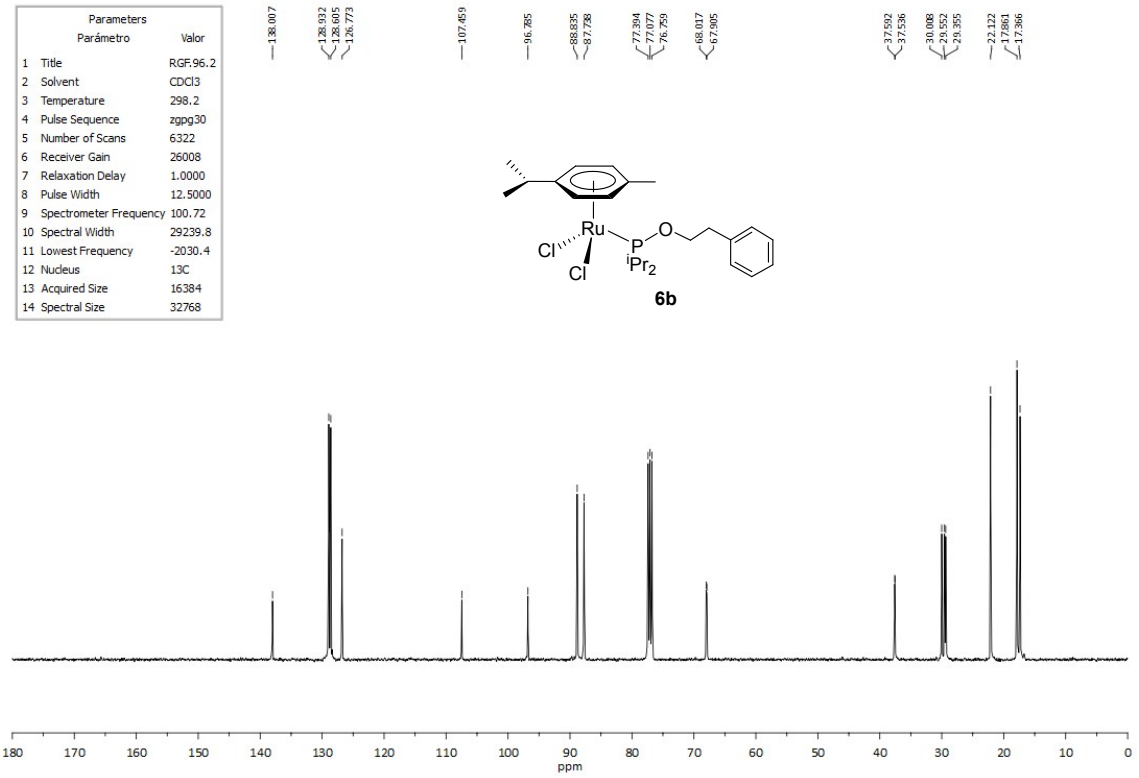

Figure S15: $^{13}C\{^{1}H\}$ NMR spectrum (100 MHz, $CDCl_3$) of complex **6b**.

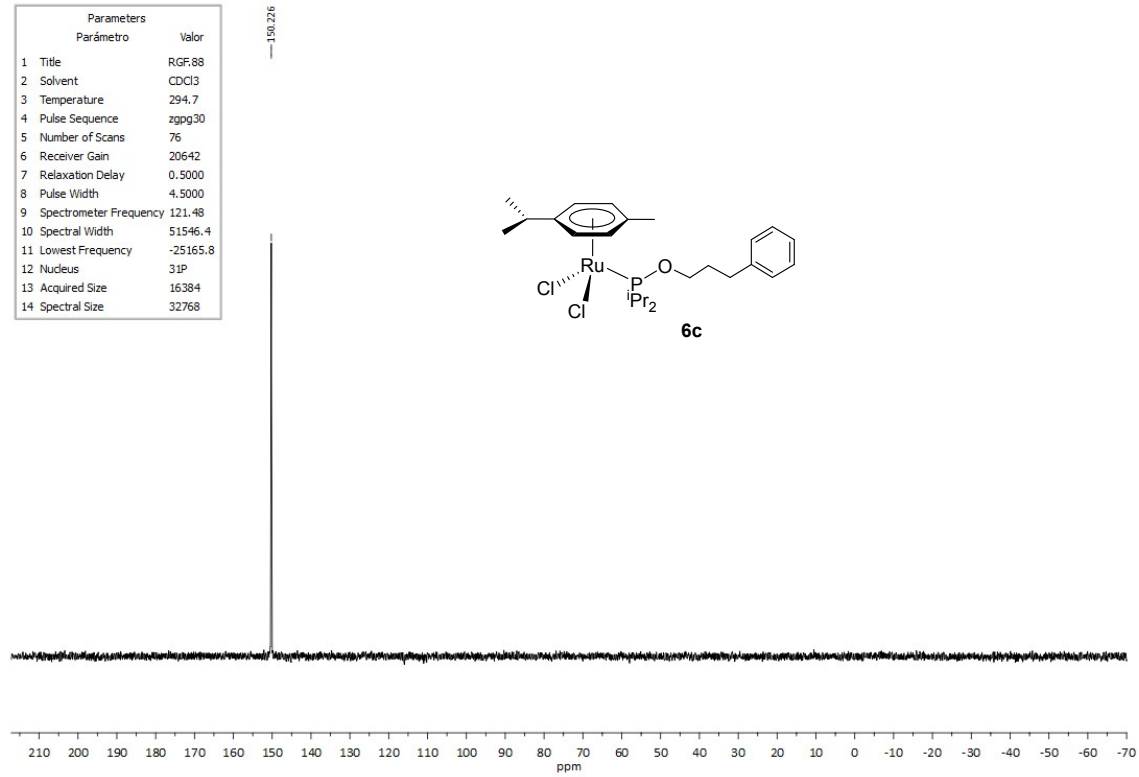

Figure S16: $^{31}P\{^{1}H\}$ NMR spectrum (121 MHz, $CDCl_3$) of complex **6c**.

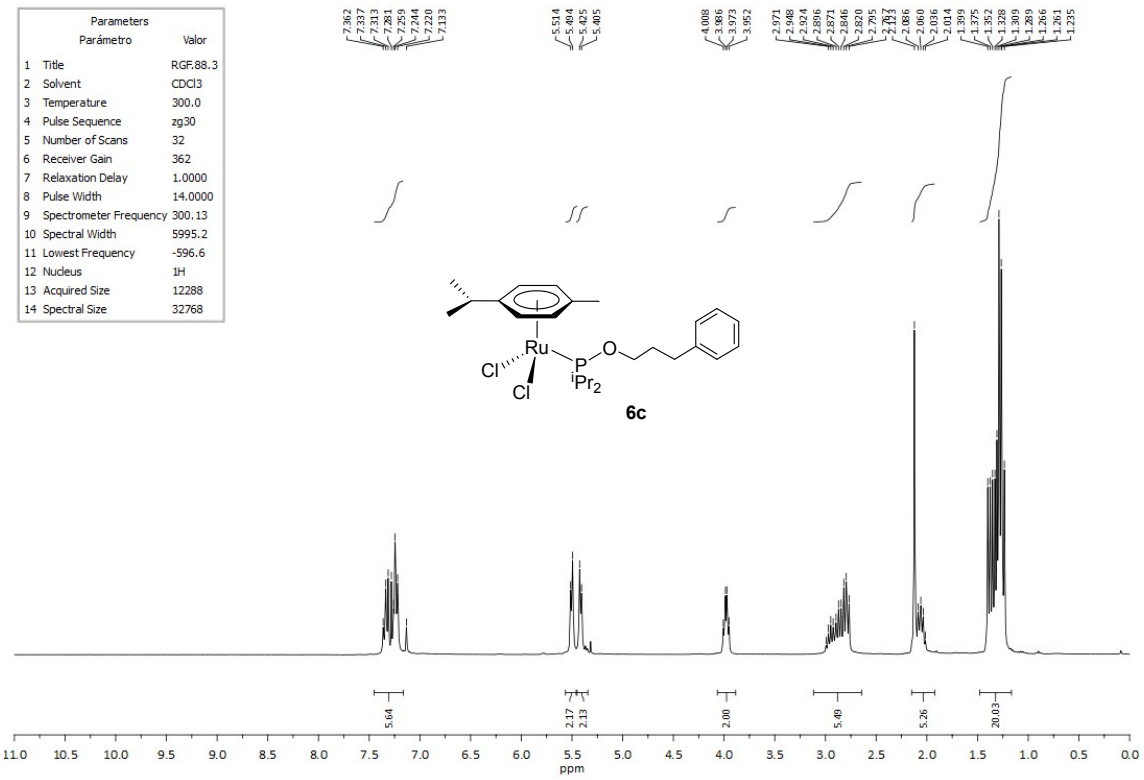

Figure S17: ^{1}H NMR spectrum (300 MHz, $CDCl_3$) of complex **6c**.

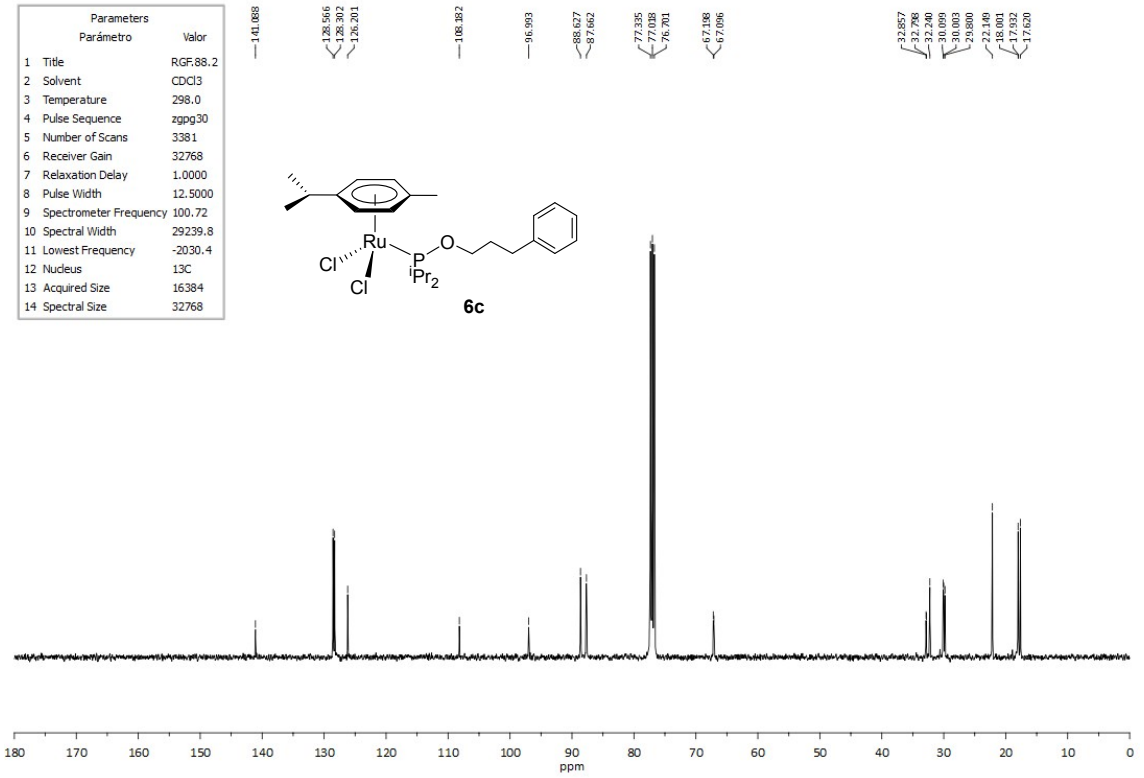

Figure S18: $^{13}C\{^{1}H\}$ NMR spectrum (100 MHz, $CDCl_3$) of complex **6c**.

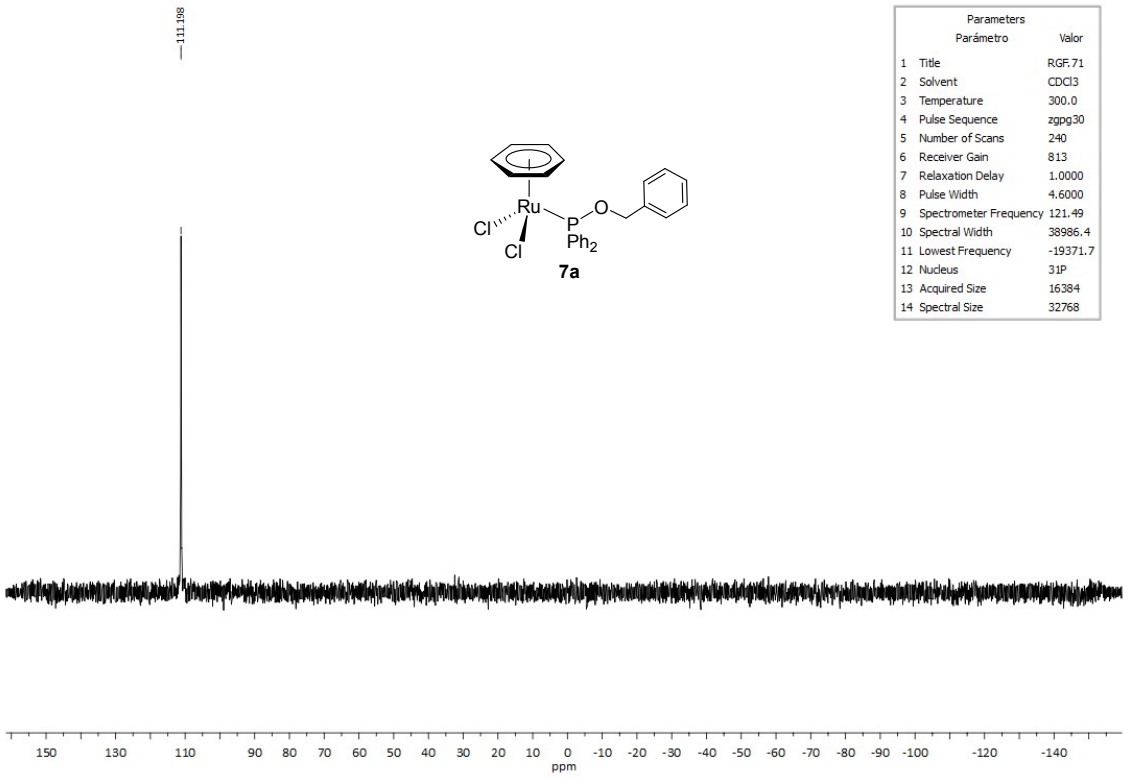

Figure S19: $^{31}P\{^{1}H\}$ NMR spectrum (121 MHz, $CDCl_3$) of complex **7a**.

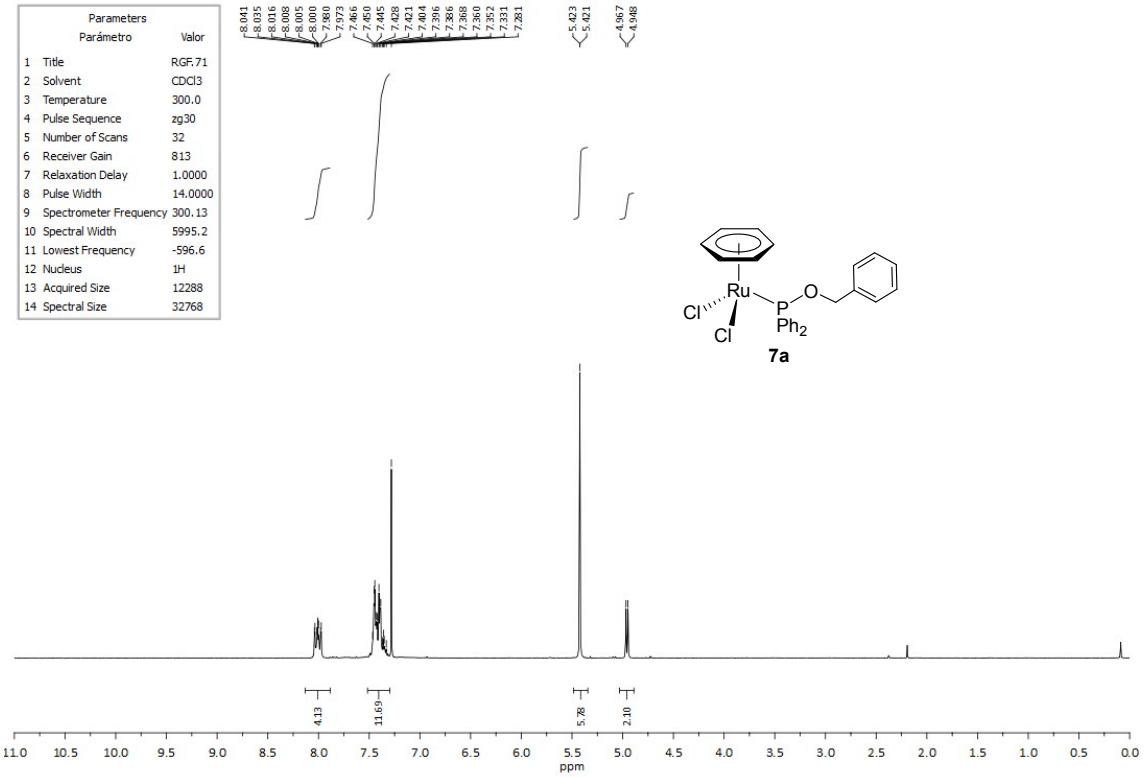

Figure S20: ^{1}H NMR spectrum (300 MHz, $CDCl_3$) of complex **7a**.

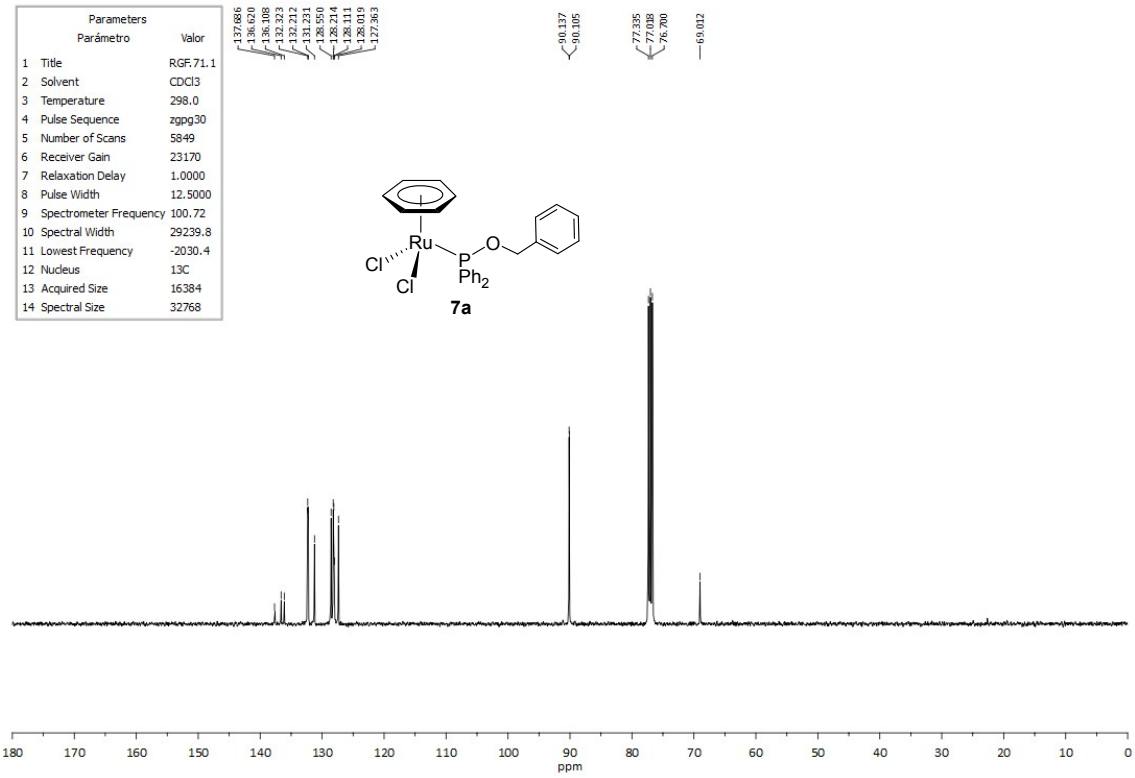

Figure S21: $^{13}C\{^{1}H\}$ NMR spectrum (100 MHz, $CDCl_3$) of complex **7a**.

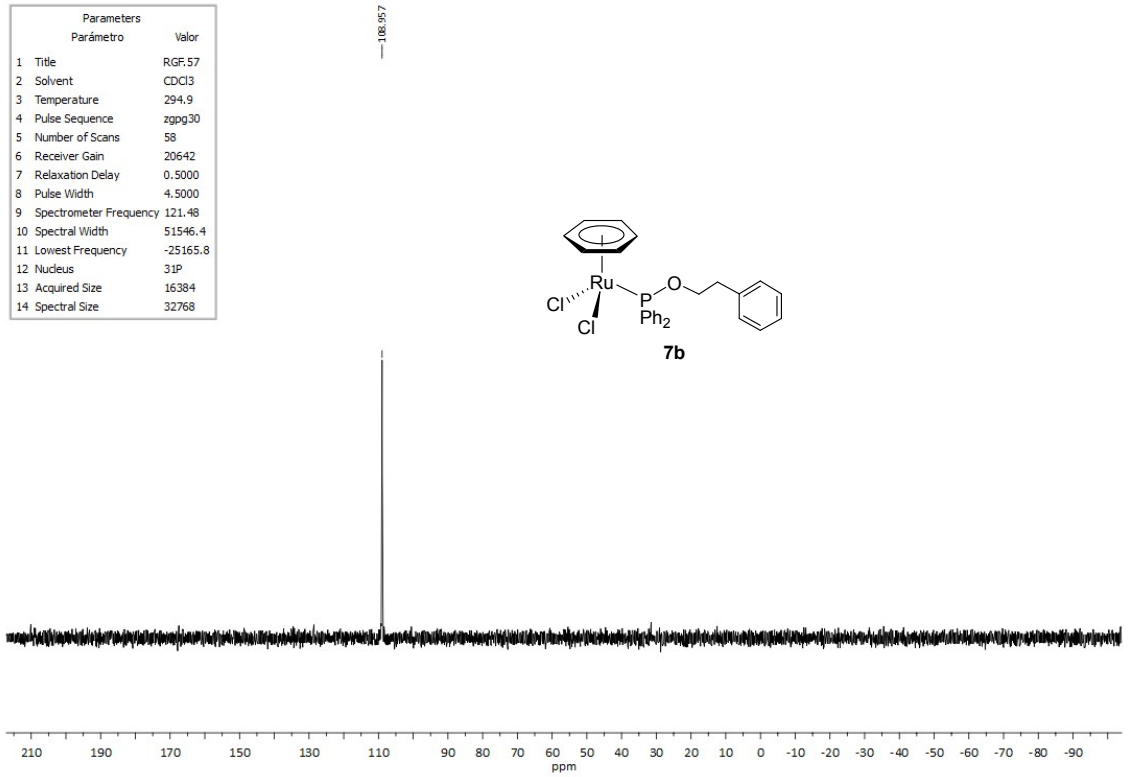

Figure S22: $^{31}P\{^{1}H\}$ NMR spectrum (121 MHz, CD_2Cl_2) of complex **7b**.

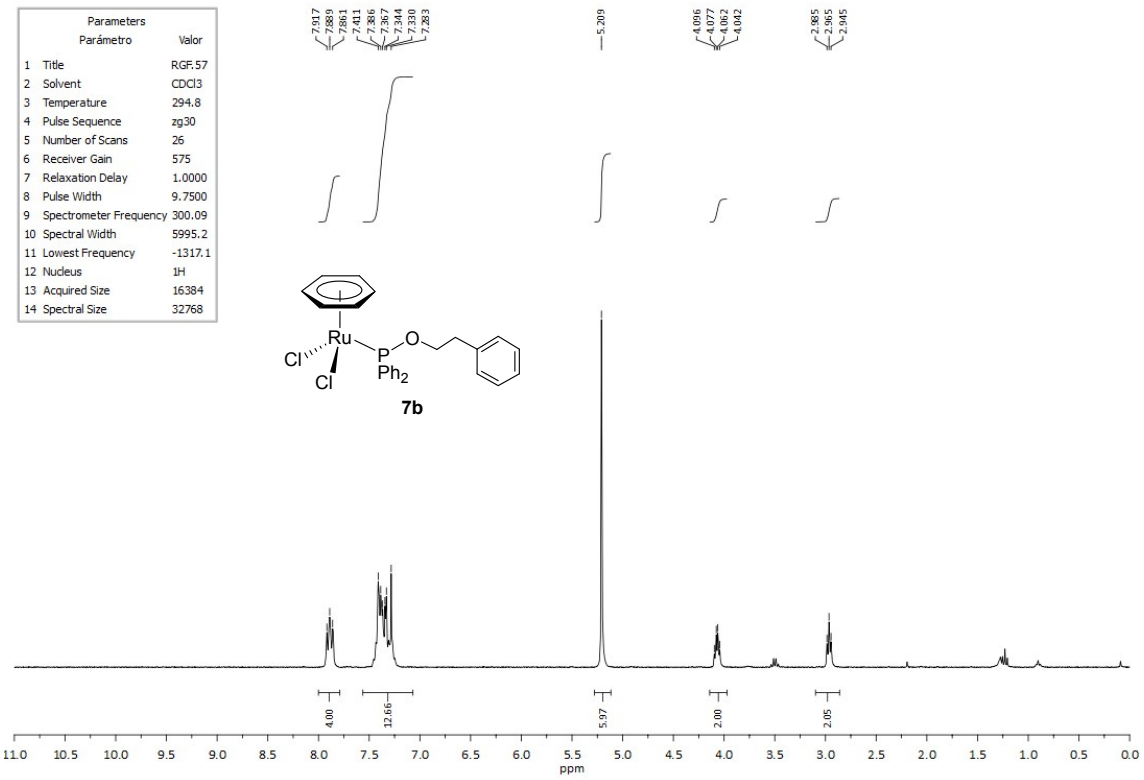

Figure S23: ^{1}H NMR spectrum (300 MHz, CD_2Cl_2) of complex **7b**.

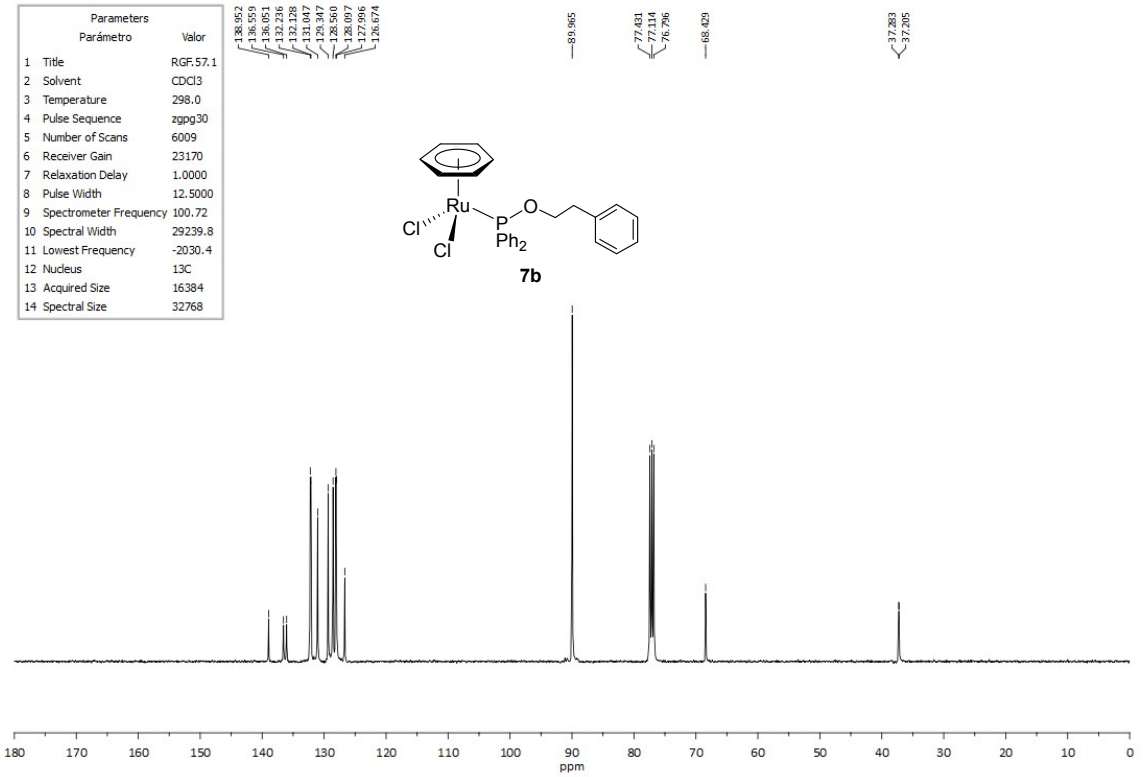

Figure S24: $^{13}C\{^{1}H\}$ NMR spectrum (100 MHz, CD_2Cl_2) of complex **7b**.

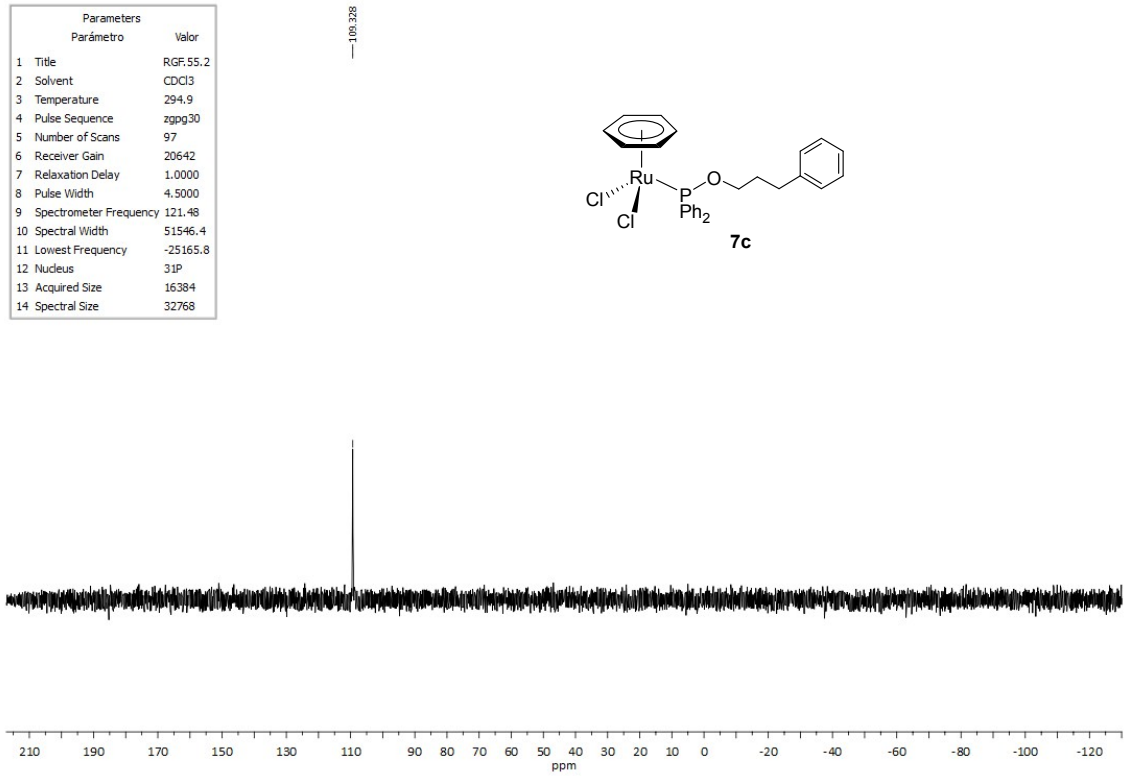

Figure S25: $^{31}P\{^{1}H\}$ NMR spectrum (121 MHz, CD_2Cl_2) of complex **7c**.

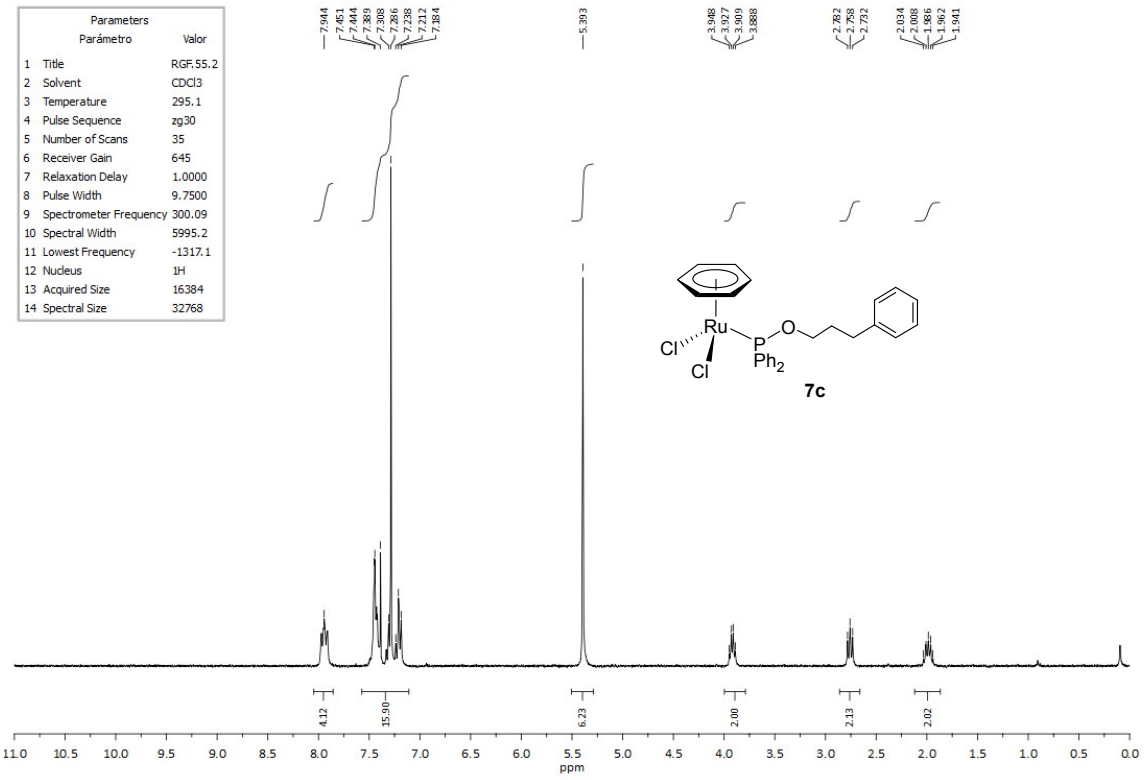

Figure S26: ^{1}H NMR spectrum (300 MHz, CD_2Cl_2) of complex **7c**.

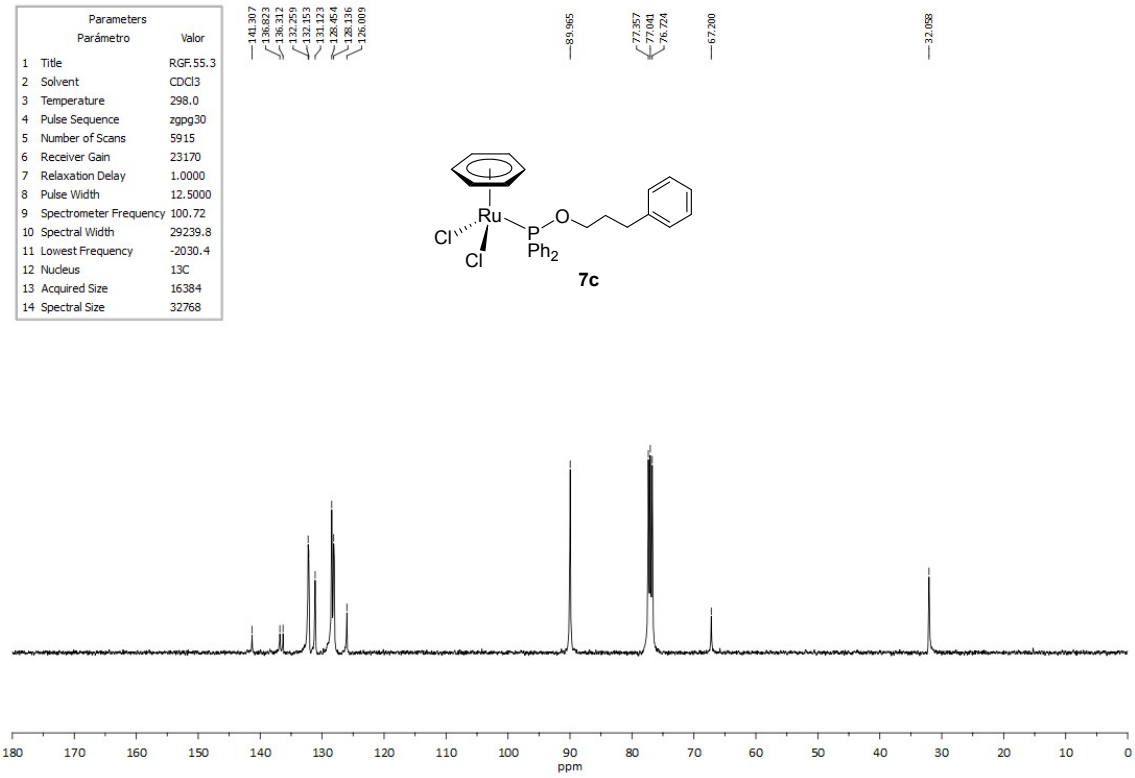

Figure S27: $^{13}C\{^{1}H\}$ NMR spectrum (100 MHz, CD_2Cl_2) of complex **7c**.

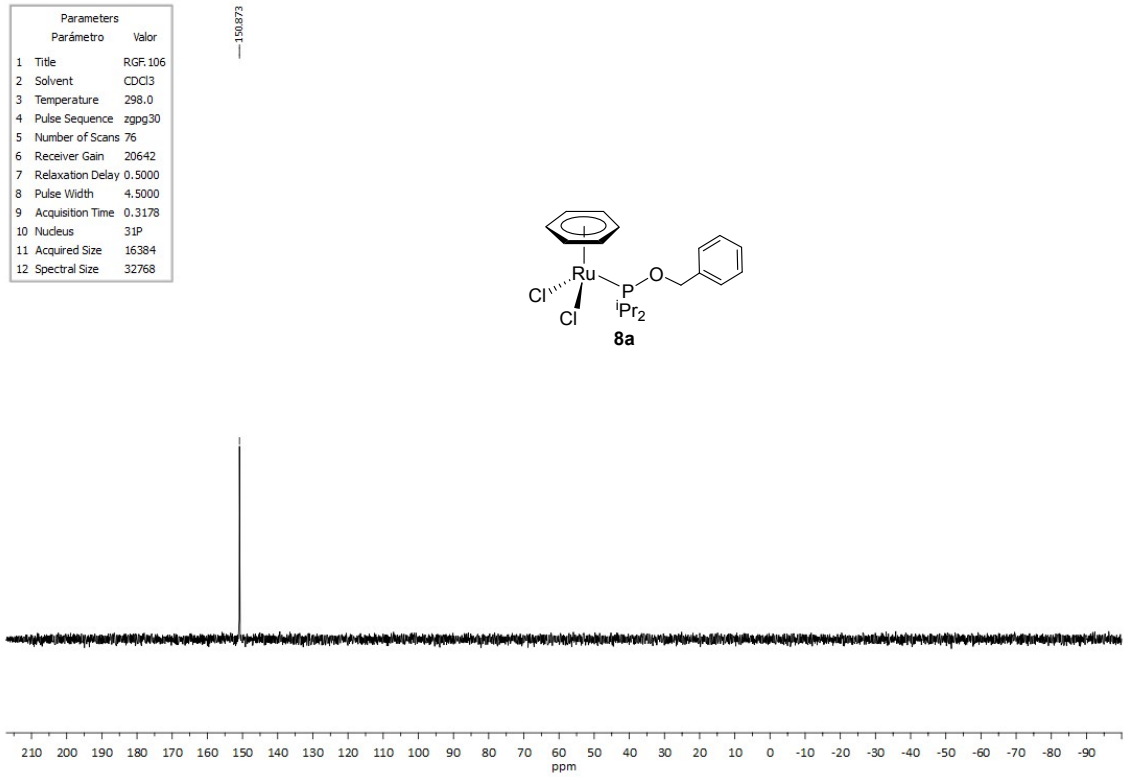

Figure S28: $^{31}P\{^{1}H\}$ NMR spectrum (121 MHz, $CDCl_3$) of complex **8a**.

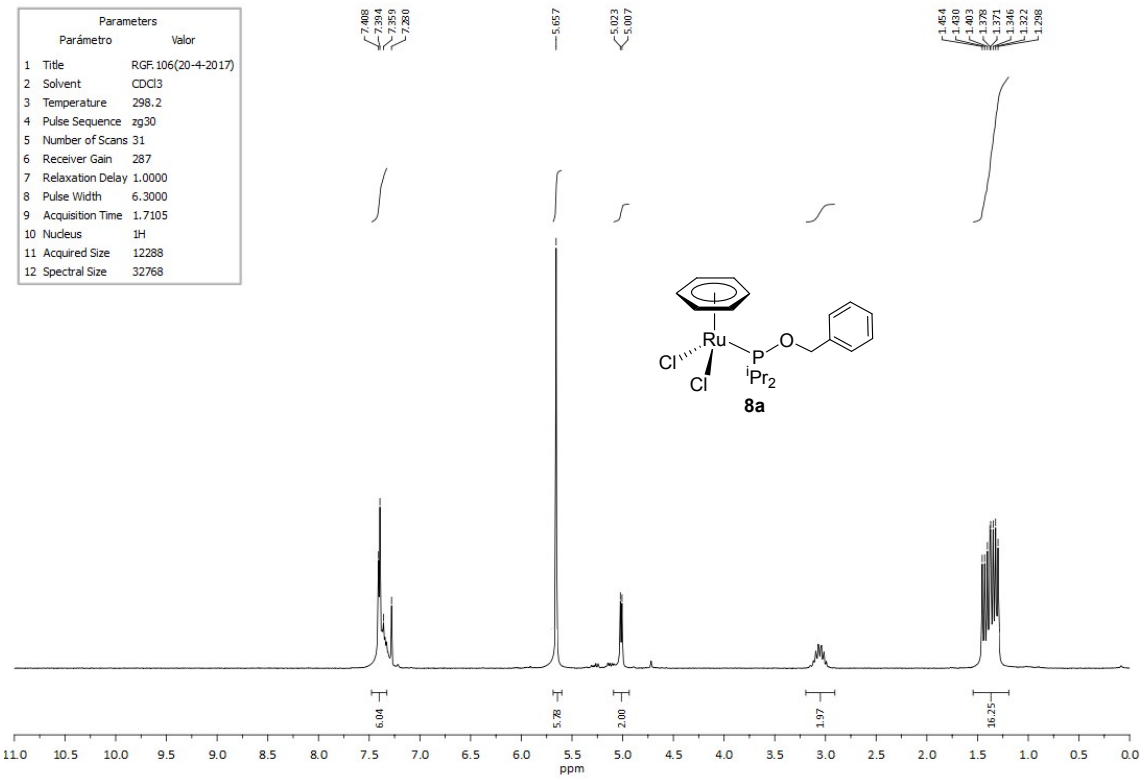

Figure S29: ^{1}H NMR spectrum (300 MHz, $CDCl_3$) of complex **8a**.

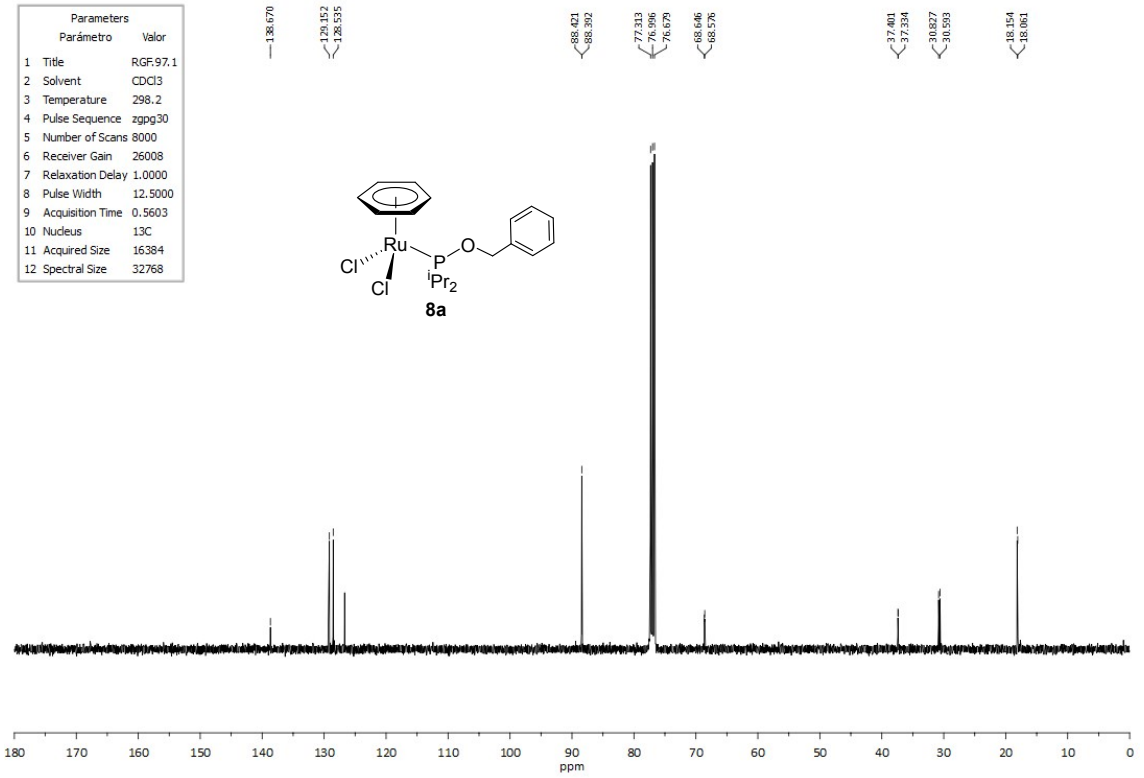

Figure S30: $^{13}C\{^{1}H\}$ NMR spectrum (100 MHz, $CDCl_3$) of complex **8a**.

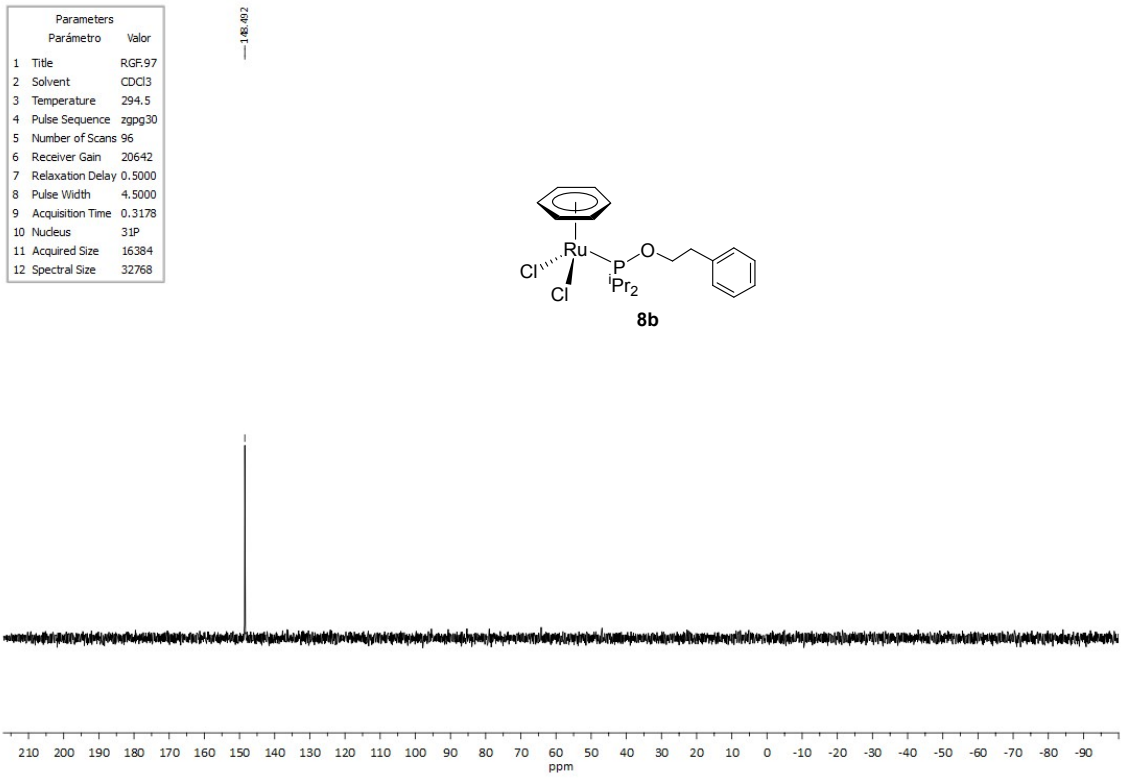

Figure S31: $^{31}P\{^{1}H\}$ NMR spectrum (121 MHz, $CDCl_3$) of complex **8b**.

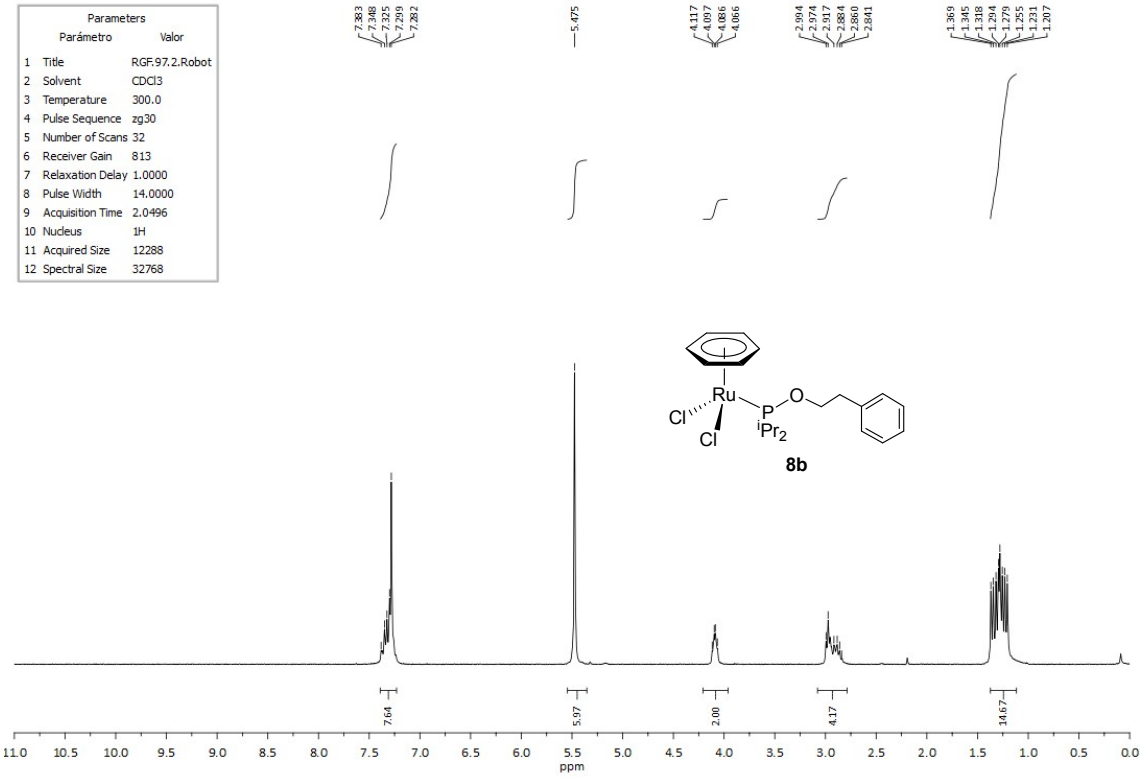

Figure S32: ^{1}H NMR spectrum (300 MHz, $CDCl_3$) of complex **8b**.

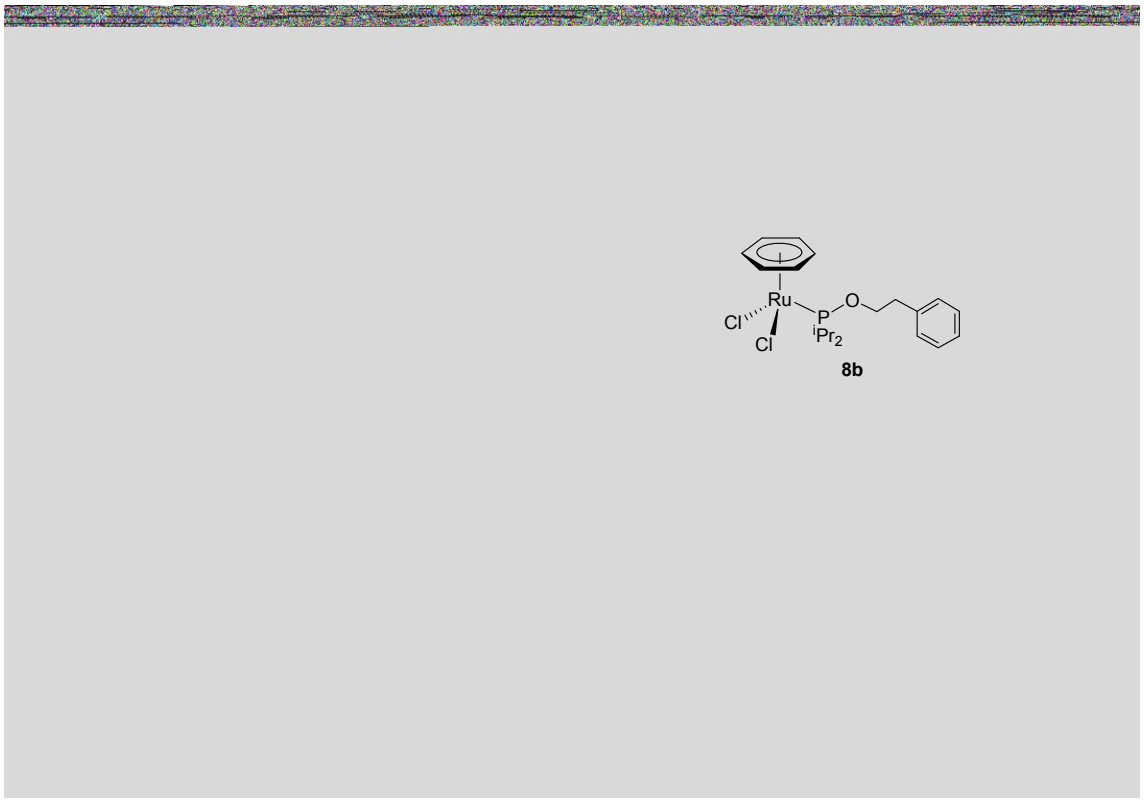

Figure S33: $^{13}C\{^{1}H\}$ NMR spectrum (100 MHz, $CDCl_3$) of complex **8b**.

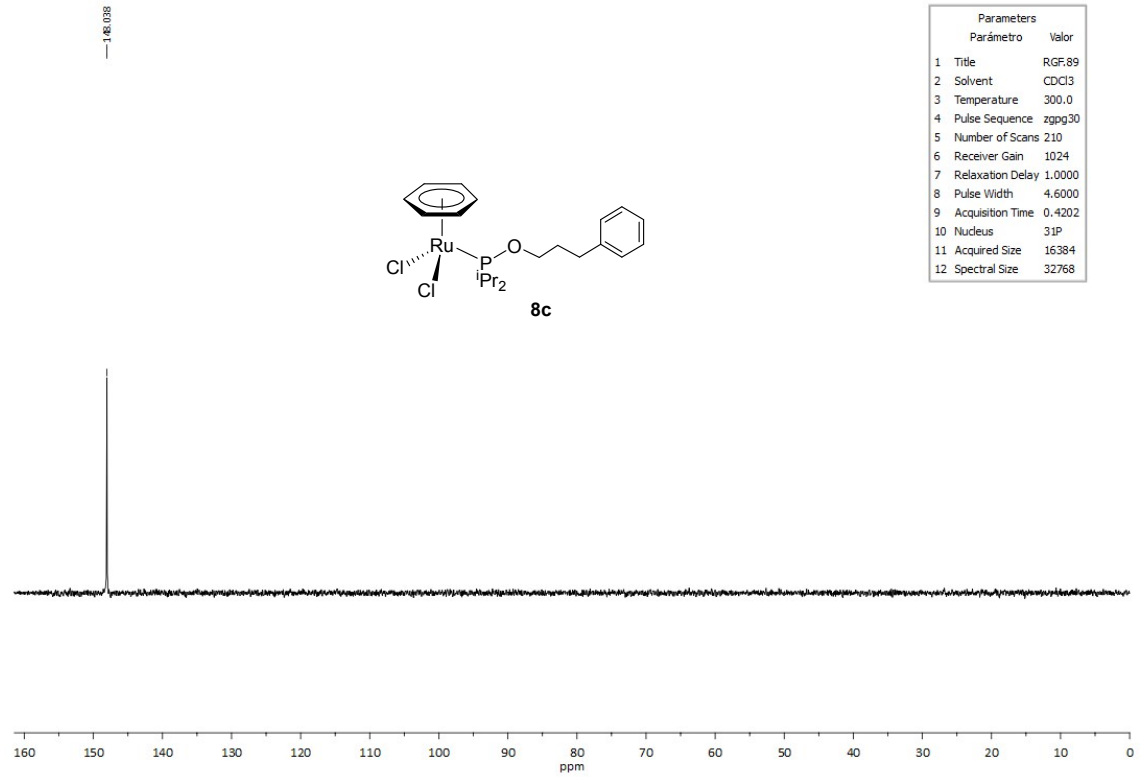

Figure S34: $^{31}P\{^{1}H\}$ NMR spectrum (121 MHz, $CDCl_3$) of complex **8c**.

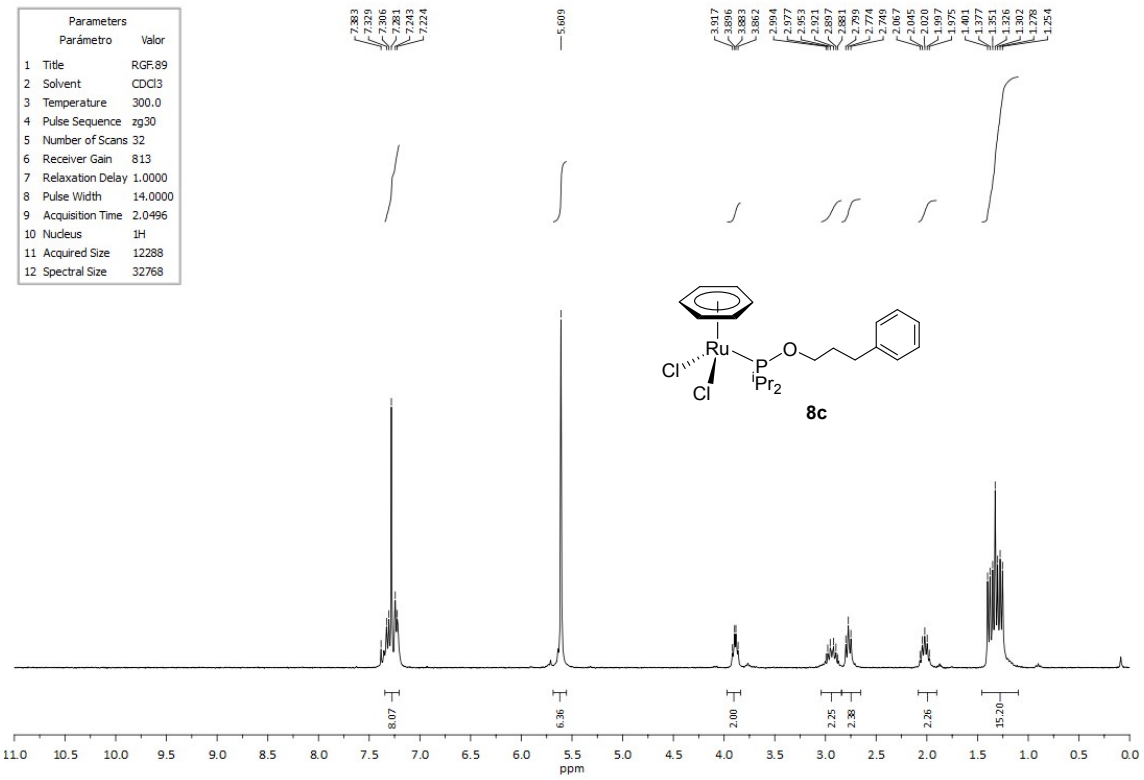

Figure S35: ^{1}H NMR spectrum (300 MHz, $CDCl_3$) of complex **8c**.

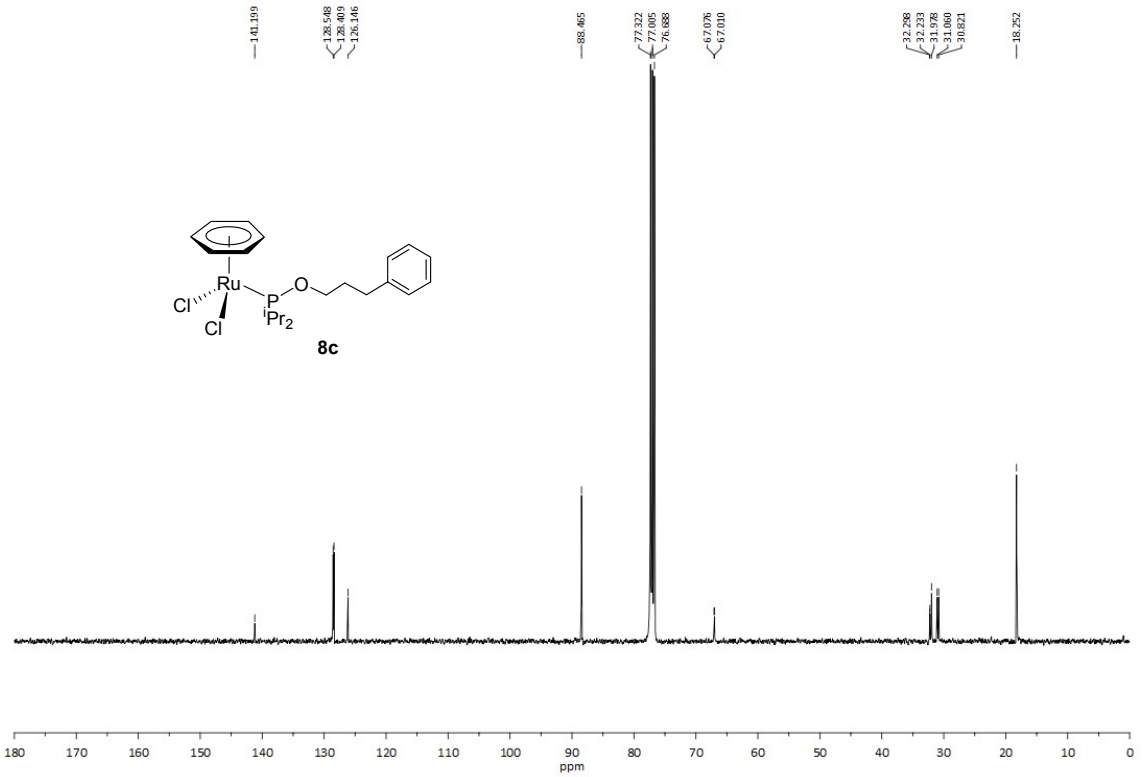

Figure S36: $^{13}C\{^{1}H\}$ NMR spectrum (100 MHz, $CDCl_3$) of complex **8c**.

NMR spectra of the tethered complexes 9-10a-c

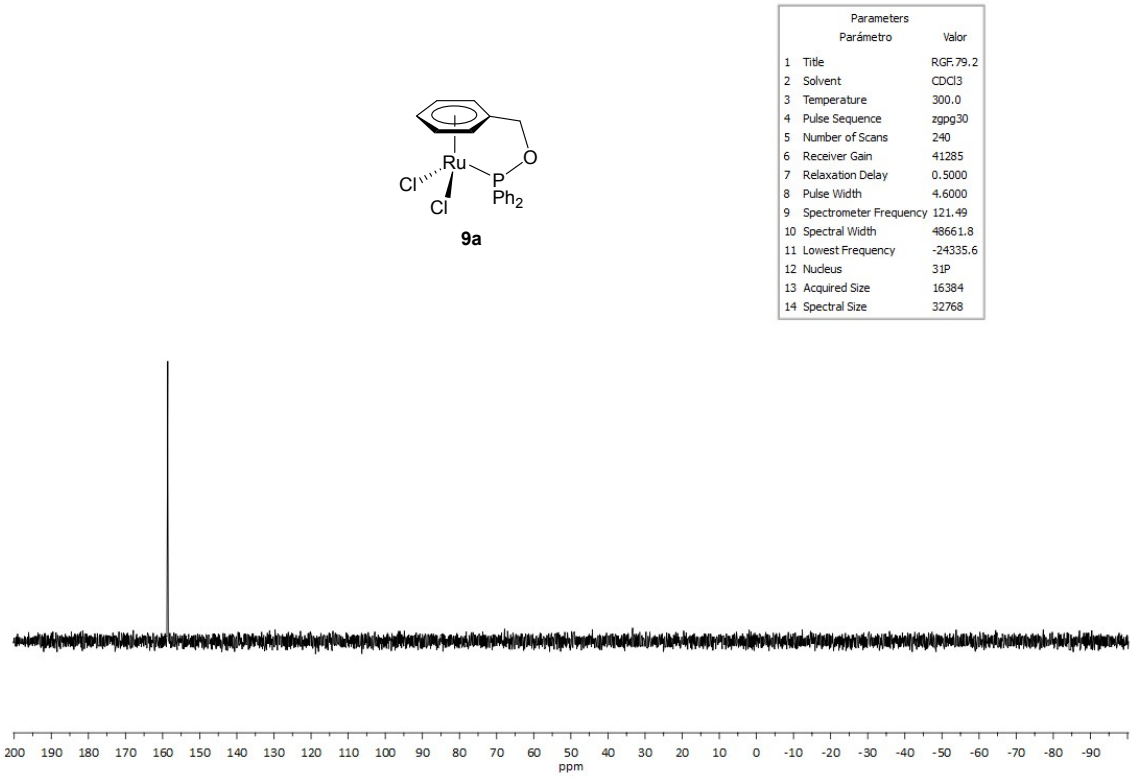

Figure S37: $^{31}P\{^{1}H\}$ NMR spectrum (121 MHz, $CDCl_3$) of complex **9a**.

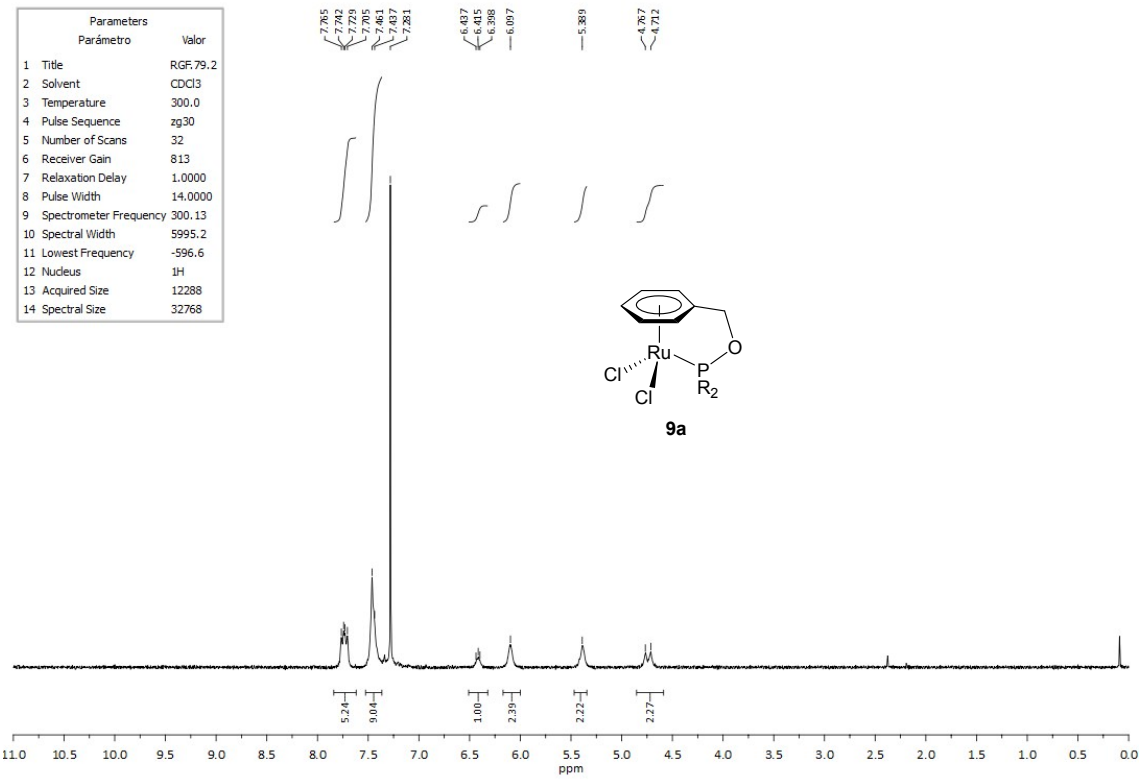

Figure S38: ^{1}H NMR spectrum (300 MHz, $CDCl_3$) of complex **9a**.

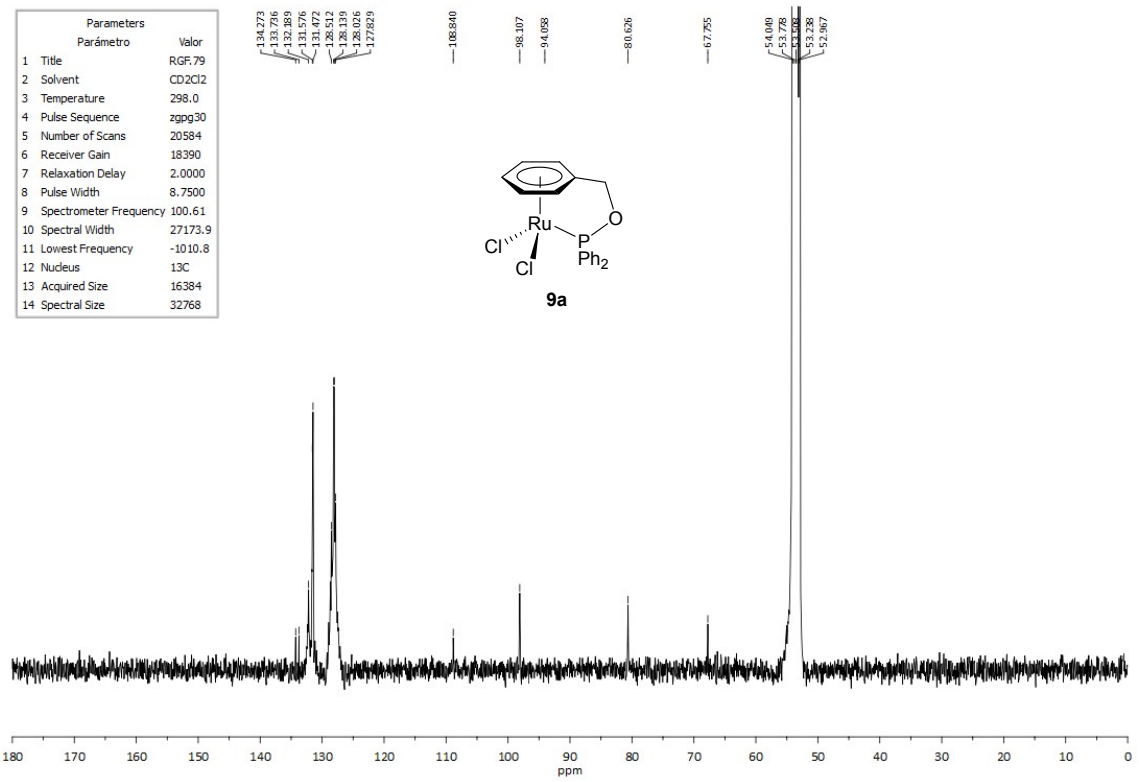

Figure S39: $^{13}C\{^{1}H\}$ NMR spectrum (100 MHz, CD_2Cl_2) of complex **9a**.

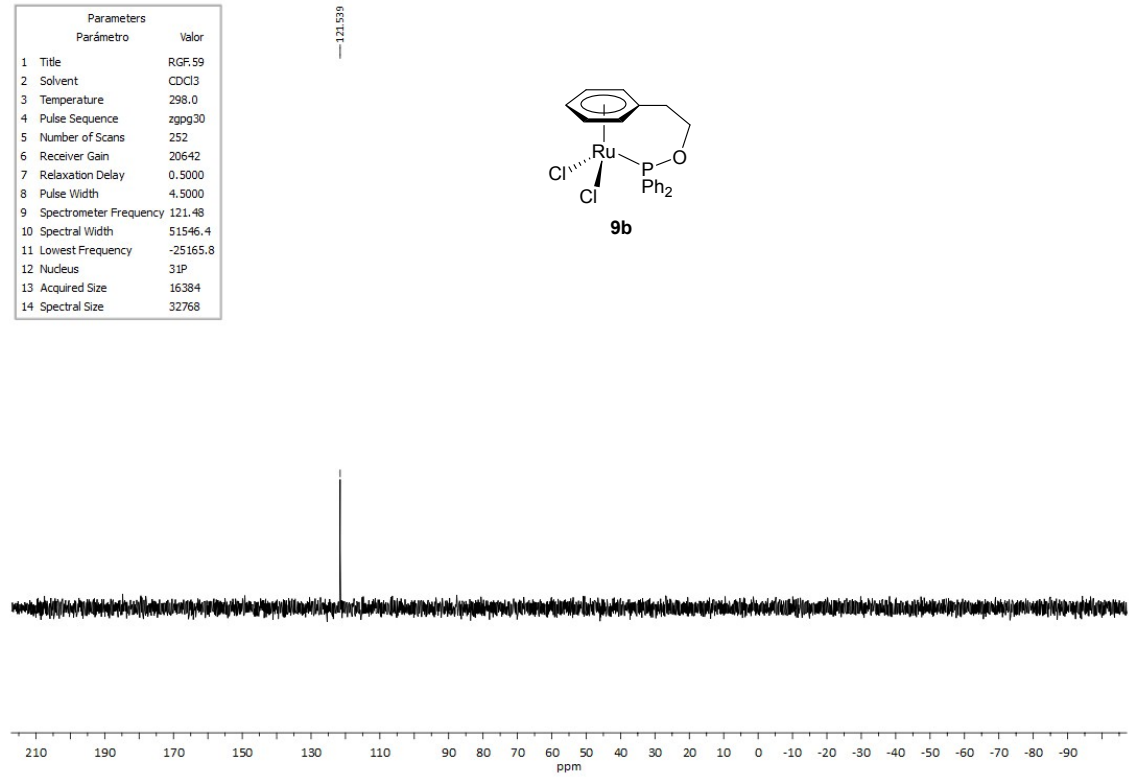

Figure S40: $^{31}P\{^{1}H\}$ NMR spectrum (121 MHz, $CDCl_3$) of complex **9b**.

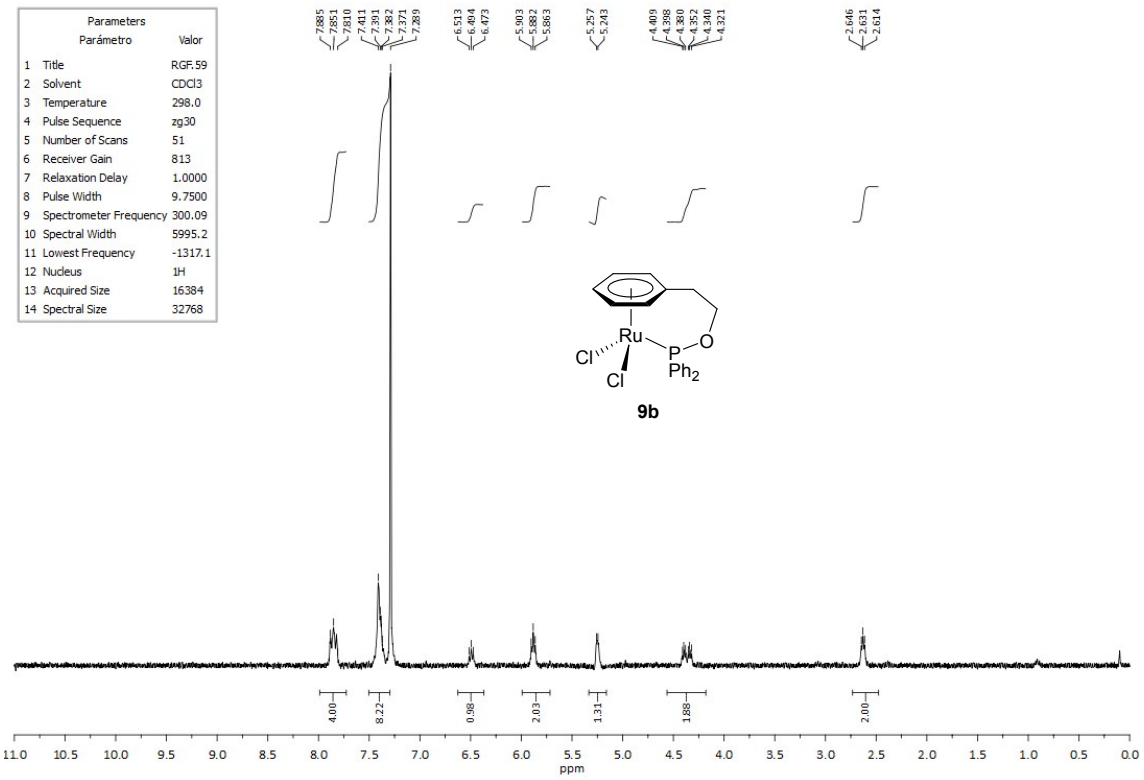

Figure S41: ^{1}H NMR spectrum (300 MHz, $CDCl_3$) of complex **9b**.

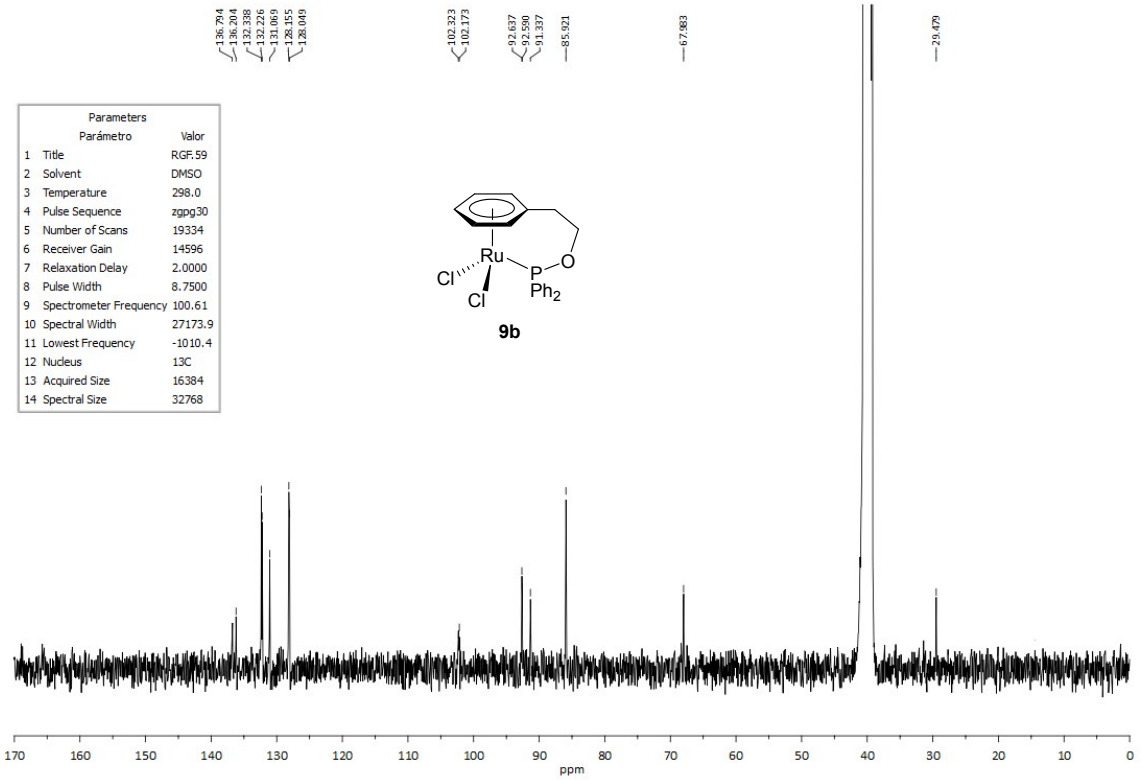

Figure S42: $^{13}C\{^{1}H\}$ NMR spectrum (100 MHz, DMSO-d_6) of complex **9b**.

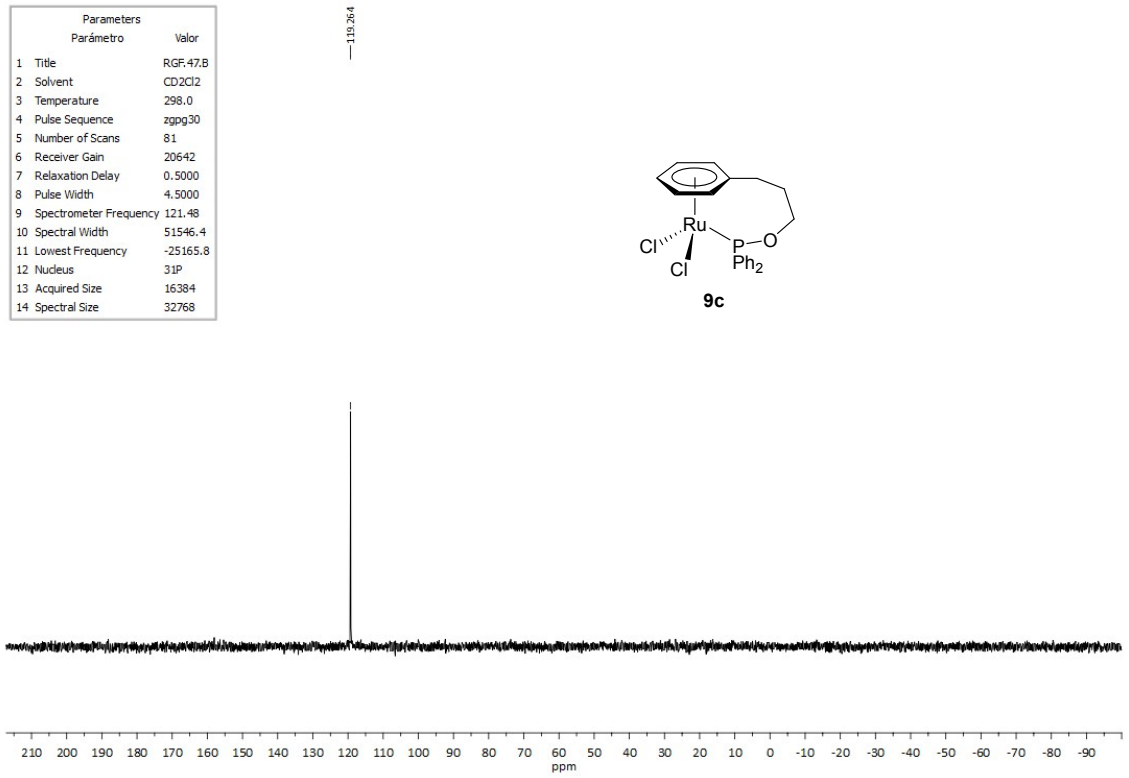

Figure S43: $^{31}P\{^{1}H\}$ NMR spectrum (121 MHz, CD_2Cl_2) of complex **9c**.

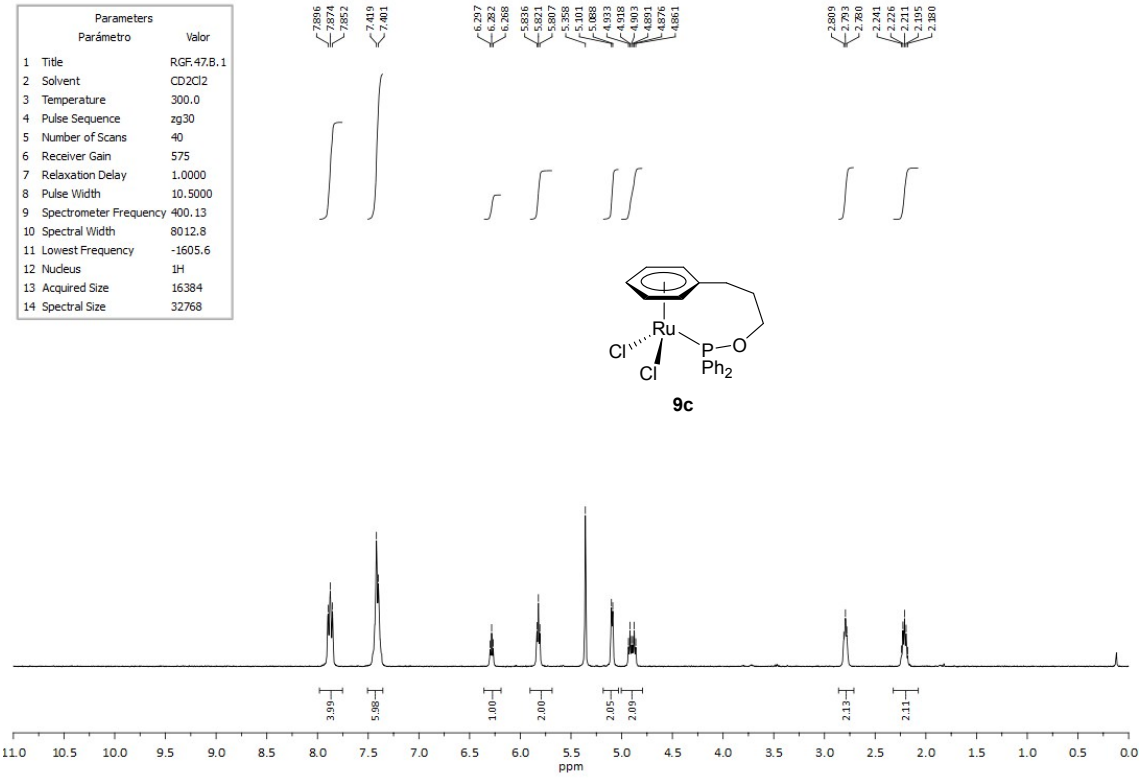

Figure S44: ^{1}H NMR spectrum (300 MHz, CD_2Cl_2) of complex **9c**.

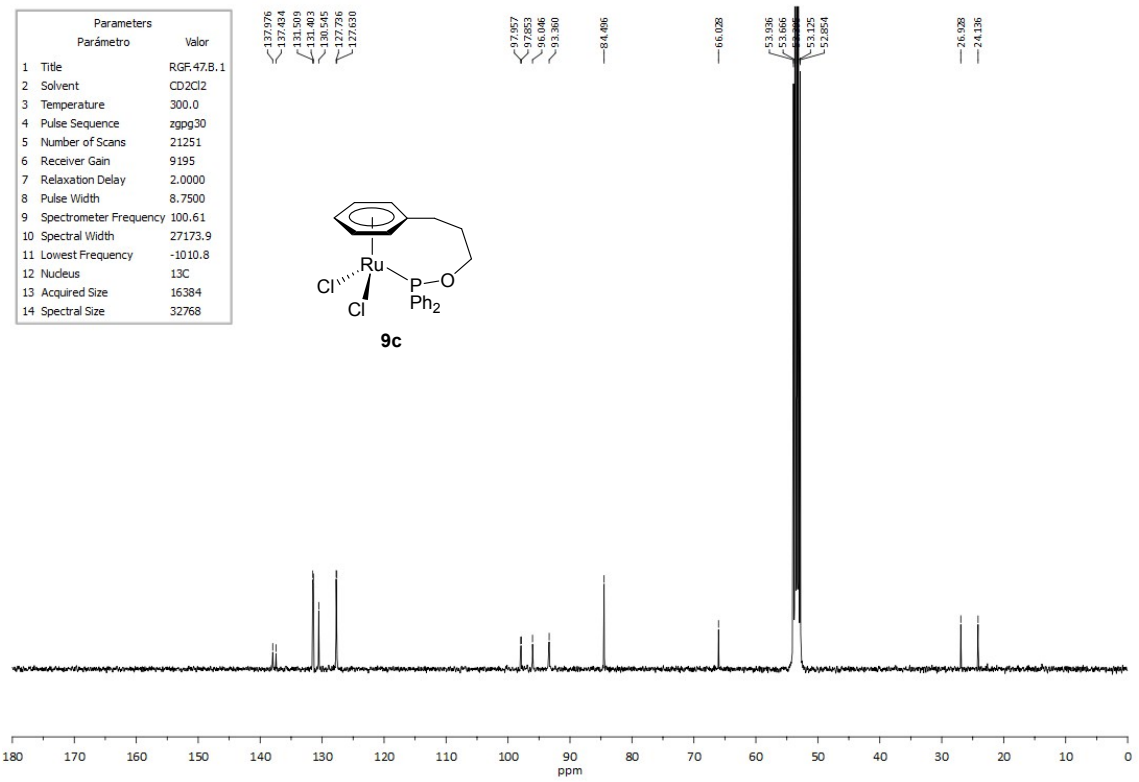

Figure S45: $^{13}C\{^{1}H\}$ NMR spectrum (100 MHz, CD_2Cl_2) of complex **9c**.

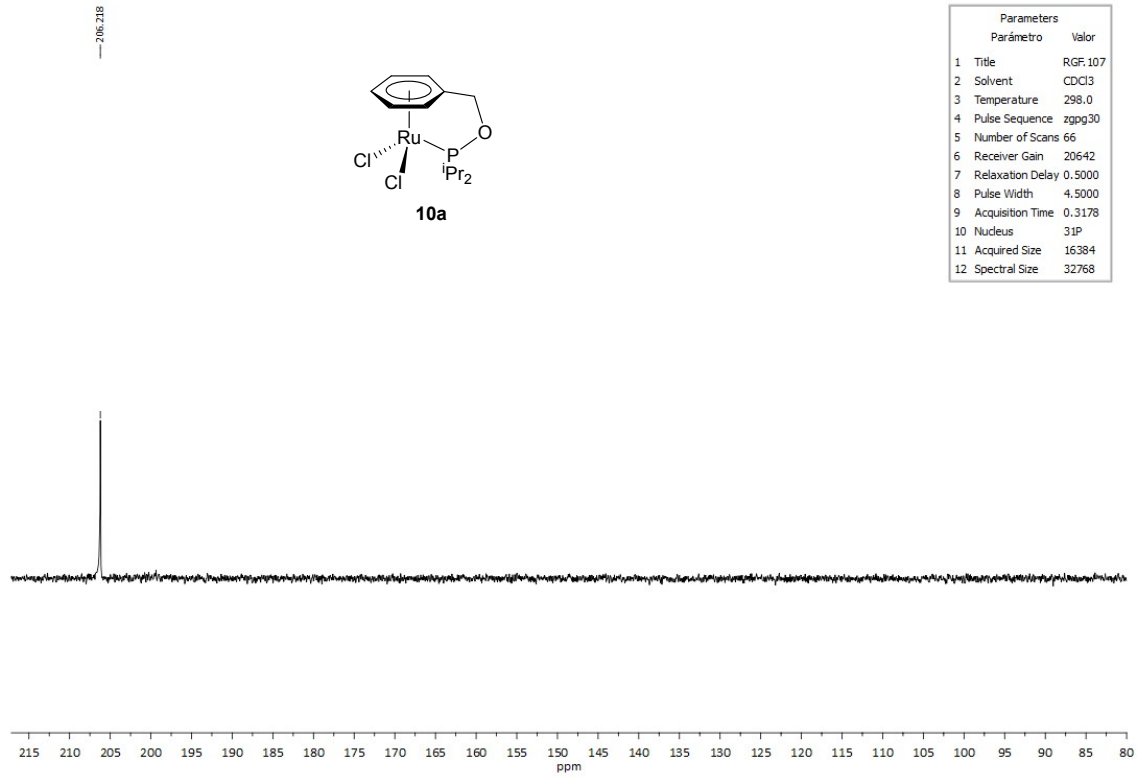

Figure S46: $^{31}P\{^{1}H\}$ NMR spectrum (121 MHz, $CDCl_3$) of complex **10a**.

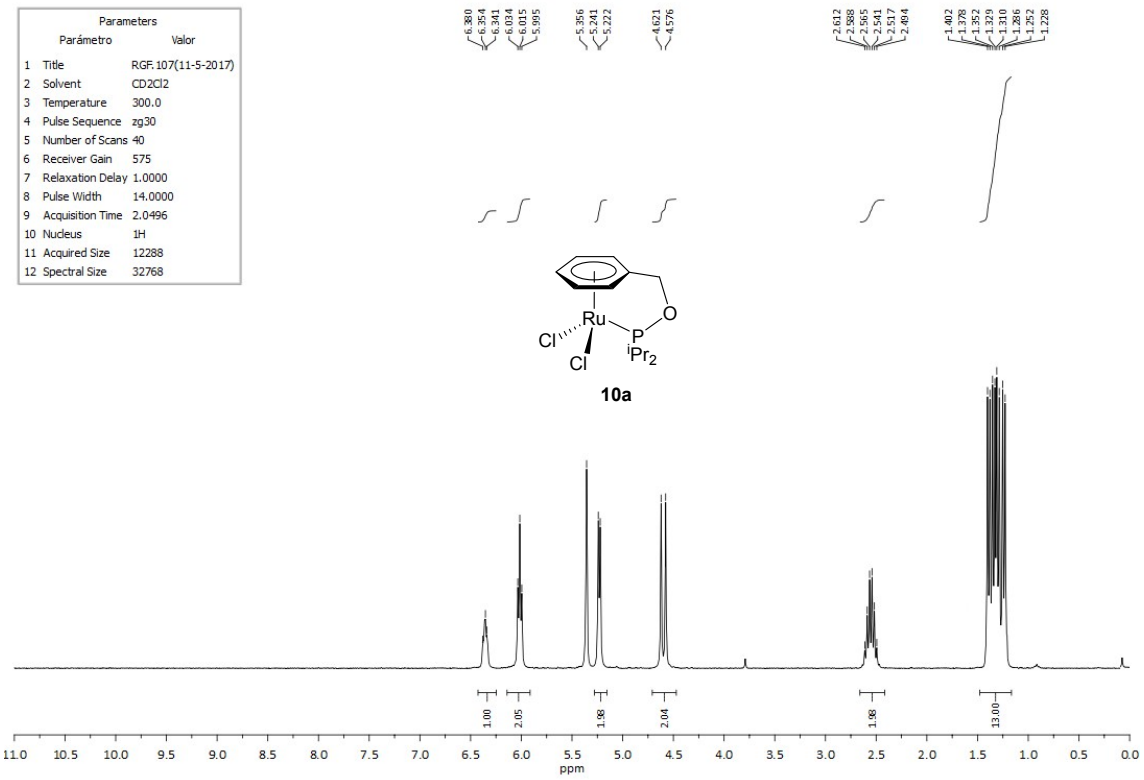

Figure S47: ^{1}H NMR spectrum (300 MHz, CD_2Cl_2) of complex **10a**.

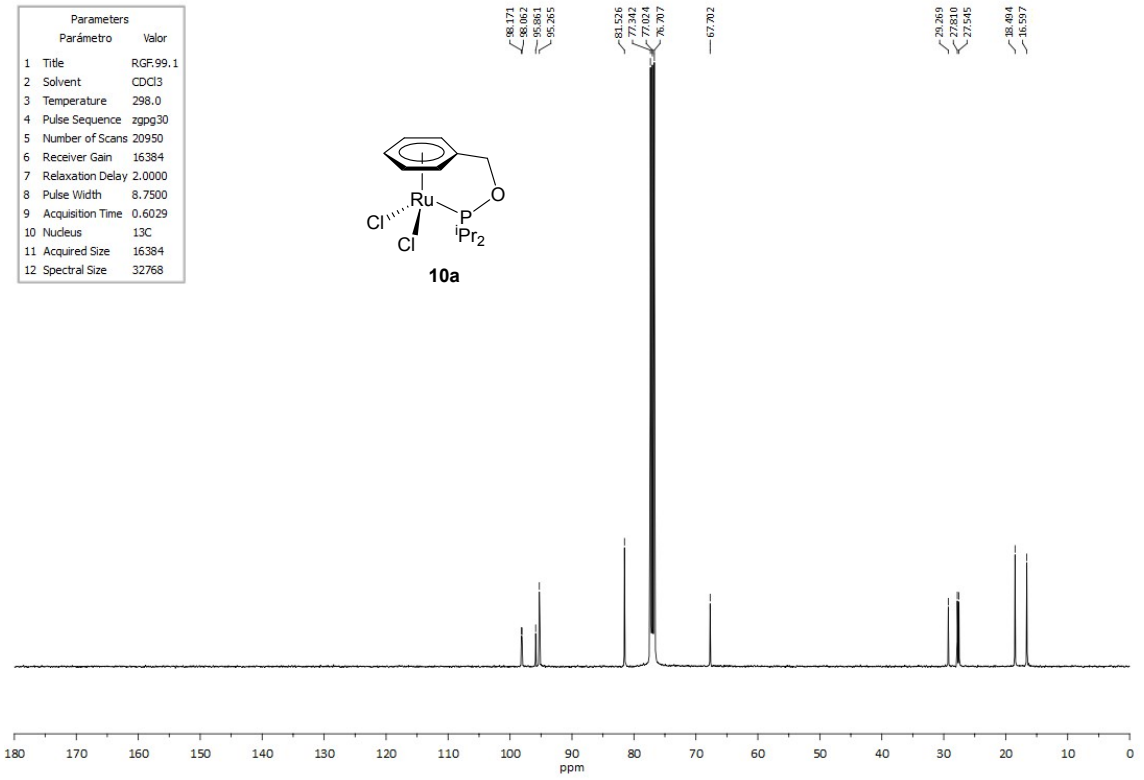

Figure S48: $^{13}C\{^{1}H\}$ NMR spectrum (100 MHz, $CDCl_3$) of complex **10a**.

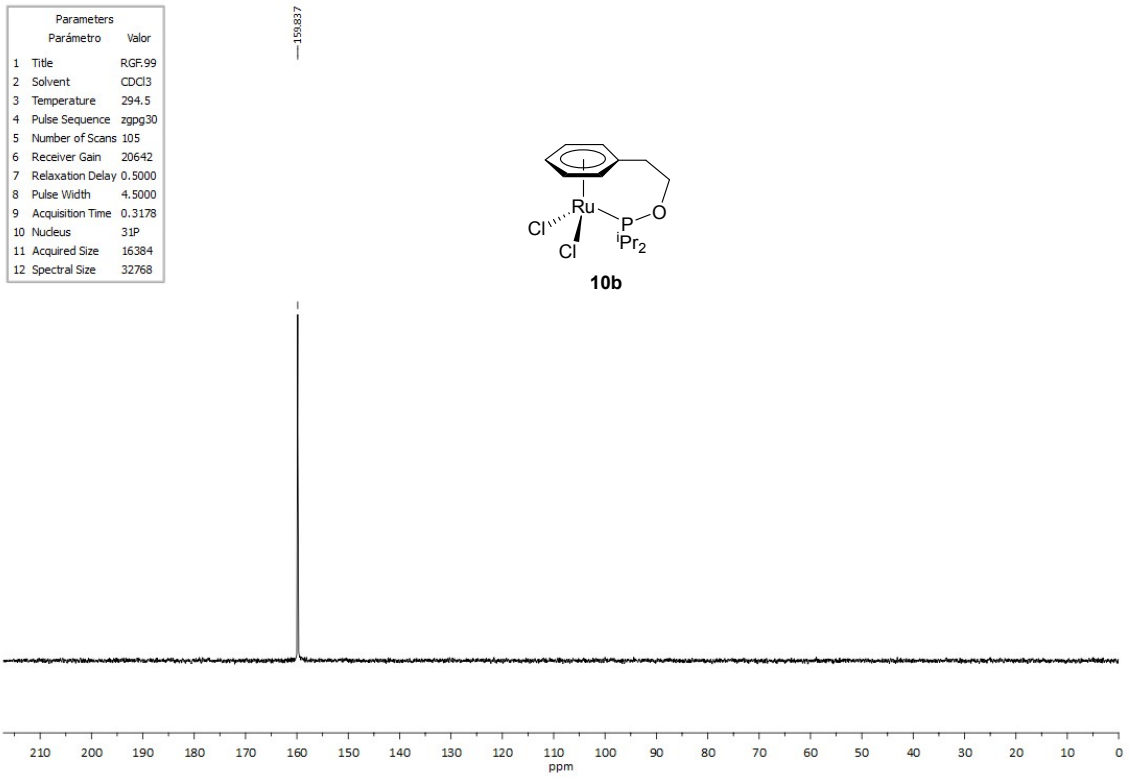

Figure S49: $^{31}P\{^{1}H\}$ NMR spectrum (121 MHz, $CDCl_3$) of complex **10b**.

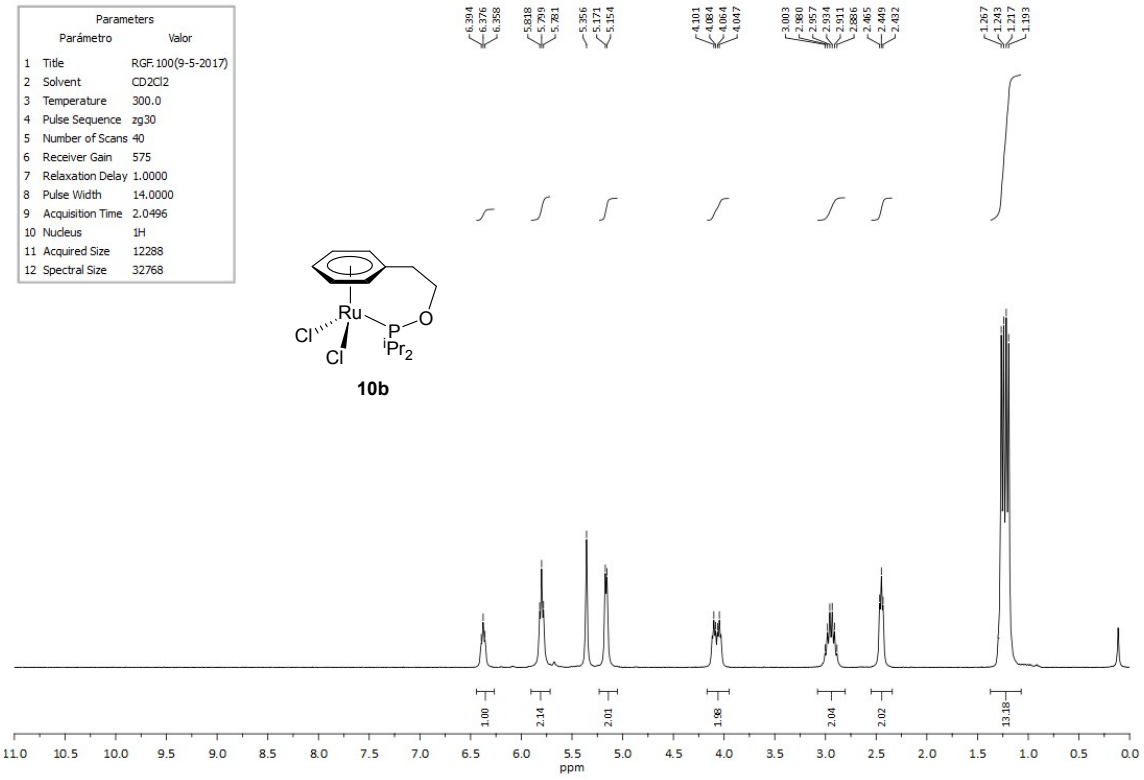

Figure S50: ^{1}H NMR spectrum (300 MHz, CD_2Cl_2) of complex **10b**.

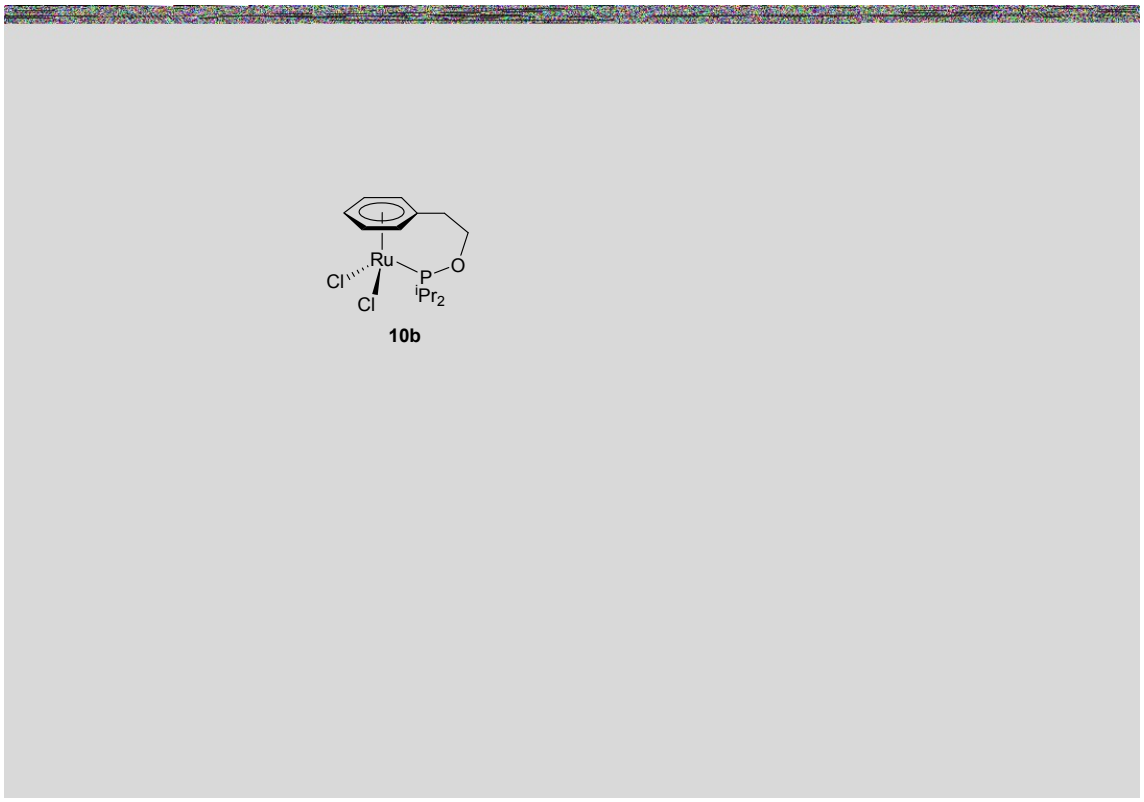

Figure S51: $^{13}C\{^{1}H\}$ NMR spectrum (100 MHz, $CDCl_3$) of complex **10b**.

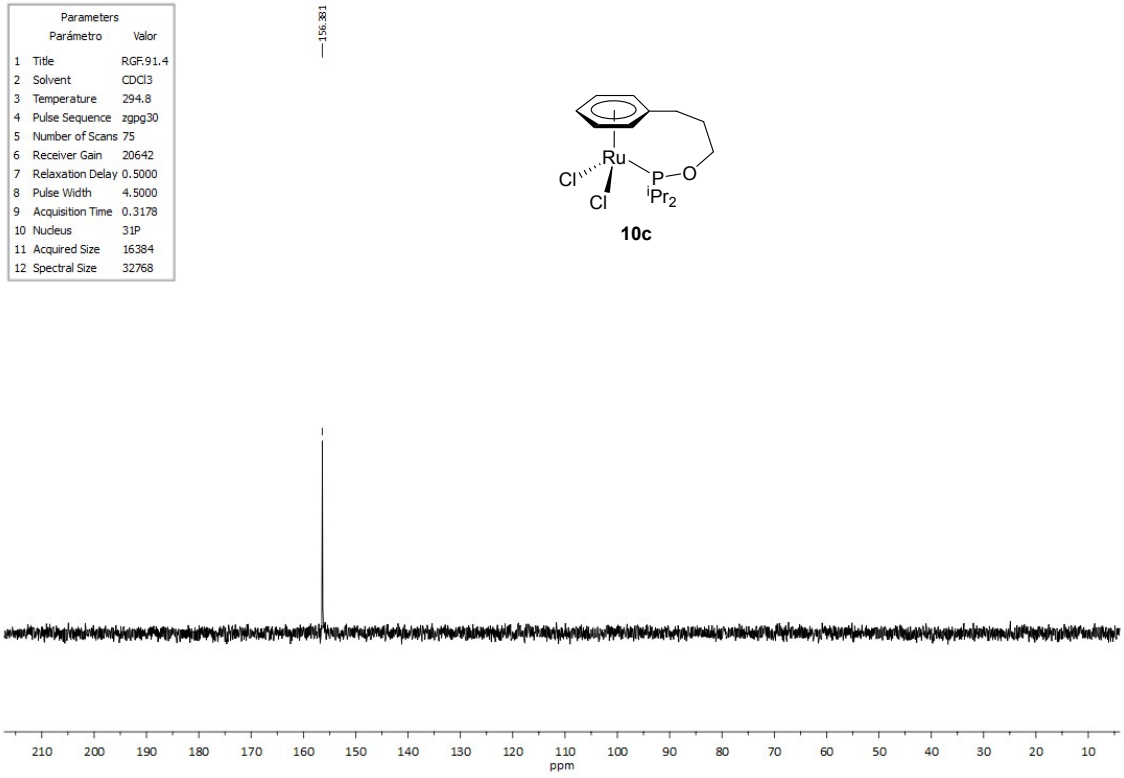

Figure S52: $^{31}P\{^{1}H\}$ NMR spectrum (121 MHz, $CDCl_3$) of complex **10c**.

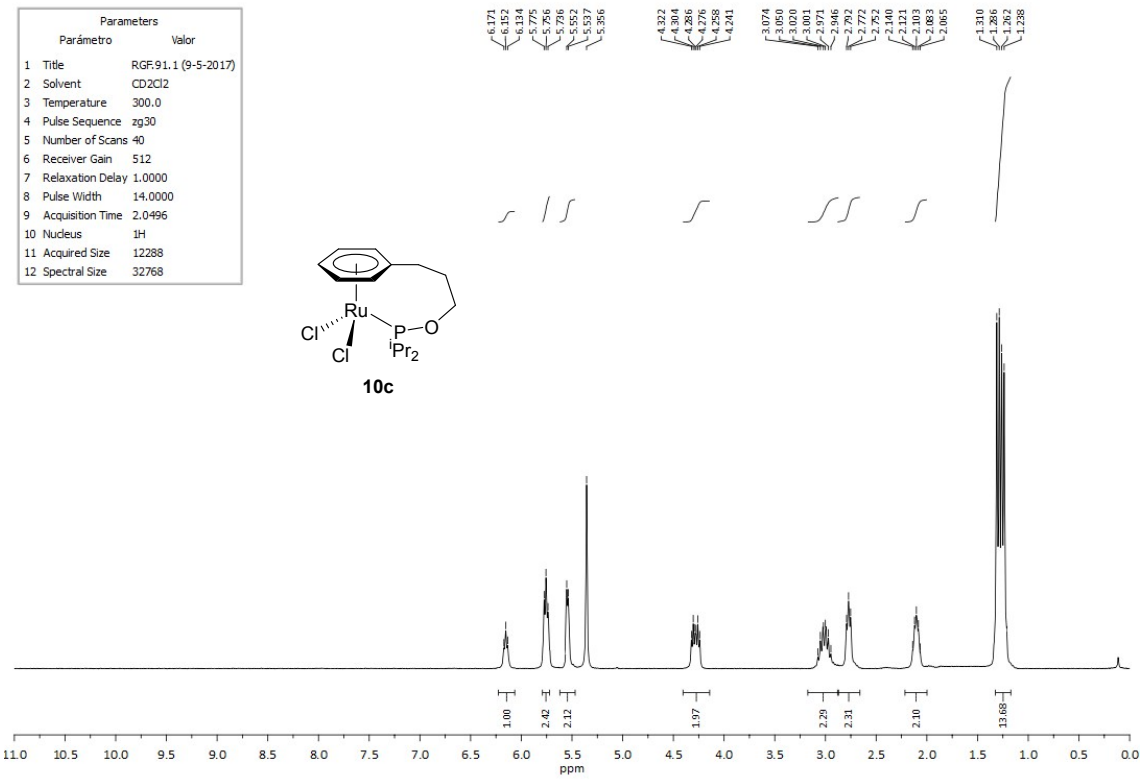

Figure S53: ^{1}H NMR spectrum (300 MHz, CD_2Cl_2) of complex **10c**.

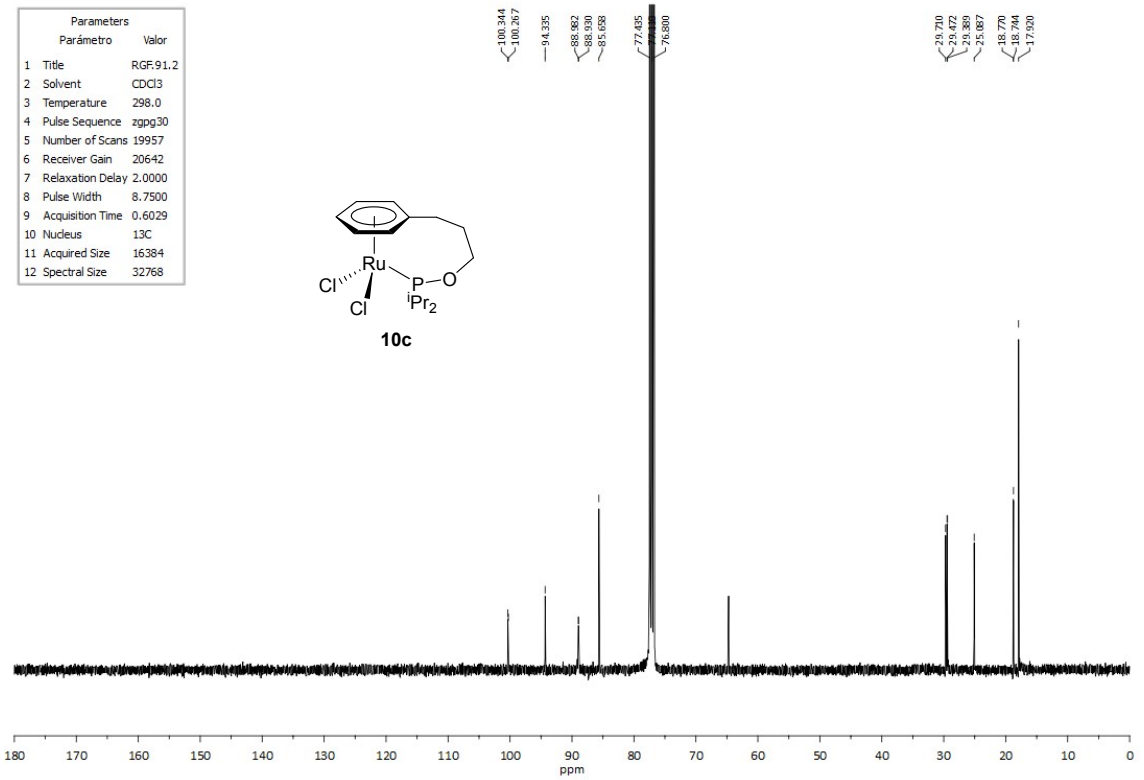

Figure S54: $^{13}C\{^{1}H\}$ NMR spectrum (100 MHz, $CDCl_3$) of complex **10c**.

NMR spectra of the alkoxysilanes isolated from the catalytic reactions

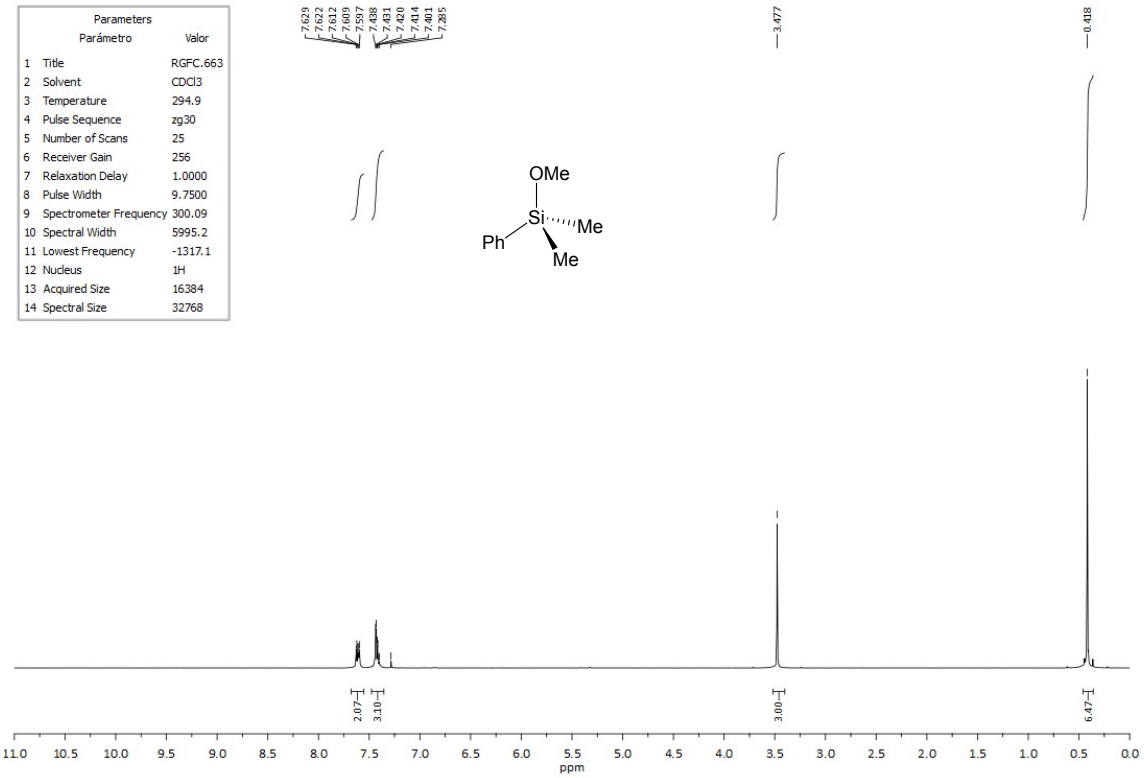

Figure S55: ^{1}H NMR spectrum (300 MHz, $CDCl_3$) of $Me_2PhSiOMe$.

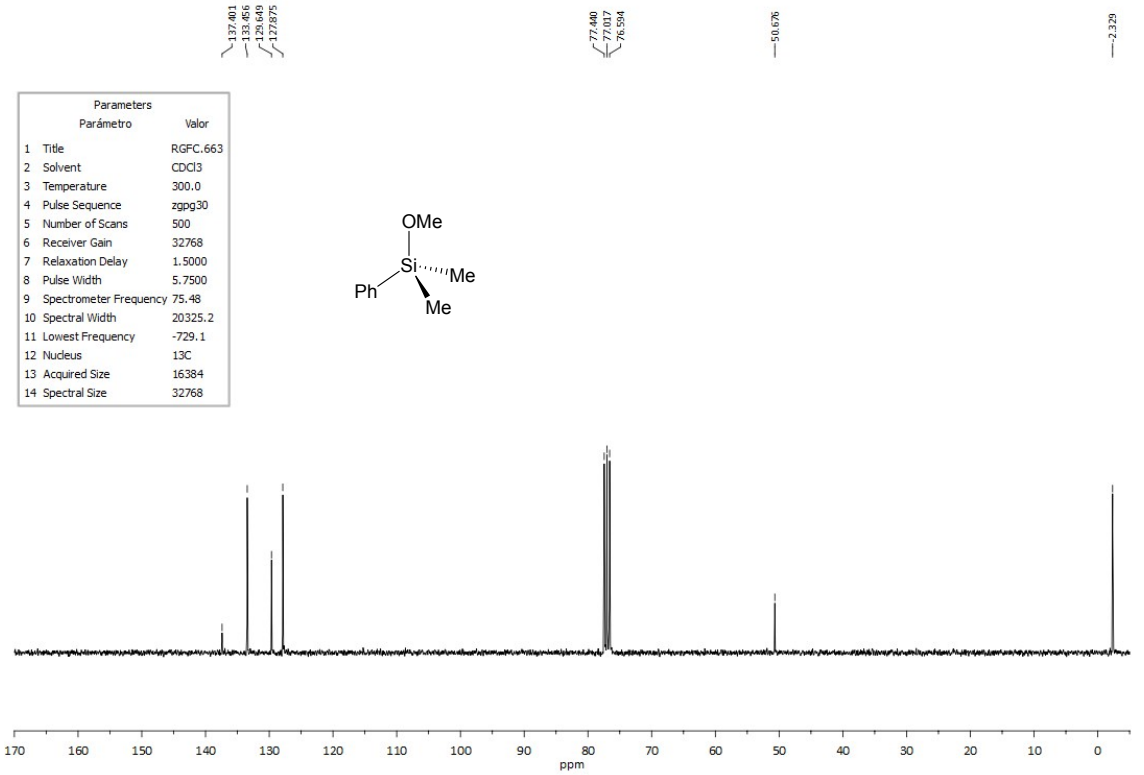

Figure S56: $^{13}C\{^{1}H\}$ NMR spectrum (75 MHz, $CDCl_3$) of $Me_2PhSiOMe$.

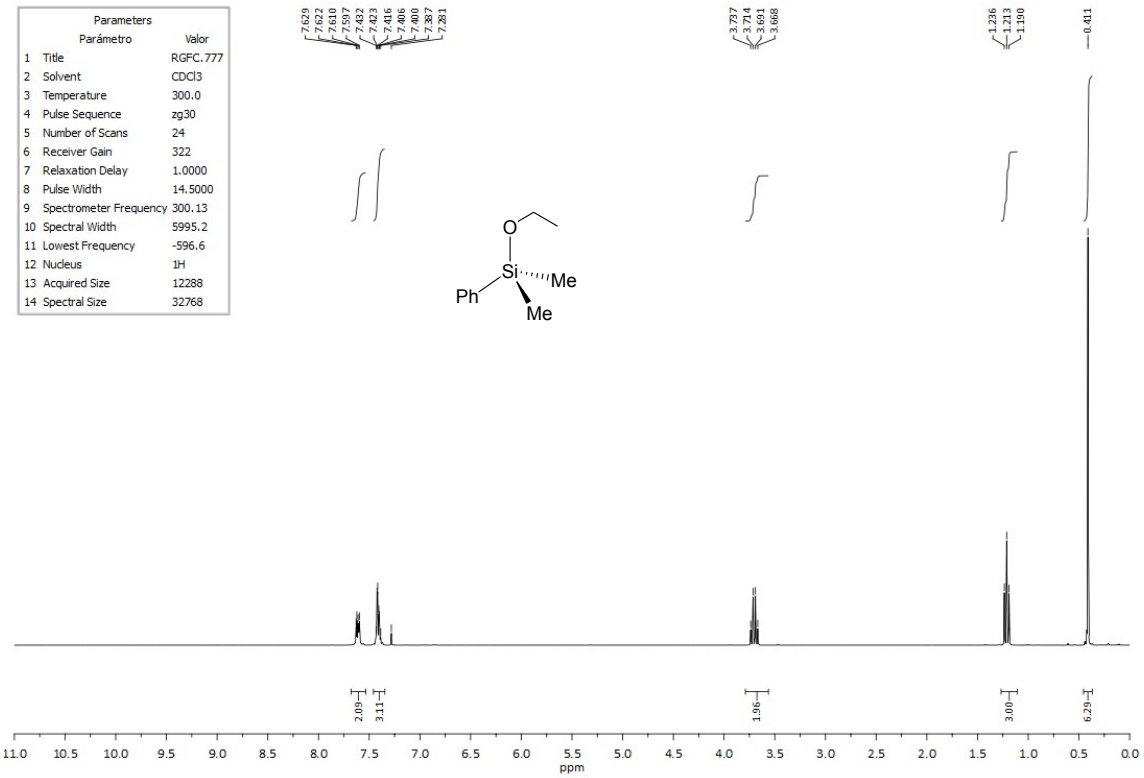

Figure S57: ^{1}H NMR spectrum (300 MHz, $CDCl_3$) of $Me_2PhSiOEt$.

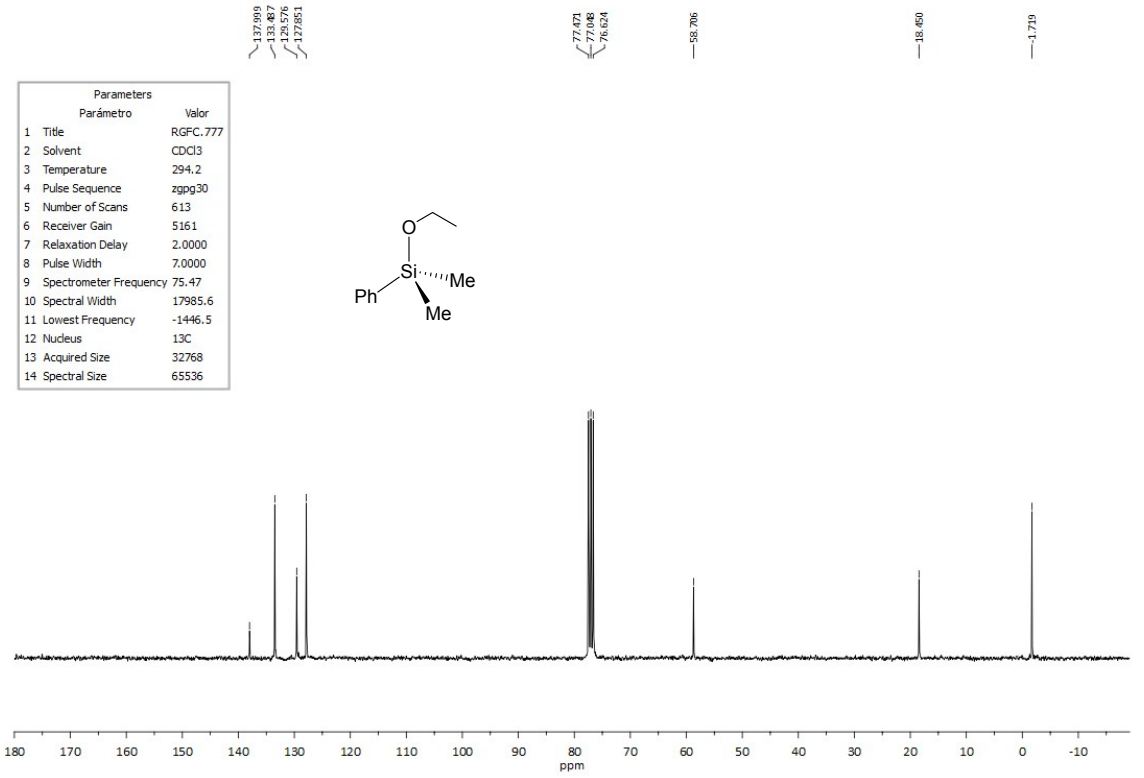

Figure S58: $^{13}C\{^{1}H\}$ NMR spectrum (75 MHz, $CDCl_3$) of $Me_2PhSiOEt$.

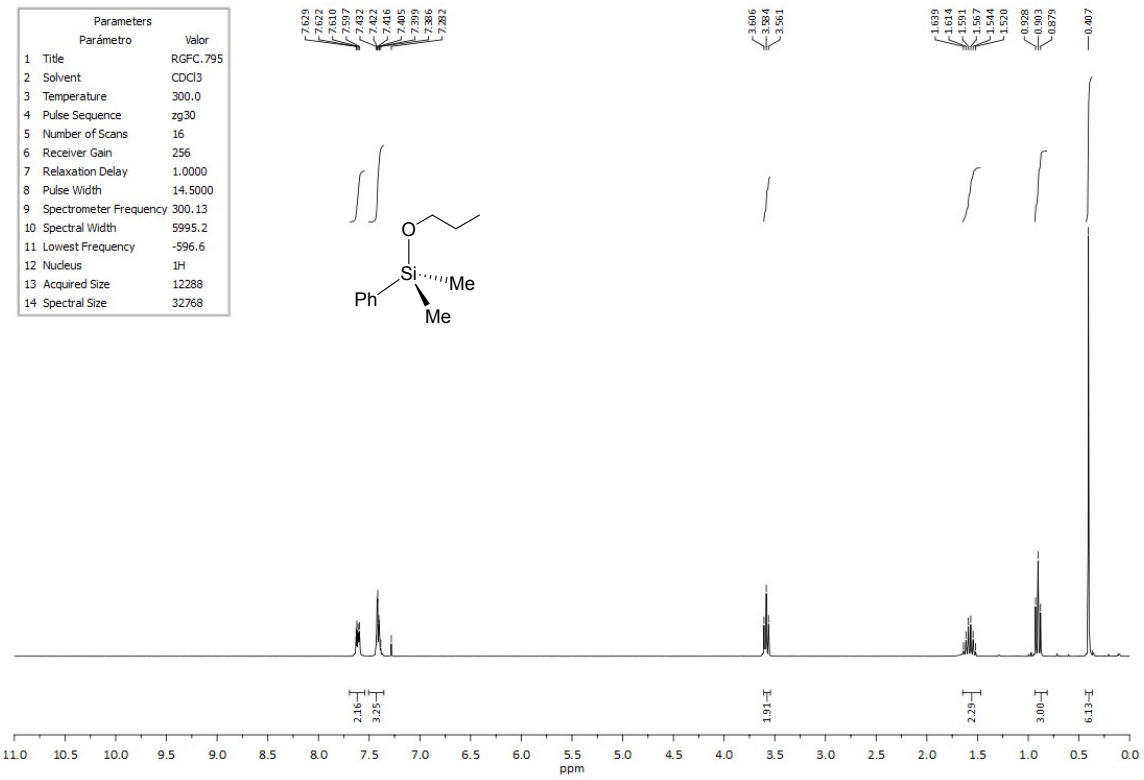

Figure S59: ^{1}H NMR spectrum (300 MHz, $CDCl_3$) of Me_2PhSiO^nPr.

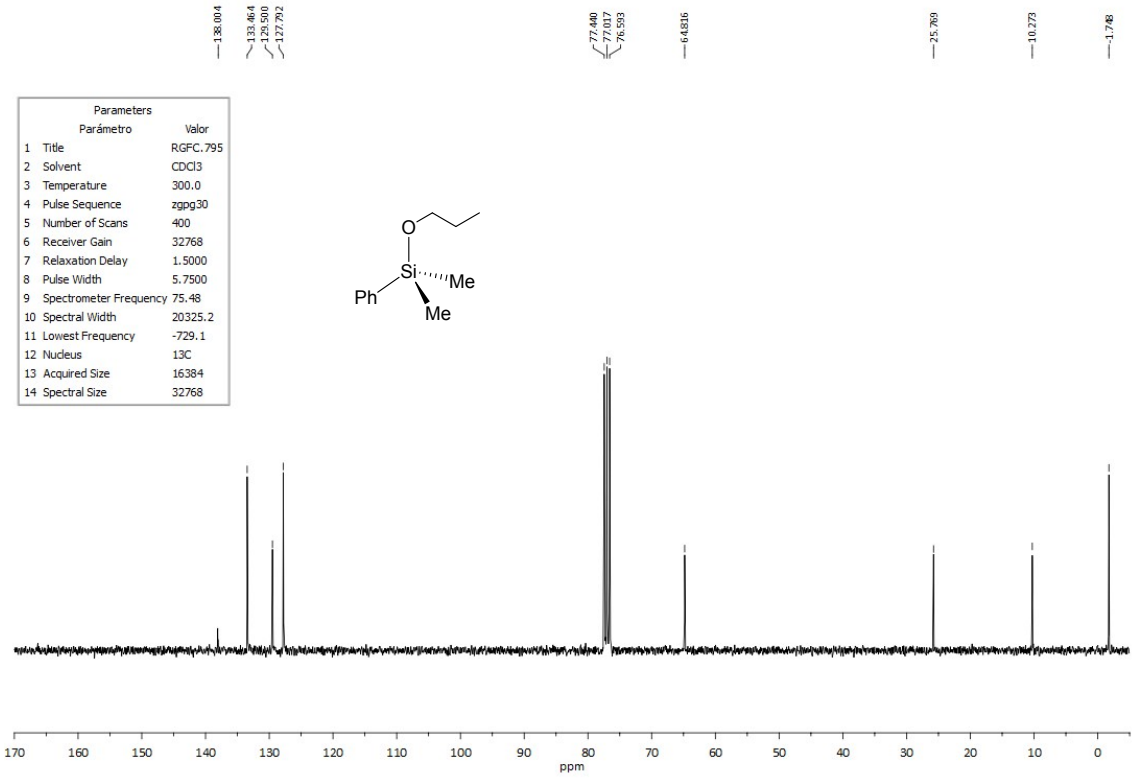

Figure S60: $^{13}C\{^{1}H\}$ NMR spectrum (75 MHz, $CDCl_3$) of Me_2PhSiO^nPr.

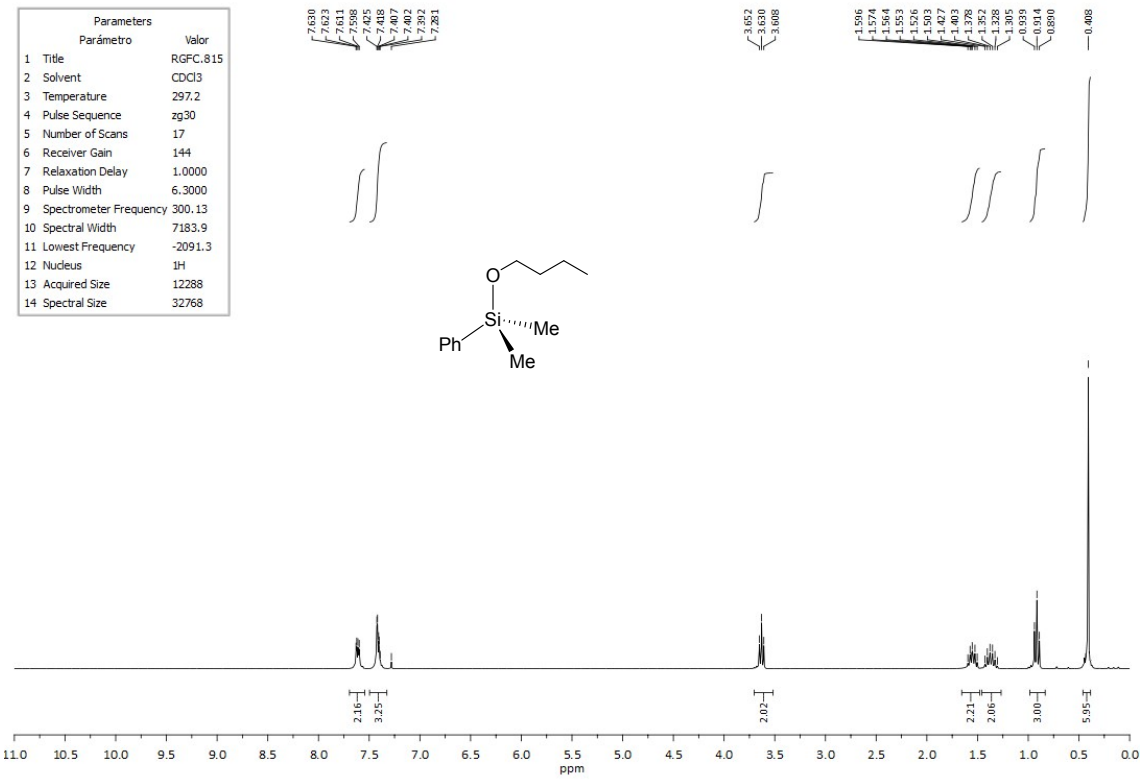

Figure S61: ^{1}H NMR spectrum (300 MHz, $CDCl_3$) of Me_2PhSiO^nBu.

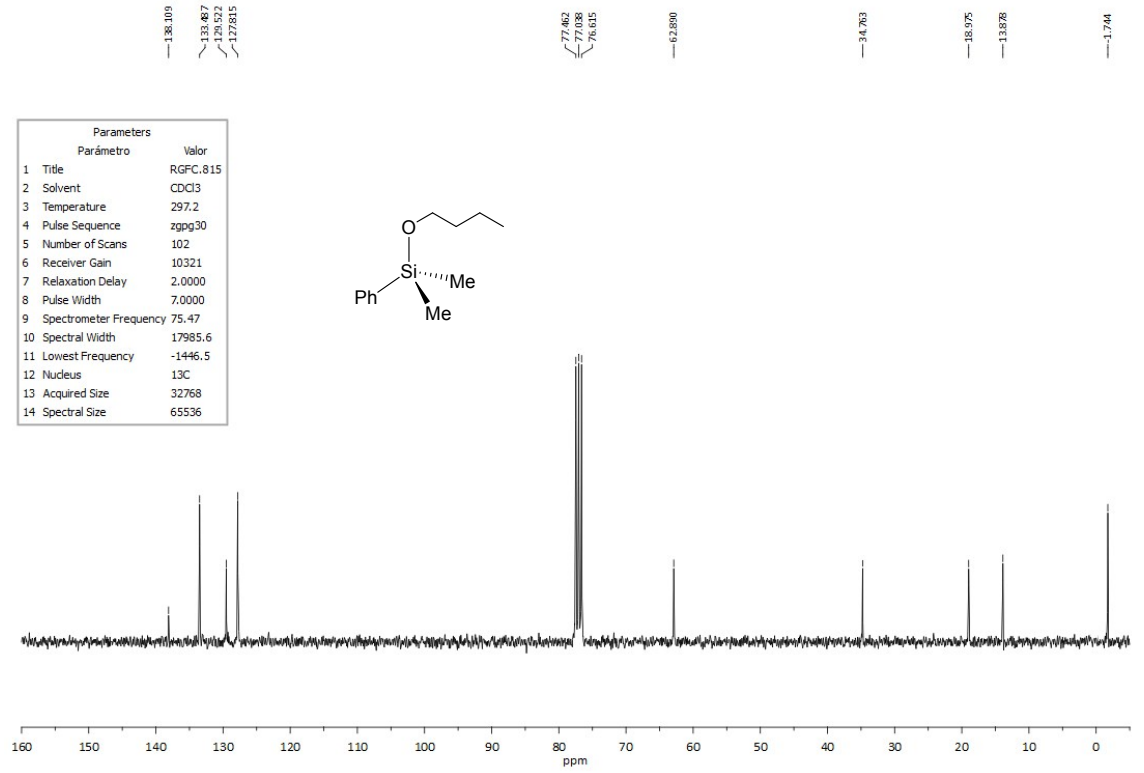

Figure S62: $^{13}C\{^{1}H\}$ NMR spectrum (75 MHz, $CDCl_3$) of Me_2PhSiO^nBu.

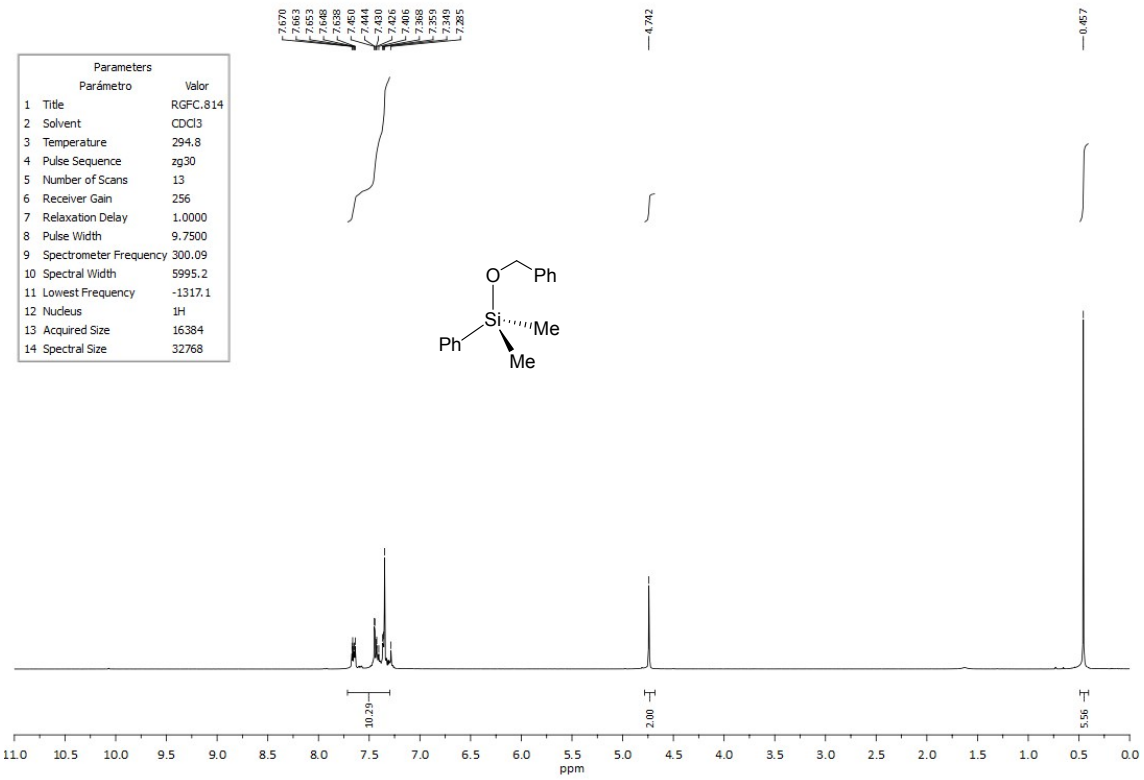

Figure S63: ^{1}H NMR spectrum (300 MHz, $CDCl_3$) of $Me_2PhSiOBn$.

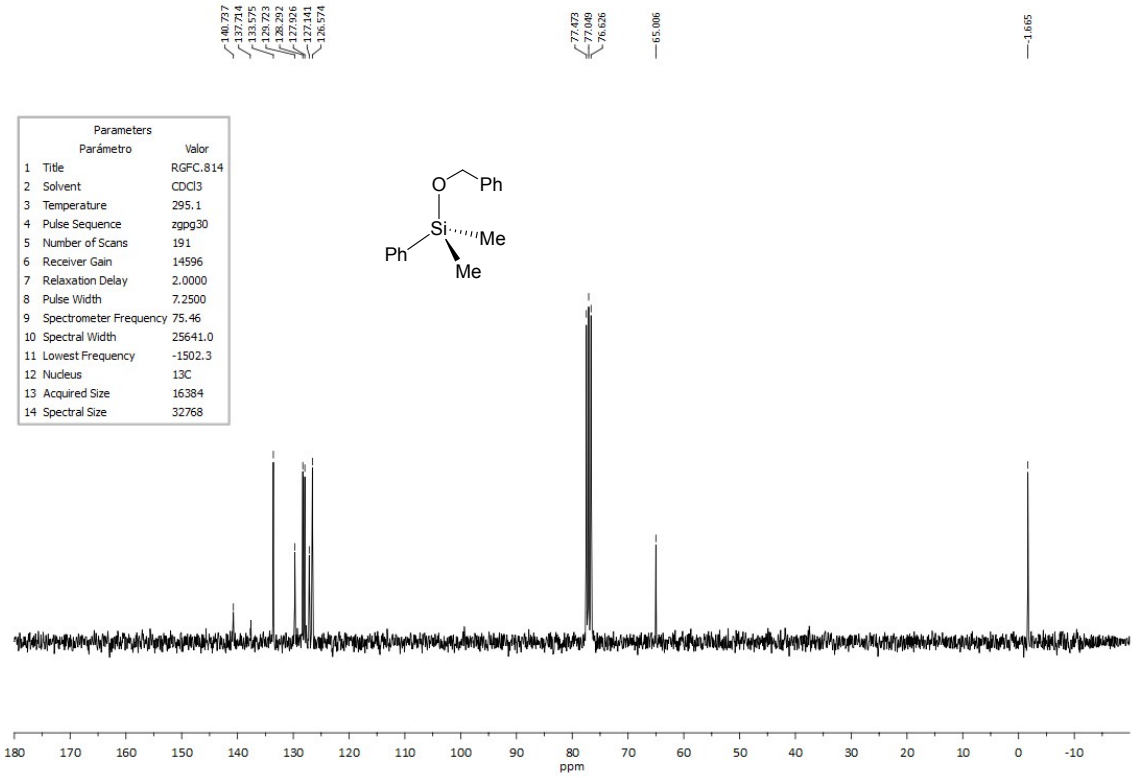

Figure S64: $^{13}C\{^{1}H\}$ NMR spectrum (75 MHz, $CDCl_3$) of $Me_2PhSiOBn$.

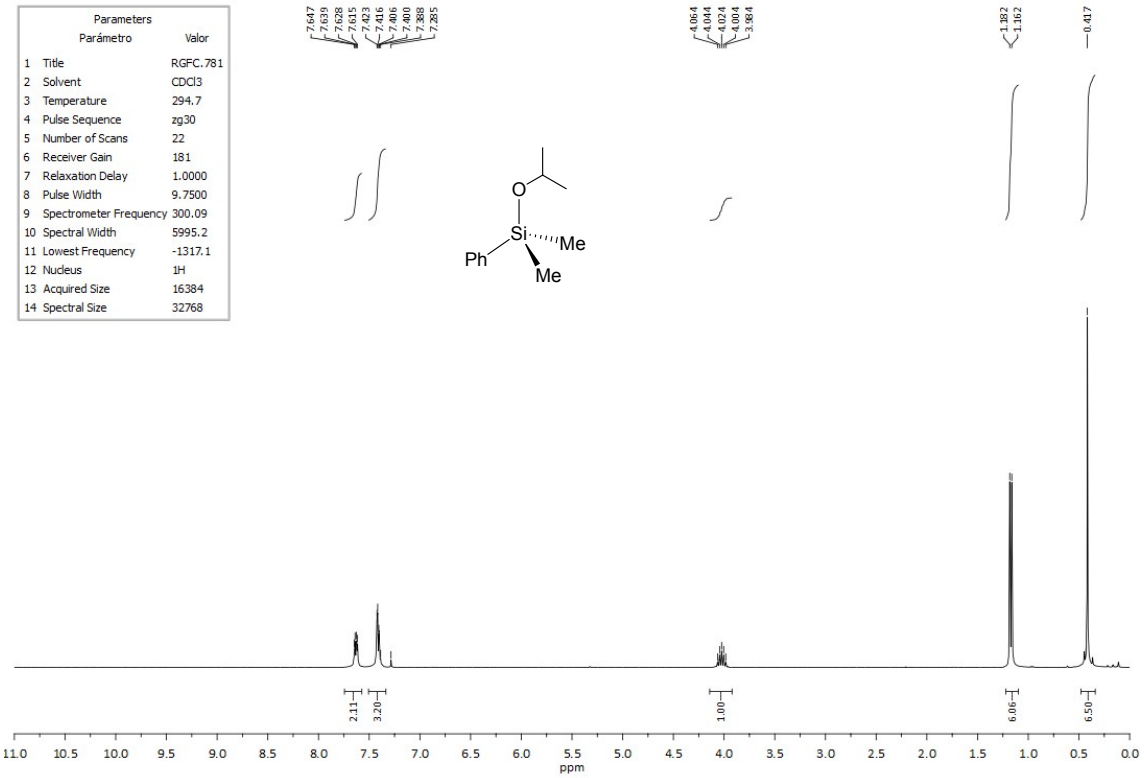

Figure S65: ^{1}H NMR spectrum (300 MHz, $CDCl_3$) of Me_2PhSiO^iPr.

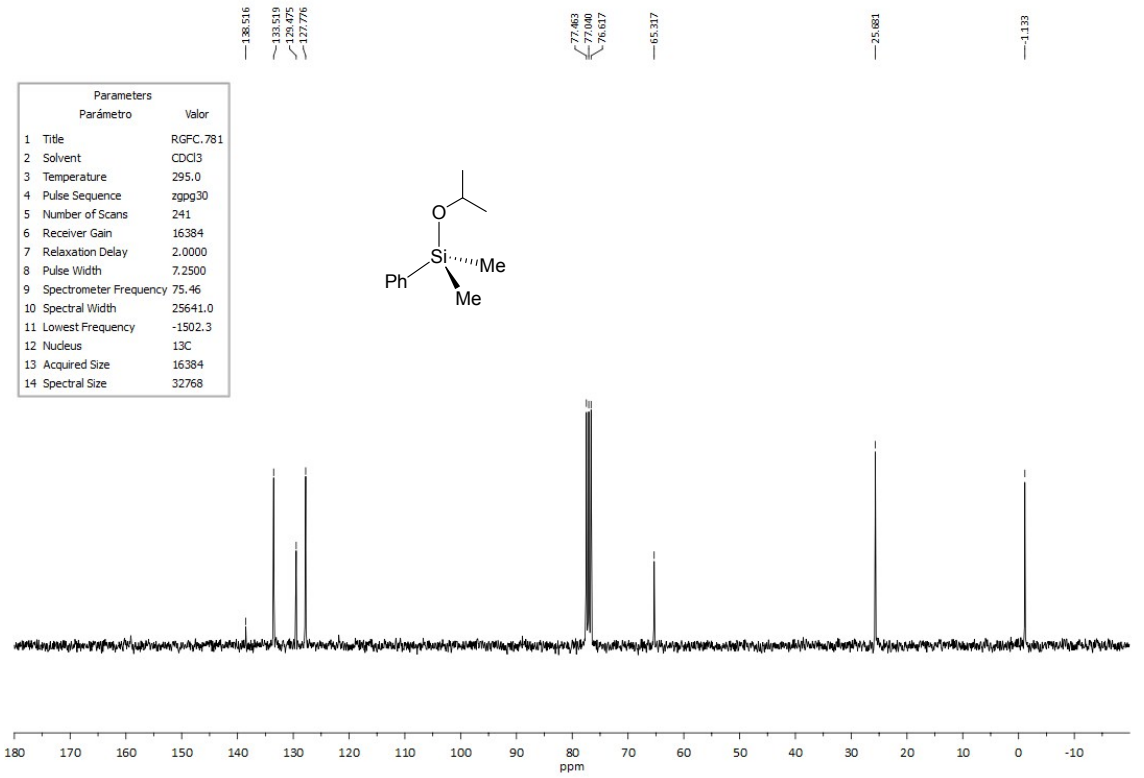

Figure S66: $^{13}C\{^{1}H\}$ NMR spectrum (75 MHz, $CDCl_3$) of Me_2PhSiO^iPr.

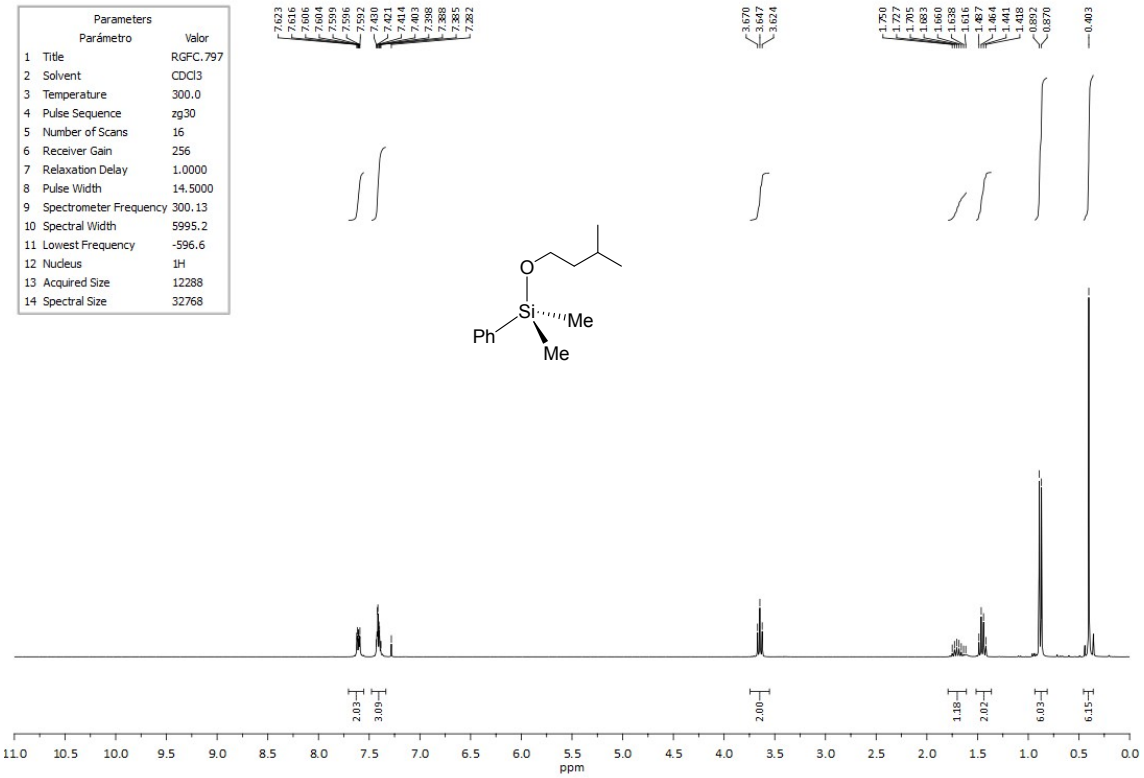

Figure S67: ^{1}H NMR spectrum (300 MHz, $CDCl_3$) of $Me_2PhSiOCH_2CH_2{}^{i}Pr$.

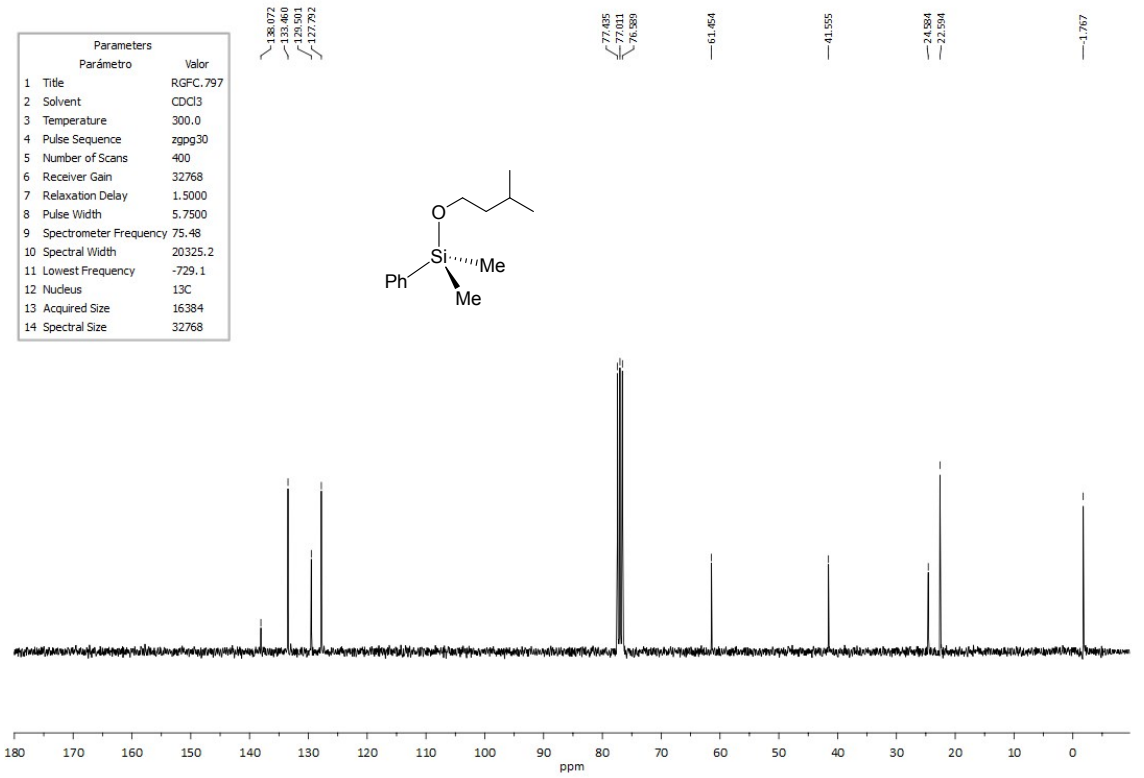

Figure S68: $^{13}C\{^{1}H\}$ NMR spectrum (75 MHz, $CDCl_3$) of $Me_2PhSiOCH_2CH_2{}^{i}Pr$.

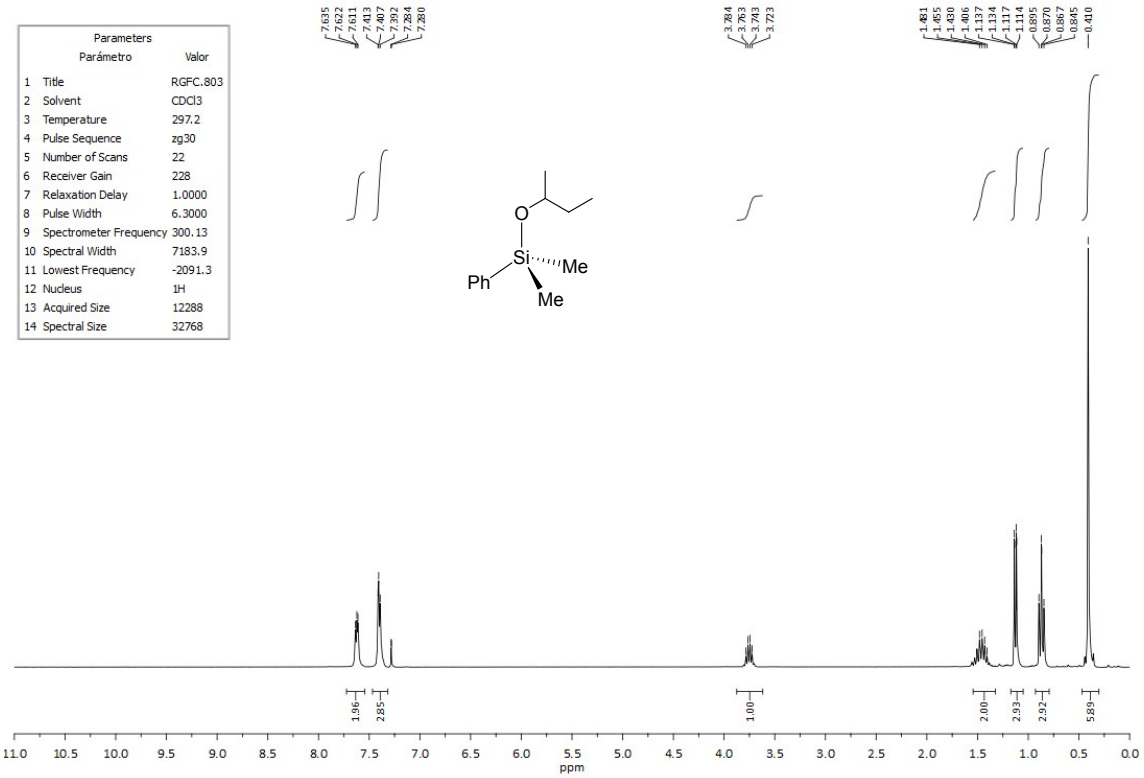

Figure S69: ^{1}H NMR spectrum (300 MHz, $CDCl_3$) of $Me_2PhSiOCHMeEt$.

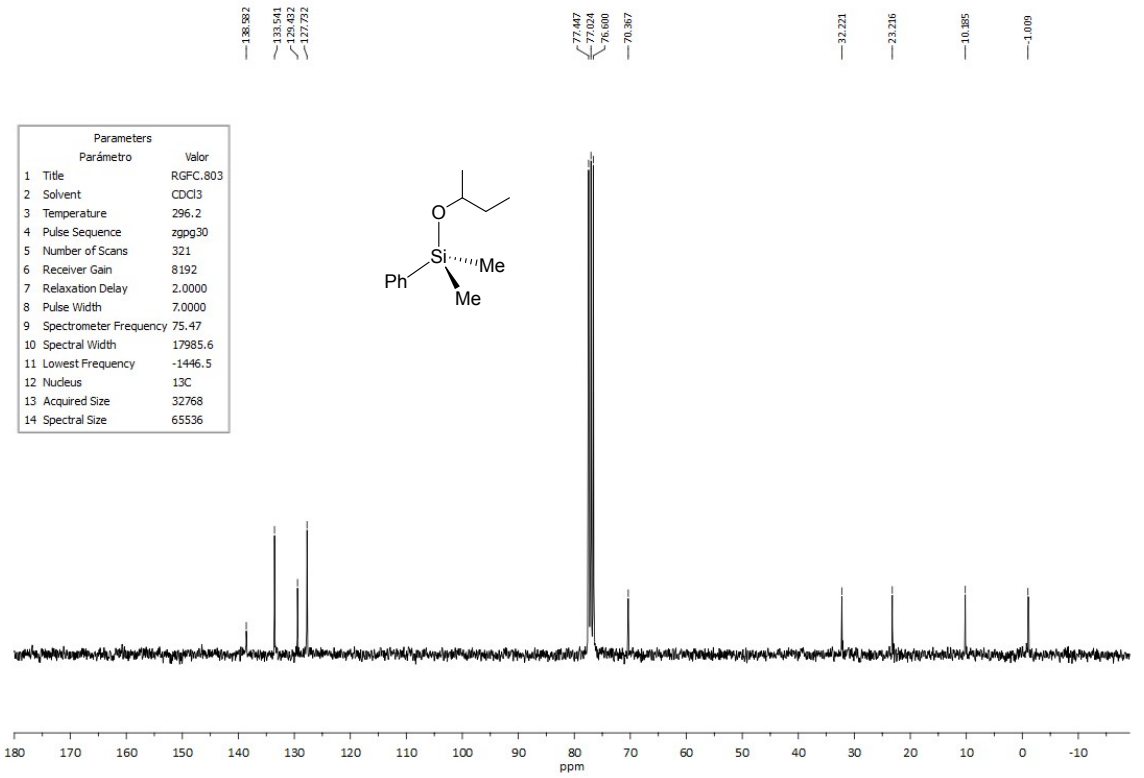

Figure S70: $^{13}C\{^{1}H\}$ NMR spectrum (75 MHz, $CDCl_3$) of $Me_2PhSiOCHMeEt$.

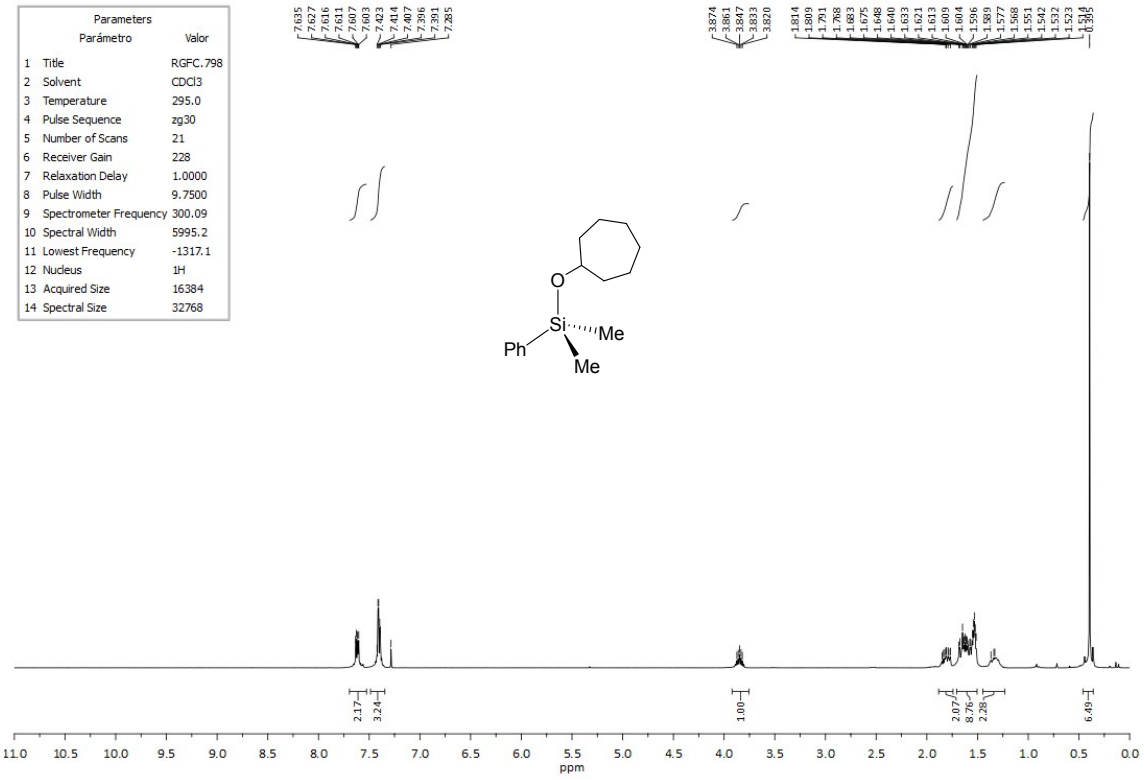

Figure S71: ^{1}H NMR spectrum (300 MHz, $CDCl_3$) of $Me_2PhSiO^cHeptyl$.

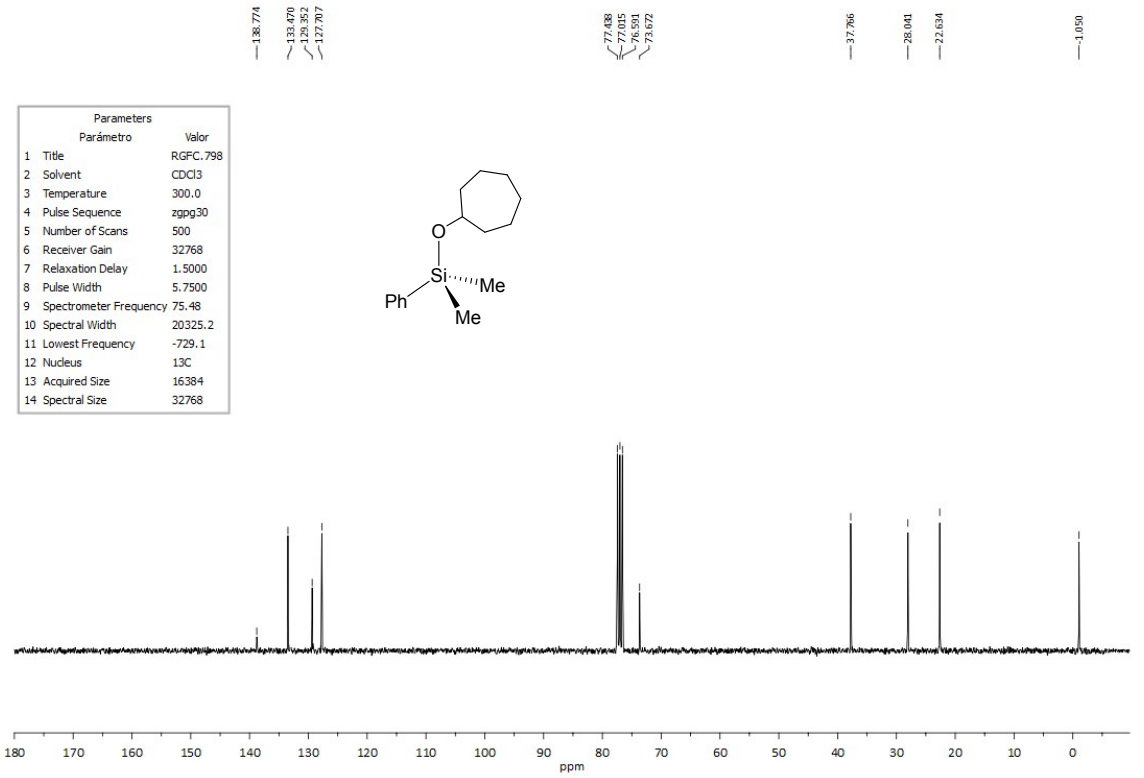

Figure S72: $^{13}C\{^{1}H\}$ NMR spectrum (75 MHz, $CDCl_3$) of $Me_2PhSiO^cHeptyl$.

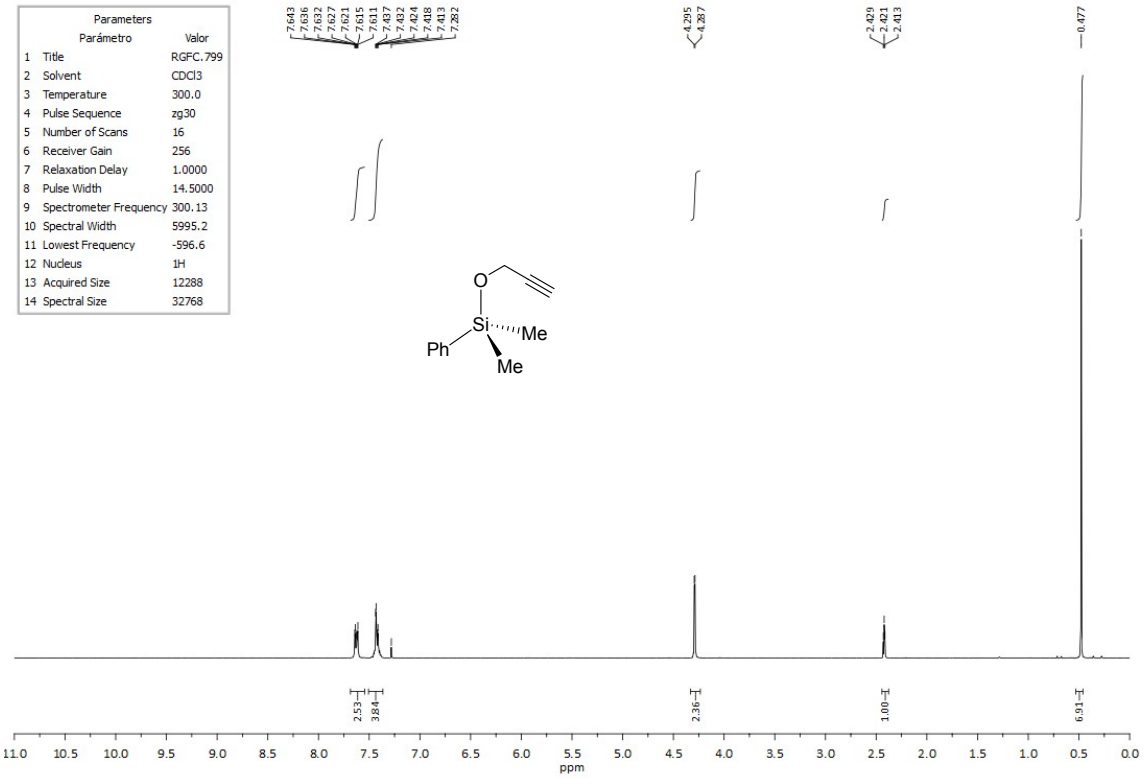

Figure S73: ^{1}H NMR spectrum (300 MHz, $CDCl_3$) of $Me_2PhSiOCH_2C{\equiv}CH$.

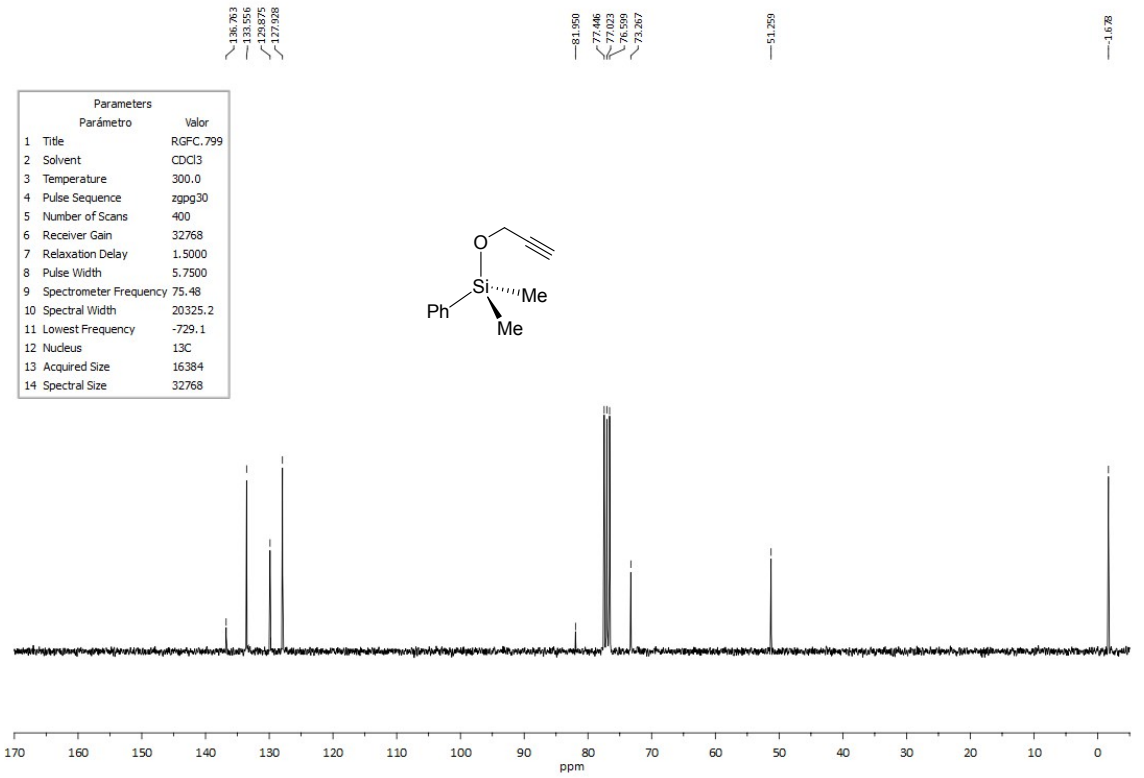

Figure S74: $^{13}C\{^{1}H\}$ NMR spectrum (75 MHz, $CDCl_3$) of $Me_2PhSiOCH_2C{\equiv}CH$.

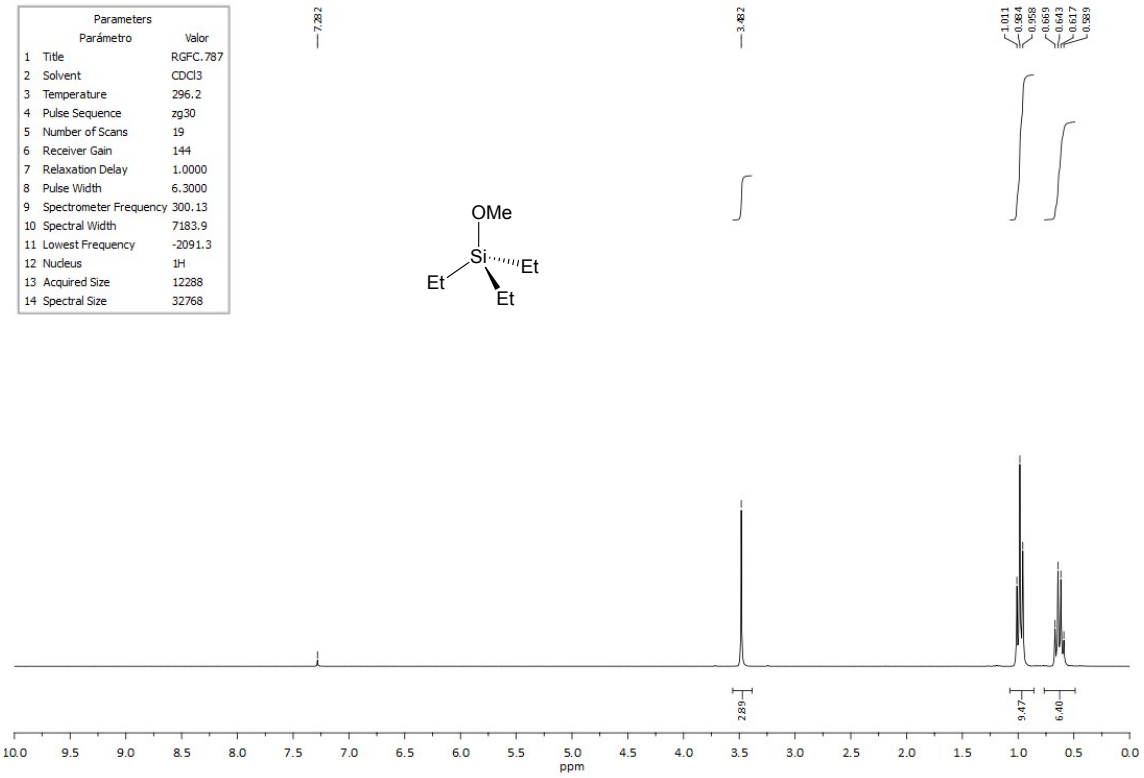

Figure S75: ^{1}H NMR spectrum (300 MHz, $CDCl_3$) of Et_3SiOMe.

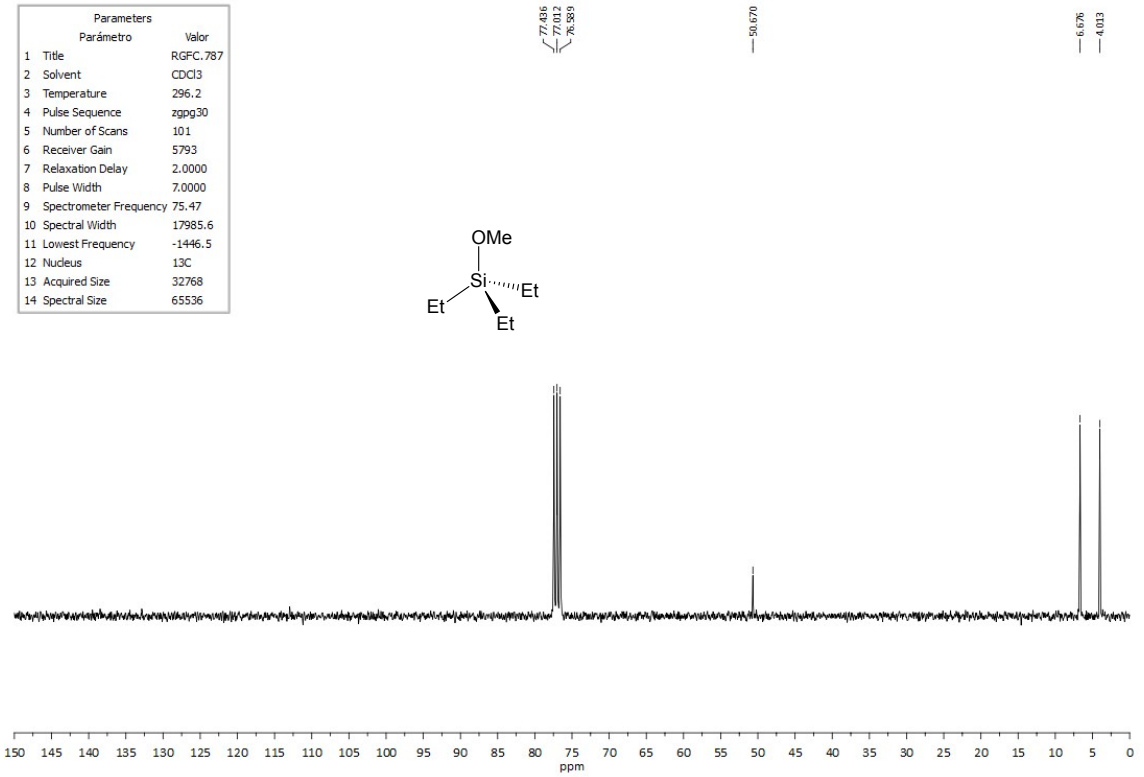

Figure S76: $^{13}C\{^{1}H\}$ NMR spectrum (75 MHz, $CDCl_3$) of Et_3SiOMe.

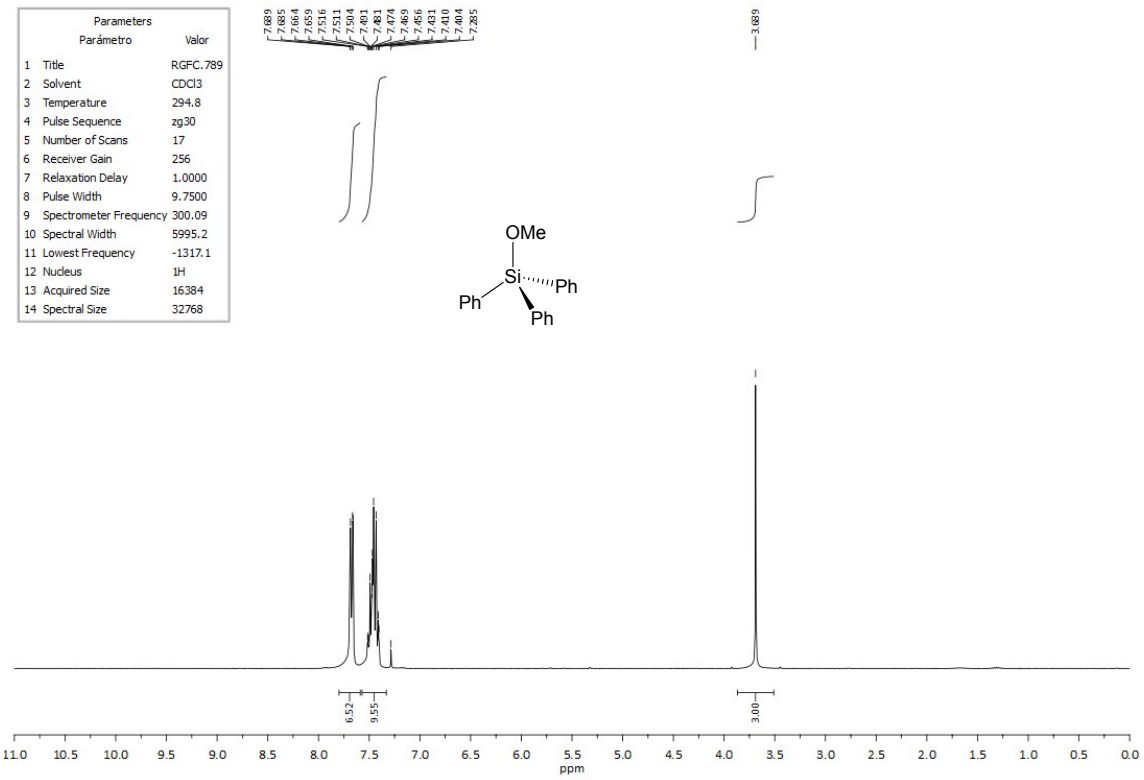

Figure S77: ^{1}H NMR spectrum (300 MHz, $CDCl_3$) of Ph_3SiOMe.

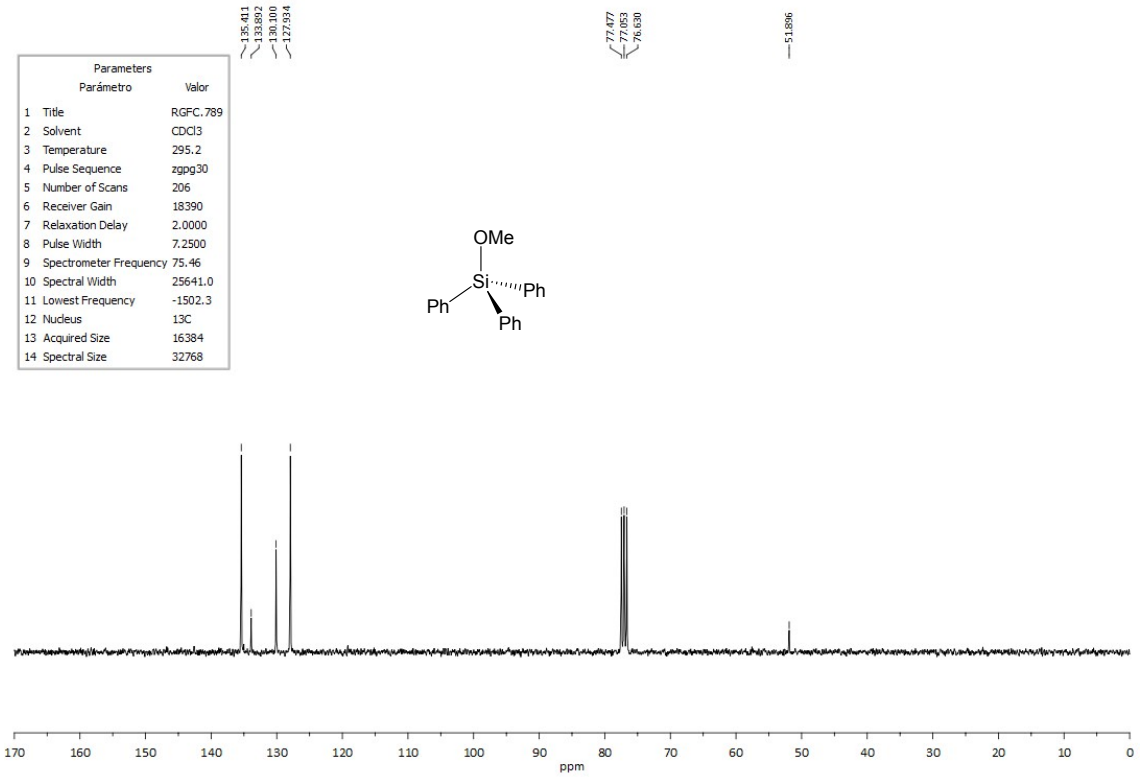

Figure S78: $^{13}C\{^{1}H\}$ NMR spectrum (75 MHz, $CDCl_3$) of Ph_3SiOMe.

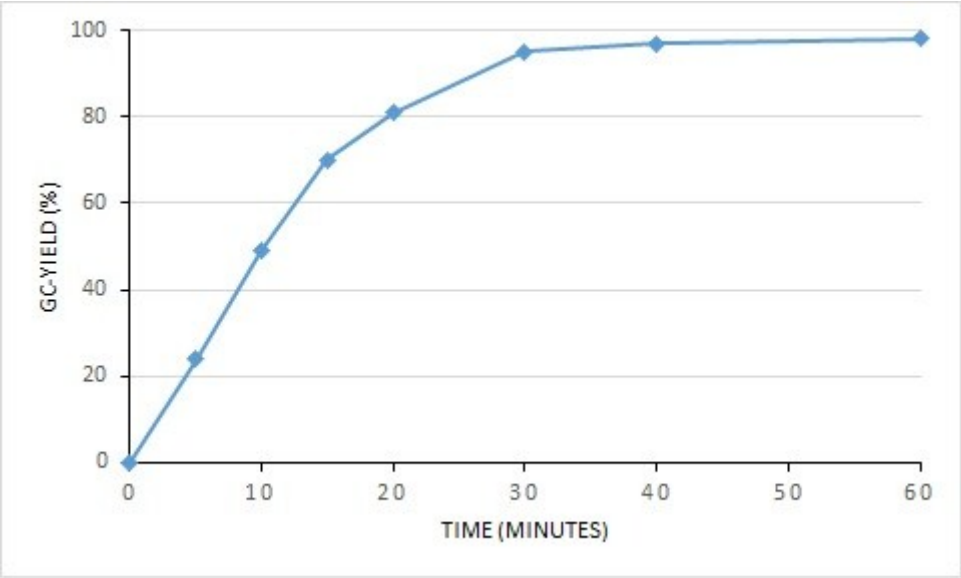

Figure S79: $^{13}C\{^{1}H\}$ NMR spectrum (75 MHz, $CDCl_3$) of Ph_3SiOMe. Kinetic profile of the dehydrogenative cross-coupling reaction of Me_2PhSiH with MeOH catalyzed by 0.005 mol% of complex **10c** (entry 13 of Table 2 of the manuscript).